

NAVAL POSTGRADUATE SCHOOL MONTEREY, CALIFORNIA



19960812 087

THESIS

EXPERIMENTAL ANALYSIS OF THE WAKE OF AN OSCILLATING AIRFOIL

by

Claus M. Dohring

June 1996

Thesis Advisor:

M. F. Platzer

Approved for public release; distribution is unlimited

DISCLAIMER NOTICE



THIS DOCUMENT IS BEST QUALITY AVAILABLE. THE COPY FURNISHED TO DTIC CONTAINED A SIGNIFICANT NUMBER OF COLOR PAGES WHICH DO NOT REPRODUCE LEGIBLY ON BLACK AND WHITE MICROFICHE.

REPORT DOCUMENTATION PAGEForm Approved
OMB No. 0704-0188

Public reporting burden for this collection of information is estimated to average 1 hour per response, including the time for reviewing instructions, searching existing data sources, gathering and maintaining the data needed, and completing and reviewing the collection of information. Send comments regarding this burden estimate or any other aspect of this collection of information, including suggestions for reducing this burden, to Washington Headquarters Services, Directorate for Information Operations and Reports, 1215 Jefferson Davis Highway, Suite 1204, Arlington, VA 22202-4302, and to the Office of Management and Budget, Paperwork Reduction Project (0704-0188), Washington, DC 20503.

1. AGENCY USE ONLY (Leave blank)		2. REPORT DATE June 1996	3. REPORT TYPE AND DATES COVERED Master's Thesis	
4. TITLE AND SUBTITLE EXPERIMENTAL ANALYSIS OF THE WAKE OF AN OSCILLATING AIRFOIL			5. FUNDING NUMBERS	
6. AUTHOR(S) Dohring, Claus M.				
7. PERFORMING ORGANIZATION NAME(S) AND ADDRESS(ES) Naval Postgraduate School Monterey, CA 93943-5000			8. PERFORMING ORGANIZATION REPORT NUMBER	
9. SPONSORING/MONITORING AGENCY NAME(S) AND ADDRESS(ES) Office of Naval Research Arlington, VA 22217-5660			10. SPONSORING/MONITORING AGENCY REPORT NUMBER	
11. SUPPLEMENTARY NOTES The views expressed in this thesis are those of the author and do not reflect the official policy or position of the Department of Defense or the U.S. Government.				
12a. DISTRIBUTION / AVAILABILITY STATEMENT Approved for public release; distribution is unlimited			12b. DISTRIBUTION CODE	
13. ABSTRACT (Maximum 200 words) The wake of an airfoil which oscillates in pure plunge mode is investigated in a water tunnel over a wide range of reduced frequency and amplitude. The main focus of this study is the comparison of the experimentally determined wake geometry with numerical results from a potential flow code. The wake vortices are visualized by two-color dye injection and velocity profiles are measured with LDV upstream and downstream of the airfoil. Wake signatures are examined with regard to thrust or drag generation. There is a good agreement between calculated and experimental data of the vortical wavelength. At high plunge velocities both approaches show a loss of wake symmetry and the emergence of a dual mode wake behavior.				
14. SUBJECT TERMS Vortical Wake Visualization Drag-/ Thrust Signature Comparison with Calculation			15. NUMBER OF PAGES 147	
			16. PRICE CODE	
17. SECURITY CLASSIFICATION OF REPORT Unclassified	18. SECURITY CLASSIFICATION OF THIS PAGE Unclassified	19. SECURITY CLASSIFICATION OF ABSTRACT Unclassified	20. LIMITATION OF ABSTRACT SAR	

Approved for public release; distribution is unlimited

**EXPERIMENTAL ANALYSIS OF THE WAKE
OF AN OSCILLATING AIRFOIL**

Claus M. Dohring
Commander, German Navy
Dipl. Ing., Universität der Bundeswehr, München, 1981

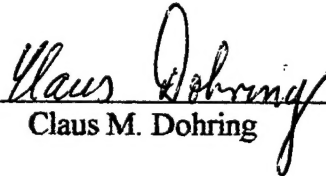
Submitted in partial fulfillment of the
requirements for the degree of

MASTER OF SCIENCE IN ASTRONAUTICAL ENGINEERING

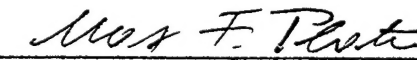
from the

**NAVAL POSTGRADUATE SCHOOL
June 1996**

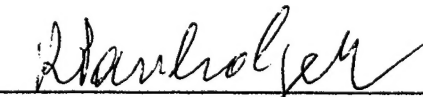
Author:

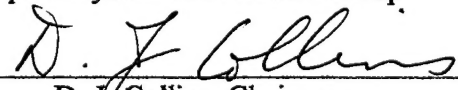

Claus M. Dohring

Approved by:


M. F. Platz, Thesis Advisor


M. S. Chandrasekhara, Second Reader


R. Panholzer, Chairman
Space Systems Academic Group


D. J. Collins, Chairman
Department of Aeronautics and Astronautics

ABSTRACT

The wake of an airfoil which oscillates in pure plunge mode is investigated in a water tunnel over a wide range of reduced frequency and amplitude. The main focus of this study is the comparison of the experimentally determined wake geometry with numerical results from a potential flow code. The wake vortices are visualized by two-color dye injection and velocity profiles are measured with LDV upstream and downstream of the airfoil. Wake signatures are examined with regard to thrust or drag generation. There is a good agreement between calculated and experimental data of the vortical wavelength. At high plunge velocities both approaches show a loss of wake symmetry and the emergence of a dual mode wake behavior.

TABLE OF CONTENTS

I. INTRODUCTION.....	1
II. EXPERIMENTAL APPARATUS.....	3
A. WATER TUNNEL.....	3
B. SHAKER.....	3
C. AIRFOILS.....	5
D. LASER.....	7
III. EXPERIMENTAL PROCEDURE.....	9
A. FLOW VELOCITY.....	9
B. FREQUENCY.....	12
C. AMPLITUDE.....	12
D. DYE INJECTION.....	13
E. PHOTOGRAPHY.....	14
F. VORTICAL WAVELENGTH.....	14
G. LASER DOPPLER VELOCIMETRY.....	15
H. MATRIX OF EXPERIMENTS.....	18
IV. RESULTS AND DISCUSSION.....	25
A. WAKE OF THE FLAPPING AIRFOIL.....	25
B. VORTICAL WAVELENGTH AS FUNCTION OF AMPLITUDE.....	27
C. VORTICAL WAVELENGTH AS FUNCTION OF FREQUENCY.....	29
D. DOWNSTREAM VARIATION OF THE VORTICAL WAVELENGTH.....	29
E. DRAG/THRUST SIGNATURE.....	32
F. COMPARISON WITH CALCULATION.....	32
G. DUAL MODE BEHAVIOUR.....	38
H. VELOCITY PROFILES.....	40
V. CONCLUSIONS.....	51
APPENDIX A. WAKE PHOTOGRAPHS AND VORTICAL WAVELENGTH PLOTS.....	53
APPENDIX B. TABLES.....	95
APPENDIX C. COMPUTED WAKES.....	125
LIST OF REFERENCES.....	133
INITIAL DISTRIBUTION LIST.....	135

ACKNOWLEDGEMENT

The author would like to acknowledge the financial support of the Office of Naval Research for allowing the purchase of equipment used in this thesis.

The author wants to thank Professor M. F. Platzler for his guidance and encouragement throughout the course of this project and Dr. K. D. Jones who provided the numerical results for comparison with the experimental data.

I. INTRODUCTION

The aerodynamics of oscillating airfoils is of interest both because of the role it plays in aircraft flutter problems and because of its application in bio-fluid-dynamics as a propulsive system of birds, insects and fishes. The thrust of a flapping airfoil was also used for propulsion of an experimental catamaran by Schmidt [Ref. 1]. In both areas - aircraft aerodynamics and bio-fluid-dynamics - the interference of the wake with downstream located bodies or the interaction of wakes from two flapping airfoils may significantly improve or deteriorate flight performance or propulsive efficiency. Therefore the knowledge of the wake properties is of great importance.

Freymuth [Ref. 2] explained the generation of propulsive vortical wake signatures of plunging and pitching airfoils and documented the time sequence of the vortex generation. Koochesfahani [Ref. 3] provided experimental results of the wake structure of a pitching airfoil and its dependence on amplitude, frequency and oscillation waveform. Freymuth, Gustafson and Leben [Ref. 4] compared physical visualizations and computed vortex dynamics of an airfoil in combined plunging and pitching motion. At the Naval Postgraduate School Platzler, Tuncer, Jones and Teng [Ref. 5, 6, 7] conducted a computational analysis of flapping airfoil aerodynamics with both a Navier-Stokes solver and a potential flow code.

The objective of this investigation is to provide comprehensive experimental data about the wake of a flapping airfoil for the purpose of comparison with the computed wake structures. The wake is investigated over a wide range of frequency and amplitude. It is visualized in a water tunnel using dye injection technique. Velocity profiles are measured upstream and downstream of the airfoil using laser Doppler velocimetry.

II. EXPERIMENTAL APPARATUS

A. WATER TUNNEL

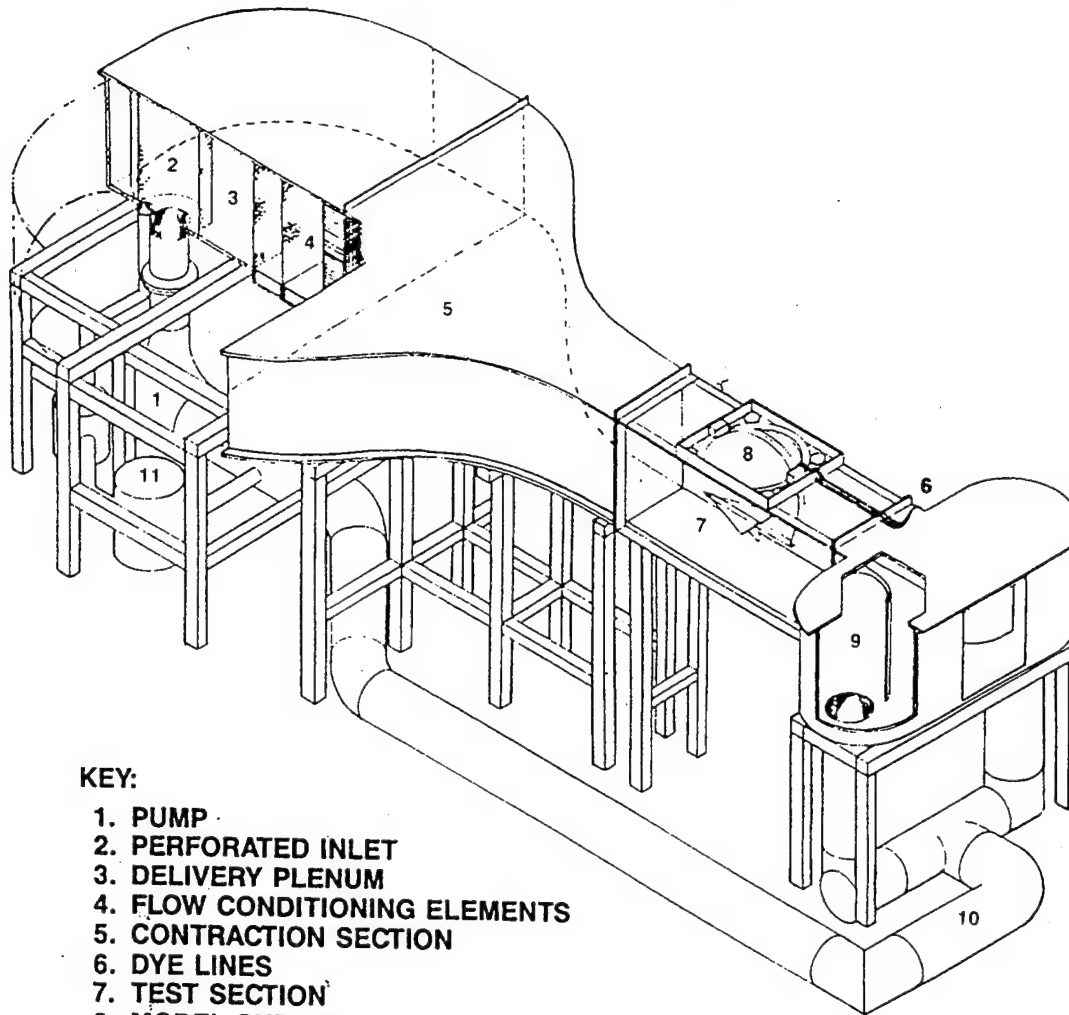
The experiments were carried out in the Naval Postgraduate School water tunnel facility, by Eidetics International, Inc., Model No 1520. This is a closed circuit, continuous flow facility with a contraction ratio of 6:1 and horizontal orientation. The test section is 38cm wide, 51cm high and 150cm long. Glass side walls, rear wall and bottom permit maximum optical access. There is no sealed top, thus providing simple access to the model. The side walls of the test section slightly diverge to compensate for boundary layer growth and to maintain uniform flow velocity. The flow velocity can be set in a range from 0 to 0.5 m/s. It is measured by a flow meter at the end of the test section and digitally displayed. Figure 1 depicts the layout of the water tunnel.

For flow visualization water soluble food coloring is used. Pressurized canisters for 6 different colors are available. The pressurization for the dye canisters is provided by a small compressor and a pressure regulator is used to control the pressure level. The dye is injected either through dye ports in the model or with a rake upstream of the model. The rake provides two individually routed lines with adjustable horizontal and vertical position.

B. SHAKER

A shaker is mounted vertically on top of the test section. A Model 113 ELEKTRO-SEIS shaker from APS Dynamics Inc. is used [Ref. 8]. This is a long stroke, light weight electrodynamic shaker. On its bottom end is the armature where differnt

EIDETICS INTERNATIONAL FLOW VISUALIZATION WATER TUNNEL



KEY:

- 1. PUMP
- 2. PERFORATED INLET
- 3. DELIVERY PLENUM
- 4. FLOW CONDITIONING ELEMENTS
- 5. CONTRACTION SECTION
- 6. DYE LINES
- 7. TEST SECTION
- 8. MODEL SUPPORT
- 9. DISCHARGE PLENUM
- 10. RETURN PIPING
- 11. FILTER SYSTEM

Figure 1. EIDETICS Model 1520 flow visualization water tunnel

models can be attached. The shaker is operated with an APS Model 114 amplifier [Ref. 9] and a frequency generator which can be varied in a range from 5Hz to 60Hz. The amplitude can be adjusted on both the power supply (rough) and the frequency generator (fine). However, it cannot be set to a constant value. For a fixed amplitude setting (fixed current) the actual amplitude is a function of the frequency. With increasing frequency the amplitude decreases. This is because the unit employs a permanent magnet and is configured such that the armature coil remains in a uniform magnetic field over the entire stroke range. It is fundamentally a force generator. If a constant amplitude is desired, the force must be increased with increasing frequency. Unless the force, i.e. the current, is increased the amplitude decreases with increasing frequency. The magnitude of the generated force is directly proportional to the instantaneous value of the current. Since the waveform of the current is sinusoidal, the waveforms of acceleration, velocity and displacement are sinusoidal as well.

C. AIRFOILS

Two different airfoils were used: most flow visualization experiments were conducted with a 1cm chord steel airfoil resembling a NACA 0010. For the LDV measurements, a wooden NACA 0012 airfoil with a chord of 10cm was used. Both airfoils have a wing span of 37 cm and stretch across the whole test section. The larger airfoil also has dye injection ports on both surfaces. Both airfoils are shown in Figure 2.

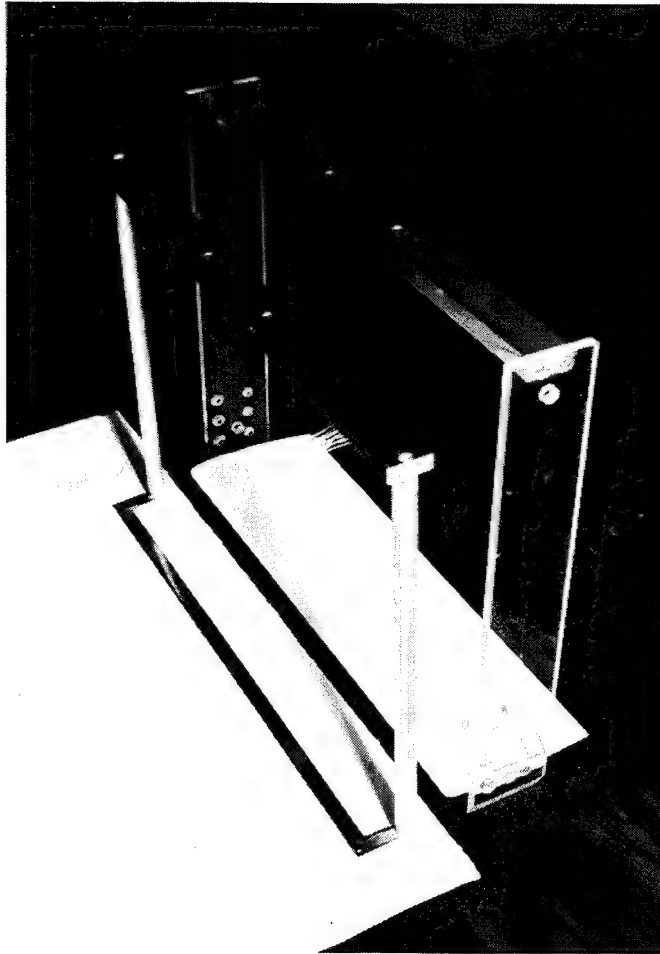


Figure 2. Airfoils $c = 10\text{mm}$ and $c = 100\text{mm}$

D. LASER

The LDV measurements are performed with an OMNICHROME Model 543-300A Argon Ion Laser with a maximum output of 300 mW. The OMNICHROME Model 160 power supply is used. The multiline argon beam is color-separated by a TSI Model 9201 Colorburst Multicolor Beam Separator [Ref. 10]. The three lines generated are green (514.5nm), blue (488.0nm), and violet (476.5nm). Frequency shift can be added to each color to allow measurements in reverse flow. Thus the beam separator outputs six laser beams. The TSI LV Frequency Shifter Model 9186 A-4 is used. It offers upshift and downshift from 2 KHz to 10MHz. Shifted and unshifted beams are transmitted by a TSI Model 9275 two-component fiberoptic probe system [Ref. 11], consisting of four Model 9271-D input couplers, four single mode polarization-preserving transmitting fibers, one multimode receiving fiber, the probe head and a junction box. In the probe head, the beams are collimated and focused with a transmitting lens. The beam separation is 50mm and the focal length is 350mm. The backscatter receiving optics focuses the scattered light onto the aperture of a TSI Model 9162 photomultiplier which is supplied by a TSI Model 916503 photomultiplier power supply. The signal processing is done by an IFA 550 Intelligent Flow Analyzer [Ref. 12] and the data are processed and displayed using the TSI Flow Information Display (FIND) software version 3.5 [Ref. 13]. The fiberoptic probe head is mounted on a LINTECH Model 41583 traverse table which allows movements in x-, y- and z-direction with an accuracy of 0.1mm. It is driven by an Applied Motion Products System 1618 supply unit. Figure 3 shows the water tunnel test section with shaker, traverse table and laser probe.

Since the existing setup provides only one photomultiplier, only one component measurements (in x-direction) using the blue beams were performed.

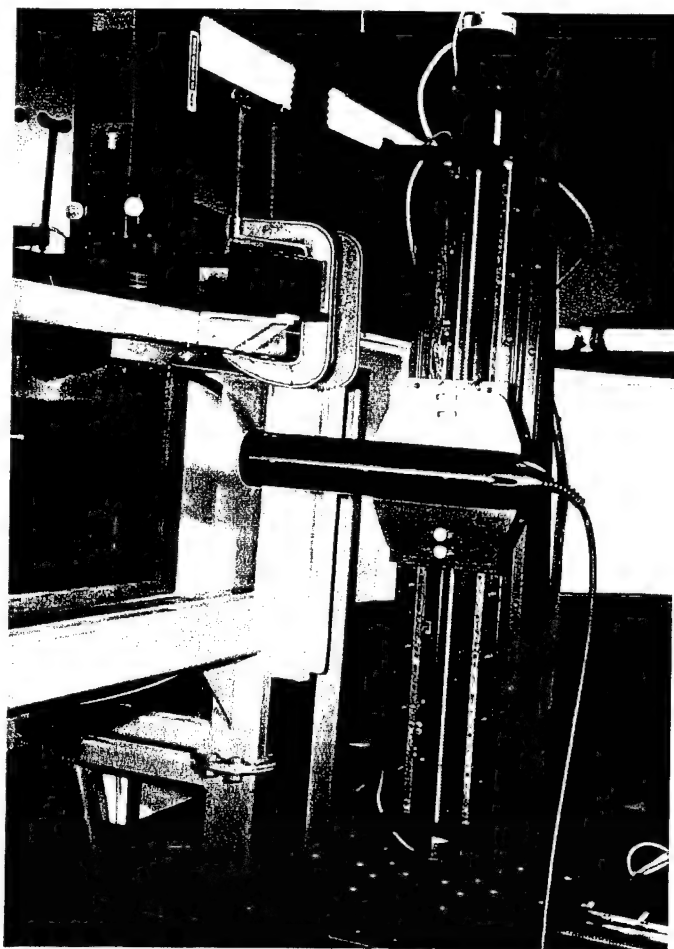


Figure 3. Water Tunnel test section with shaker, traverse table and laser probe

III. EXPERIMENTAL PROCEDURE

A. FLOW VELOCITY

The flow velocity in the water tunnel is set with a dial which allows settings from 0.00 to 9.99 with an accuracy of 0.01. This setting corresponds to a velocity range from 0 to approximately 0.5 m/s. The velocity is measured by a turbine flow meter at the end of the test section and digitally displayed in units ft/s. This flow meter has a poor sensitivity at low flow velocities. It measures the free stream velocity about 150 cm downstream of the position where the airfoils are mounted to the shaker. The actual flow velocity in the test section may be somewhat different, especially when large models or airfoils are used.

Prior to the experiments a calibration curve was set up which relates the velocity setting, the displayed velocity and the actual velocity in the test section. The calibration data are summarized in Table 1 and the calibration curve is shown in Figure 4. The calibration data slightly vary with deviations of the voltage that drives the pump and with the amount of water filled into the tunnel. Therefore all velocity data are backed up by LDV measurement.

Velocity Setting	Displayed Velocity [ft/s]	Actual Velocity [ft/s]	Actual Velocity [m/s]	Standard Deviation [m/s]	Error [%]
0.00	0.00	0.000	0.000		
0.20	0.00	0.016	0.005	0.003	
0.40	0.00	0.046	0.014	0.004	
0.60	0.02	0.082	0.025	0.004	-76
0.80	0.06	0.118	0.036	0.004	-49
1.00	0.10	0.148	0.045	0.004	-32
1.20	0.13	0.180	0.055	0.004	-28
1.40	0.17	0.217	0.066	0.004	-22
1.60	0.20	0.249	0.075	0.004	-20
1.80	0.24	0.282	0.086	0.004	-15
2.00	0.28	0.318	0.097	0.005	-12
2.20	0.32	0.354	0.108	0.005	-10
2.40	0.36	0.384	0.117	0.005	-6
2.60	0.40	0.419	0.128	0.006	-5
2.80	0.43	0.453	0.138	0.006	-5
3.00	0.47	0.490	0.148	0.006	-4
3.20	0.51	0.515	0.157	0.006	-1
3.40	0.55	0.548	0.167	0.005	0
3.60	0.58	0.587	0.179	0.006	-1
3.80	0.63	0.616	0.188	0.006	2
4.00	0.66	0.650	0.198	0.006	2
4.20	0.70	0.682	0.208	0.006	3
4.40	0.74	0.714	0.218	0.007	4
4.60	0.78	0.741	0.226	0.007	5
4.80	0.81	0.770	0.235	0.007	5
5.00	0.85	0.801	0.244	0.007	6
5.20	0.88	0.827	0.252	0.008	6
5.40	0.92	0.856	0.261	0.007	7
5.60	0.95	0.892	0.271	0.007	7
5.80	0.99	0.918	0.280	0.008	8
6.00	1.02	0.942	0.287	0.008	8

Table 1. Water tunnel calibration data

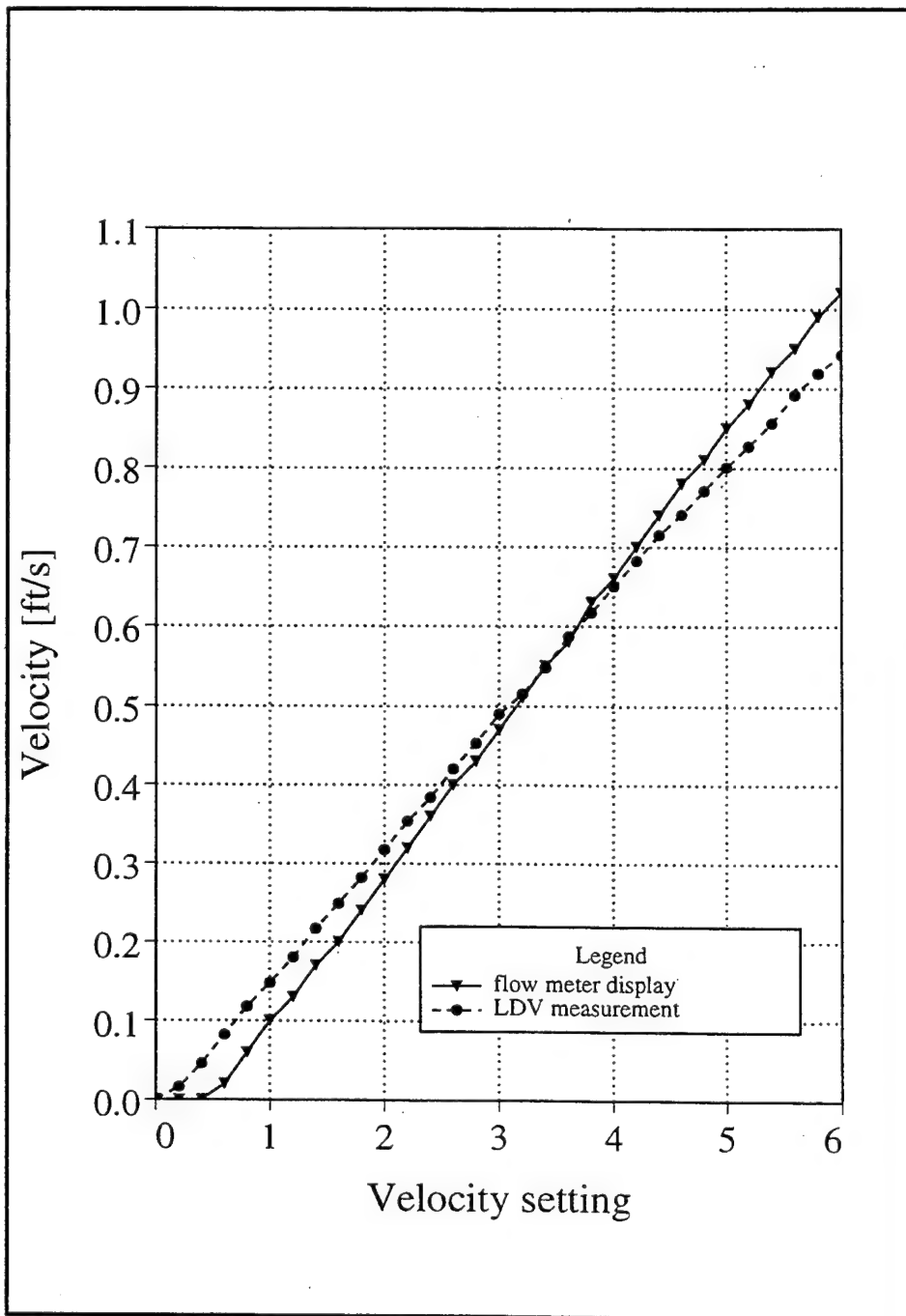


Figure 4. Water tunnel calibration curve

B. FREQUENCY

The frequency at which the shaker is operated is set on an analog dial on the frequency generator with a resolution of 1 Hz and a range from 5 Hz to 60 Hz. All experiments were carried out with frequencies between 5 Hz and 10 Hz. Larger frequencies produce very small vortices which make it difficult to measure the wake geometry. Furthermore, the wake patterns tend to become blurred at high frequencies.

All results are presented in terms of the reduced frequency k which is defined as

$$k = \frac{\omega \cdot c}{U}$$

where

$$\omega = 2\pi f$$

f = frequency in Hz

c = chordlength of the flapping airfoil

U = free stream velocity in the tunnel

High reduced frequencies are obtained with low flow velocities.

C. AMPLITUDE

The amplitude is set with a dial on the frequency generator which ranges from 1 to 10. The amplitude is measured from the writing of a fixed position pencil on a paper which is attached to the armature of the shaker. Later, this method was improved by using a sharp steel needle and a wax coated paper. Thus an accuracy of $\pm 0.25 \text{ mm} = 0.025 \text{ h/c}$ can be obtained. For a fixed amplitude setting, the amplitude was measured at least five times and a mean value is calculated. It is assumed that the airfoil performs the same

movement as the shaker armature. For the 1 cm chordlength airfoil this is true only for low frequencies (5 to 10 Hz). At higher frequencies the thin airfoil starts to bend and vibrate.

For a fixed amplitude setting the actual amplitude is a function of the frequency as explained in section II.B. Therefore constant amplitude measurements had to be done at a constant frequency.

All graphs and tables show the dimensionless amplitude h/c .

D. DYE INJECTION

Most experiments were done with one dye injection tube placed upstream of the flapping airfoil, horizontally leveled with the airfoil's zero position. The distance between the dye tube and the airfoil was varied in a range from a few millimeters to about 2 cm so that clear wake signatures were produced at the different flow velocities and amplitudes. Vortices originating from the lower surface during the downward motion and vortices originating from the upper surface during the upward motion can be clearly distinguished by their direction of rotation.

Some experiments were done with two dye injection tubes with red and green dye in order to visualize the clockwise and the counterclockwise rotating vortices in different colors. This procedure was successful as well, (see Appendix A, Figure 7A through 11A and 18A) however, adjusting the tubes was much more difficult and time consuming.

E. PHOTOGRAPHY

The vortical wake patterns are photographed with a 35 mm Nikon 2000 camera with manual focusing, manual aperture control and automatic shutter speed, mounted on a tripod. For all photographs a 100 ASA film for colour prints is used. The light is provided by one or more 600 watt floodlights as required.

F. VORTICAL WAVELENGTH

After every set of measurements and photographs a ruler was placed in the test section downstream of the airfoil location and photographed with unchanged camera position. The vortical wavelength is measured from the wake photographs using the photograph of the ruler. Figure 5 shows an example.

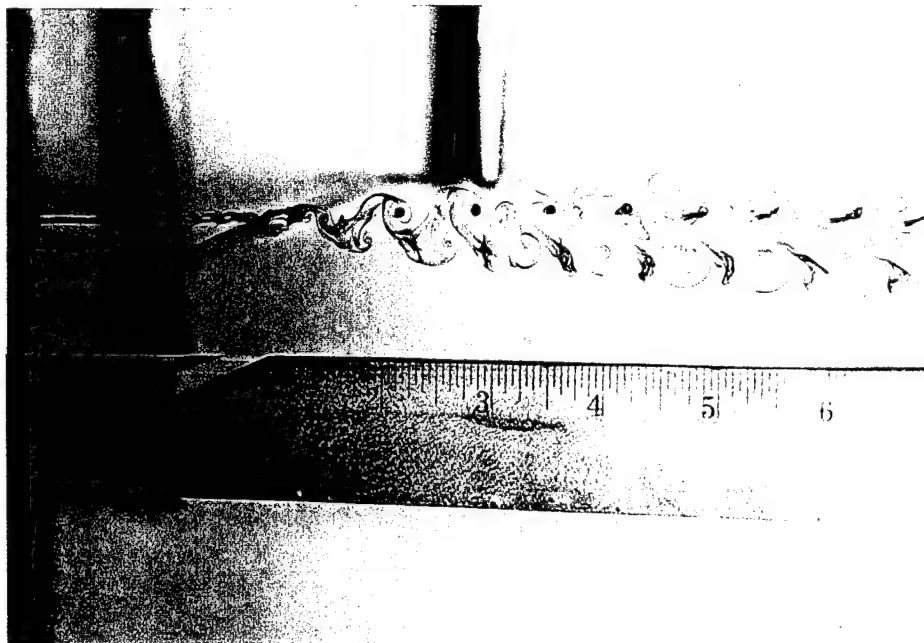


Figure 5. Measurement of the vortical wavelength

An accuracy of $1/32$ inch = 0.8 mm = 0.08 L/c is assumed. Whenever possible the mean value of the first three periods of fully developed vortices is calculated. If the vortical wavelength changes further downstream in the wake, it is not taken into account.

G. LASER DOPPLER VELOCIMETRY

The available LDV equipment is simple to use and does not need calibration, nevertheless some important points need to be considered:

1. Alignment of the fiberoptic input couplers

Both laser beams entering the test section must be of equal intensity. The higher the intensity, the better the data rate. Both - maximum intensity and equality - can be achieved by proper alignment of the fiberoptic input couplers. The x-, y- and z-position of the fiber entry must be adjusted to the beam that exits the colour separator. The TSI manual [Ref. 11] describes the procedure in detail.

2. Frequency shift

To obtain a good data rate at low flow velocities and to account for negative flow velocities a frequency shift of 100 KHz is applied. This means that 100 KHz is added to each measured Doppler frequency. The frequency shifter must be set to "100 KHz down" and in the Optics Configuration menu of the FIND software a frequency shift of 0.1 MHz must be entered.

3. Filter setting

According to the expected frequencies (=Doppler frequency + frequency shift) the filter setting for the flow analyzer must be chosen. 10 different settings are available in the Processor Setup menu of the FIND software:

100 Hz	-	1 KHz
300 Hz	-	3 KHz
1 KHz	-	10 KHz
3 KHz	-	30 KHz
10 KHz	-	100 KHz
30 KHz	-	300 KHz
100 KHz	-	1 MHz
300 KHz	-	3 MHz
1 MHz	-	10 MHz
3 MHz	-	15 MHz

Selected filter: 30 - 300 KHz.

The software also offers an automatic filter selection mode where the optimum filter setting is chosen according to the frequencies received.

4. Seeding

Seeding was not necessary. There were sufficient natural particles in the water to obtain a reasonable data rate. However, it was recognized that the data rate drops rapidly as the amount of dye in the water increases. Best results are obtained with clear water.

5. Sample Size and Data Rate

The Doppler bursts occur randomly. Therefore one has to decide how many samples shall be collected for one data point. The sample size is entered in the Realtime Histogram menu. Most measurements were done with a sample size of 200 or 400. The data rate is the number of valid samples collected per second. It is displayed in the Realtime Histogram window. The data rate varied between a few Hz for low flow velocities in dye polluted water up to 20 or 30 Hz for higher flow velocities and clear water. Thus the time for collecting the data was between a few seconds and a few minutes. When the airfoil is flapping at 5 Hz the velocity in the wake also varies at 5 Hz i.e. it has many periods within the data collection time span. Therefore the LDV measurements produce a mean velocity.

6. Alignment of the traverse table

Since the Laser precisely measures the velocity component that is perpendicular to the bisector of the angle formed by the two beams the traverse table has to be exactly aligned so that its front face is parallel to the test section side wall.

7. Accuracy

The standard deviations obtained for measurements with a stationary airfoil (Tables 33 through 36, Appendix B) indicate that the accuracy of the LDV measurements of the flow velocity is between three and four percent. Therefore it is assumed that the accuracy of the quotient u/U is between six and eight percent unless the error estimate based on half the least significant digits results in a bigger error.

H. MATRIX OF EXPERIMENTS

1. Vortical Wake Pictures

For observation and photography of vortical wake signatures experiments were carried out both with constant reduced frequency/variable amplitude and constant amplitude/variable reduced frequency.

a. Constant reduced frequency measurements

All measurements were done at a frequency of 5 Hz. The reduced frequency was set by choosing the flow velocity in the water tunnel. Table 2 shows the selected flow velocities, the resulting reduced frequency and Reynolds number, the amplitude range and the number of the relevant table and figure.

b. Constant amplitude measurements

Most measurements were done at a frequency of 5 Hz. One series was measured at a frequency of 10 Hz. The reduced frequency was varied by changing the flow velocity in the water tunnel. One series was measured at constant flow velocity and with a variable frequency between 5 Hz and 12 Hz. This was very complicated because it required a readjustment of the amplitude after every frequency change. This procedure is not recommended. Table 3 shows the selected amplitude and frequency, the range of flow velocity, reduced frequency and Reynolds number and the number of the relevant table and figure.

Table 4 shows the 119 evaluated combinations of reduced frequency and amplitude in one matrix.

velocity setting	velocity u [m/s]	reduced frequency k	Reynolds number Re	amplitude h/c	table No	figure No
2.10	0.105	3.0	1037	0.05-0.65	6	6A, 6B
1.60	0.077	4.1	760	0.01-0.35	7	7A, 7B
1.00	0.046	6.8	454	0.03-0.65	8	8A, 8B
0.80	0.037	8.6	365	0.03-0.65	9	9A, 9B
0.70	0.031	10.1	306	0.03-0.65	10	10A, 10B
0.60	0.025	12.3	247	0.03-0.65	11	11A, 11B

Table 2. Measurements at constant reduced frequency
frequency $f = 5$ Hz

amplitude h/c	frequency f [Hz]	velocity u [cm/s]	reduced frequency k	Reynolds number Re	table No	figure No
0.05	5	10.5- 1.0	3.0-32.2	1037- 99	13	13A, 13B
0.08	5	8.8- 0.5	3.6-64.4	869- 49	14	14A, 14B
0.12	5	8.8- 1.4	3.6-21.9	869- 138	16	16A, 16B
0.15	10	28.8- 4.6	2.2-13.7	2844- 454	17	17A, 17B
0.20	5	15.8- 4.6	2.0- 6.8	1560- 454	18	18A, 18B
0.40	5	28.8- 4.6	1.1- 6.8	2844- 454	19	19A, 19B
0.65	5	28.8-15.8	1.1- 2.0	2844-1560	20	20A, 20B
0.08	5-12	7.7	4.1- 9.7	760	15	15A, 14B

Table 3. Measurements at constant amplitude

Freq. k	Amplitude h/c													
	0.01	0.03	0.04	0.05	0.08	0.12	0.15	0.16	0.20	0.27	0.35	0.40	0.47	0.65
1.1												19		20
1.2												19		20
1.3												19		20
1.5												19		20
1.7												19		20
2.0									18			19		20
2.2							17							
2.4							17		18			19		
2.7							17							
3.0				0613		06	17		0618		06	19		06
3.4							17							
3.6					14	16								
4.0							17		18					
4.1	07	07		07	0715	0716		07	07		07	19		
4.7					14	16								
4.8							17							
4.9					15									
5.1				13										
5.3				13										
5.6					14	16								
5.7					15									
6.0							17		18					
6.5					15									
6.8		08		0813	0814	0816		08	0818	08	08	19	08	08
7.3					15									
7.6				13										
8.1					15		17							
8.6		09		0913	0914	0916		09	09	09	09		09	09
8.9					15									
9.7					15									
10.1		10		1013	10	10		10	10		10			10
11.1				13										
12.3		11	11	1113	1114	1116		11	11		11			11
13.7							17							
15.9				13										
21.9				13	14	16								
32.2				13	14									
64.4					14									

Table 4. Experimental Matrix
 first two digits: Fig.No. of measurements with constant reduced frequency
 second two digits: Fig.No. of measurements with constant amplitude

2. LDV Velocity Profiles

For the first LDV measurements the same airfoil was used as for the flow visualization experiments. Since the airfoil is mounted to a horizontal support strut located downstream only upstream velocity profiles were measured. The probe volume was vertically traversed 1 cm upstream of the leading edge. Velocity profiles were measured both with and without airfoil. When the first measurements revealed a dual mode behaviour of the flow, a measurement of the streamwise velocity distribution above and below the airfoil was added in order to find an explanation for this behavior.

For further LDV measurements a larger airfoil with 10 cm chord was used because

- it provided better optical access for the measurement of downstream velocity profiles.
- it was very stiff and thus guaranteed that the dual mode behaviour if observed again was not due to airfoil bending or vibration.
- it could be adjusted to different angles of attack. Two velocity profiles were measured at 10° AOA.

Table 5 shows all performed measurements and parameters.

airfoil	measure- ment No	AOA	ampl. h/c	freq. f [Hz]	velocity U [cm/s]	red. freq. k	x-pos.	y-pos. [cm]	Table No	Figure No
small c = 1cm	①	0°	0.12	5	0.85	37	-1c	-16...+10	23	28
			without airfoil		0.85		-1c	-10...+10	24	28
	②	0°	0..0.65	5	0.85	37	-1c	-1.5	25	29
	③	0°	0	0	10.5	0	-5c...+5c	+0.4	26	30
large c = 10cm	④	0°	0.35	5	0.9	35	-1c	-10...+10	27,28	31,32
	⑤	0°	0.04	5	9.0	35	-0.1c	-18...+14	29	33
		0°	0	0	9.0	0	-0.1c	-18...+14	30	33
	⑥	0°	0.04	5	8.6	36.5	-0.1c	-18...+14	31	33
		0°	0	0	8.6	0	-0.1c	-18...+14	32	33
	⑦	0°	0.04	5	21.0	15	-0.1c	-14...+14	33	34
		0°	0	0	21.0	0	-0.1c	-14...+14	33	34
	⑧	0°	0.04	5	21.0	15	1.4c	-14...+14	34	35
		0°	0	0	21.0	0	1.4c	-14...+14	34	35
	⑨	10°	0.04	5	21.0	15	-0.1c	-14...+14	35	36
		10°	0	0	21.0	0	-0.1c	-14...+14	35	36
	⑩	10°	0.04	5	21.0	15	1.4c	-14...+14	36	37
		10°	0	0	21.0	0	1.4c	-14...+14	36	37

Table 5. Summary of LDV measurements.
Origo of x-pos. and y-pos. coordinates is the leading edge of the airfoil

IV. RESULTS AND DISCUSSION

A. WAKE OF THE FLAPPING AIRFOIL

The wake photographs are shown in Appendix A. Figure 6A through 11A are each taken at a constant reduced frequency and show the changing wake pattern as the amplitude h/c is increased. Appendix A, Figure 13A through 20A are each taken at a constant amplitude and show the changing wake pattern as the reduced frequency is increased.

All Figures have some common features which are listed below. Some effects observed with increasing amplitude are similar to the effects of increasing reduced frequency while others are not as will be outlined.

- At low amplitudes a clear vortical pattern can be observed a long way downstream. With increasing amplitude (see Figure 9A) or increasing reduced frequency (see Figure 15A) the burst location moves upstream and finally only two or three discrete vortex pairs remain visible.
- The vortical pattern changes with increasing amplitude/increasing reduced frequency. For example see Figure 8A: at low amplitudes ($h/c=0.03$) the wake is basically symmetric. With increasing amplitude ($h/c=0.08$) remnant vorticity breaks off and finally ($h/c=0.20$) an asymmetric wake pattern develops. Typical asymmetric patterns are also found in Figure 9A($h/c=0.20$), 10A($h/c=0.16$), 11A($h/c=0.12$) and 16A($k=8.6$ and $k=12.3$)

- The vertical position of the cw and ccw vortices changes with increased amplitude/increased reduced frequency. For example see Figure 8A: the cw vortices are indicated by green dye which is ejected above the airfoil. The ccw vortices are indicated by red dye which is ejected below the airfoil. Initially ($h/c=0.05$) the green vortices (cw) stay above the red vortices (ccw). With increasing amplitude ($h/c=0.08$) both kinds of vortices get aligned horizontally and finally ($h/c=0.12$ through $h/c=0.20$) the red vortices (ccw) move above the green vortices (cw). The switching of the vertical position of the vortices can also be seen if only one color is used (for example see Figure 14A: $k=3.6$ cw=top, $k=8.6$ cw=bottom) and is essential for the drag/thrust classification which will be explained later.
- Some pictures show a downward orientation of the vortical pattern. For example see Figure 10A($h/c=0.03$), Figure 13A($k=15.9$ through $k=32.2$) and Figure 14A($k=12.3$ through $k=32.2$). This occurs due to settling of the dye especially at high reduced frequencies which are obtained with very low flow velocities in the tunnel and at low amplitudes i.e. when there is no thrust and no jet velocity.
- The vortical wavelength i.e. the horizontal spacing between vortices with the same direction of rotation obviously grows as the reduced frequency becomes smaller (for example see Figures 13A and 18A) or as the amplitude is increased (see Figure 9A).

The vortical wavelength, the drag/thrust classification and the development of an asymmetric wake are discussed in more detail in the following sections B through G.

B. VORTICAL WAVELENGTH AS FUNCTION OF AMPLITUDE

The experimental data from Table 6 to Table 11 are plotted as function of the amplitude and presented in Appendix A (Figure 6B through 11B). Figure 12 shows the vortical wavelength as function of the amplitude for the different reduced frequencies on one plot. For small reduced frequencies the vortical wavelength is a linear function of the amplitude. For higher reduced frequencies the linear relation only holds at large amplitudes. As the amplitude decreases the vortical wavelength rapidly drops towards zero. There is a maximum amplitude at which a vortical wake pattern can be observed. If this amplitude is exceeded the picture turns to extreme turbulence and reverse flow as observed in the water tunnel. The maximum amplitude decreases with increasing reduced frequency as shown in Table 12.

reduced frequency k	maximum amplitude h/c
3.0	0.65
6.8	0.47
8.6	0.47
10.1	0.35
12.3	0.35

Table 12. Maximum amplitude for vortical wake formation

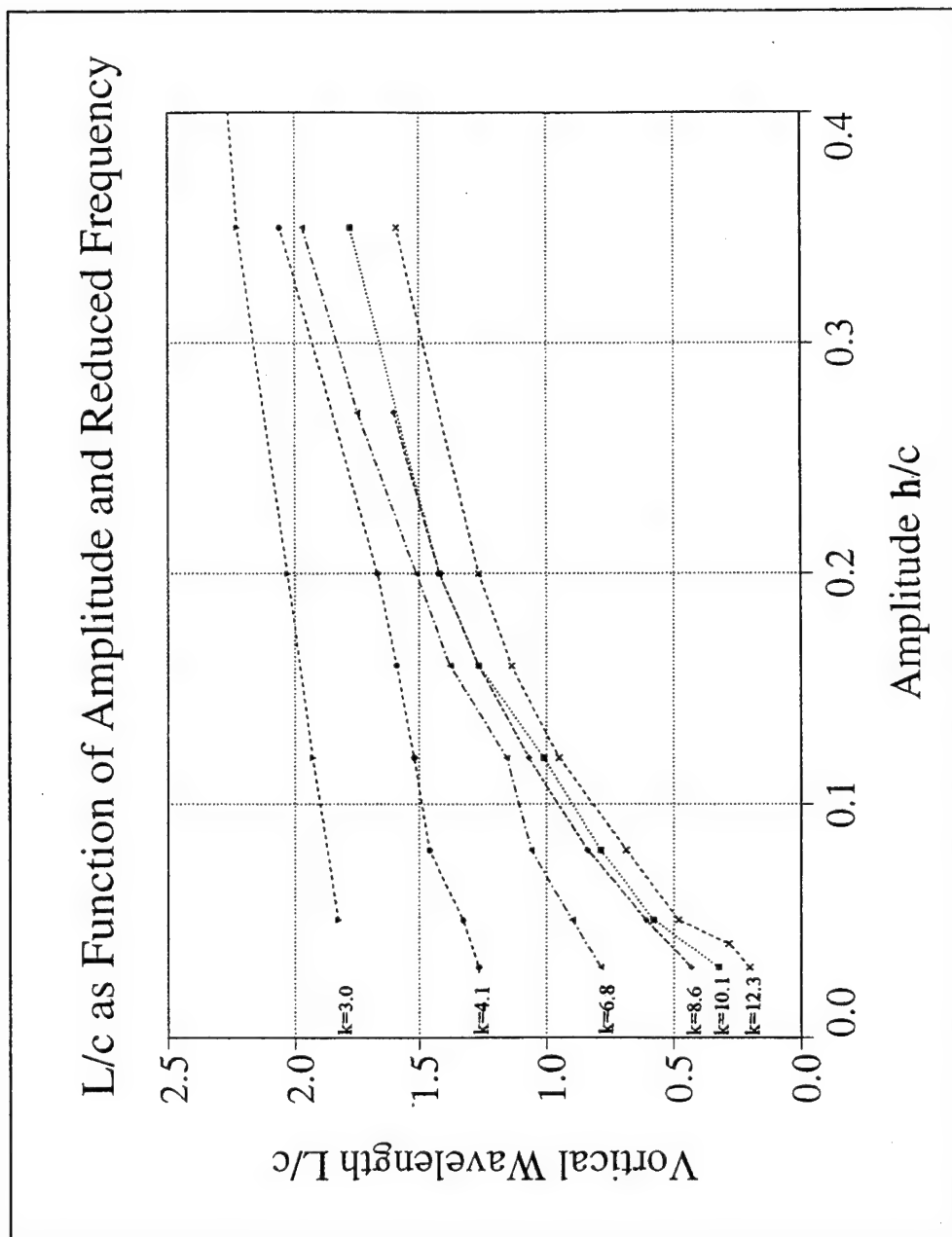


Figure 12. Vortical wavelength as function of the amplitude

C. VORTICAL WAVELENGTH AS FUNCTION OF FREQUENCY

The experimental data from Table 13 to Table 20 are plotted as function of the reduced frequency and presented in Appendix A (Figure 13B through 20B). Figure 21 shows the vortical wavelength as function of the reduced frequency for four different amplitudes on one plot. It shows that the vortical wavelength is inversely proportional to the reduced frequency. Figure 21 also shows the graph for $2\pi/k$ which represents the characteristic length for a periodic disturbance in a steady flow. It obviously is the limiting value for the vortical wavelength as the amplitude approaches zero. With increasing amplitude the deviation from the $2\pi/k$ -line and thus the vortical wavelength are increasing which corresponds to the results from the measurements at constant reduced frequency. Similar results have been reported by Koochesfahani [Ref. 3] for a pitching airfoil.

D. DOWNSTREAM VARIATION OF THE VORTICAL WAVELENGTH

A careful evaluation of the wake pictures reveals that the spacing between two vortices of same direction of rotation is not a constant. In some cases it changes as the vortices move downstream. Table 21 shows a comparison between initial and final wavelength of selected wake pictures. The wavelength is measured from the photograph and the ratio of the initial and the final (downstream) value is calculated. It can be seen that as the vortices travel downstream the wavelength becomes smaller in thrust type wakes and it becomes larger in drag type wakes. This behaviour is due to viscosity and the

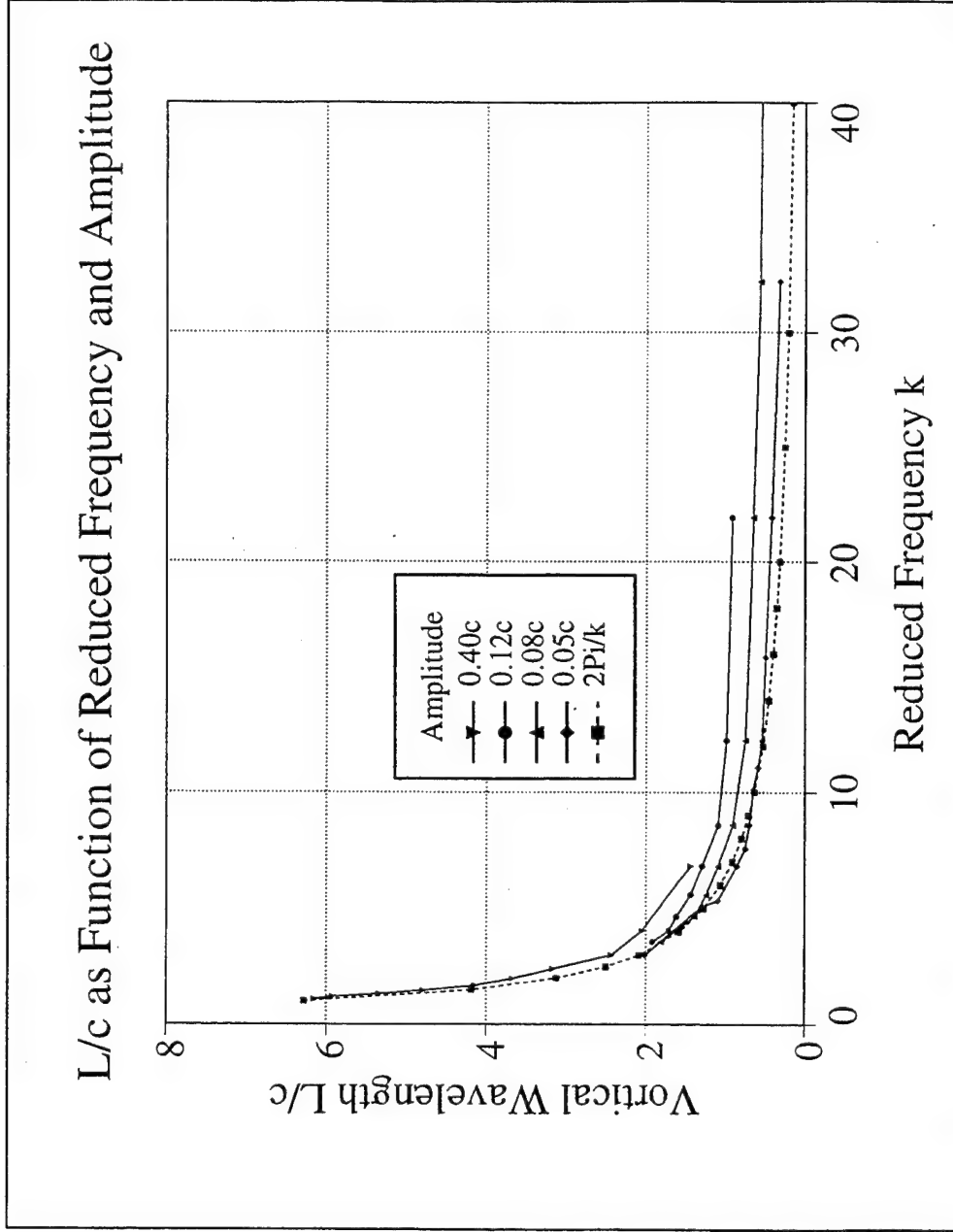


Figure 21. Vortical Wavelength as function of the reduced frequency

difference between wake velocity and free stream velocity. In a thrust type wake, friction gradually slows the wake velocity down and the vortices are compressed. In a drag type wake the velocity slowly increases until it reaches free stream velocity and the vortices are stretched.

figure No	reduced frequency k	amplitude h/c	$3 L_{\text{initial}}$ (vortices No 1 to 4) [mm]	$3 L_{\text{final}}$ [mm]	No of final vortices	ratio $L_{\text{fin}}/L_{\text{init}}$	wake type
054	3.0	0.05	3.50	4.00	6 to 9	1.14	drag
054	3.0	0.12	3.60	4.05	5 to 8	1.13	drag
062	4.1	0.01	2.30	2.65	6 to 9	1.15	drag
061	6.8	0.05	1.40	1.65	11 to 14	1.18	drag
061	6.8	0.12	1.95	1.80	11 to 14	0.92	thrust
073	8.6	0.03	0.80	1.00	25 to 28	1.25	drag
073	8.6	0.08	1.50	1.30	18 to 21	0.87	thrust
072	10.1	0.12	1.30	1.15	8 to 11	0.88	thrust
071	12.3	0.08	1.25	1.10	15 to 18	0.88	thrust

Table 21 Downstream variation of the vortical wavelength

E. DRAG/THRUST SIGNATURE

Thrust type and drag type of the vortex street can be clearly distinguished. The thrust type shows a top row of counterclockwise rotating vortices and a bottom row of clockwise rotating vortices, both inducing a downstream velocity component on each other. The drag type vortices are positioned the other way round, inducing an upstream velocity component on each other and eventually forming a vortex street similar to the Karman vortex street. Both regimes are separated by a signature where both kinds of vortices are horizontally aligned. The position of thrust, drag and neutral type wake signature as a function of reduced frequency and amplitude is shown in Figure 22. The separating line between the drag and the thrust regime is governed by the relationship

$$k \bullet \frac{h}{c} = const$$

F. COMPARISON WITH CALCULATION

Jones [Ref. 7] conducted computations of vortical wakes, using the unsteady potential flow code UPOT developed at the Naval Postgraduate School by Teng [Ref. 6]. It is a panel code that computes and plots inviscid, incompressible flows about arbitrary bodies performing defined plunging or pitching motions. From the wake plots the vortical wavelength is measured. Thirty wake plots were analyzed at reduced frequencies corresponding to the experiment ($k = 3.0, 4.1, 6.8, 8.6, 10.1, 12.3$) and at five amplitudes ($h/c = 0.025, 0.05, 0.1, 0.2, 0.3$). The evaluated wake plots are attached in Appendix C. The vortical wavelengths measured from the plots are shown in Table 22 (Appendix C) and added to Figures 6B through 11B (Appendix A). If the calculated wavelength is

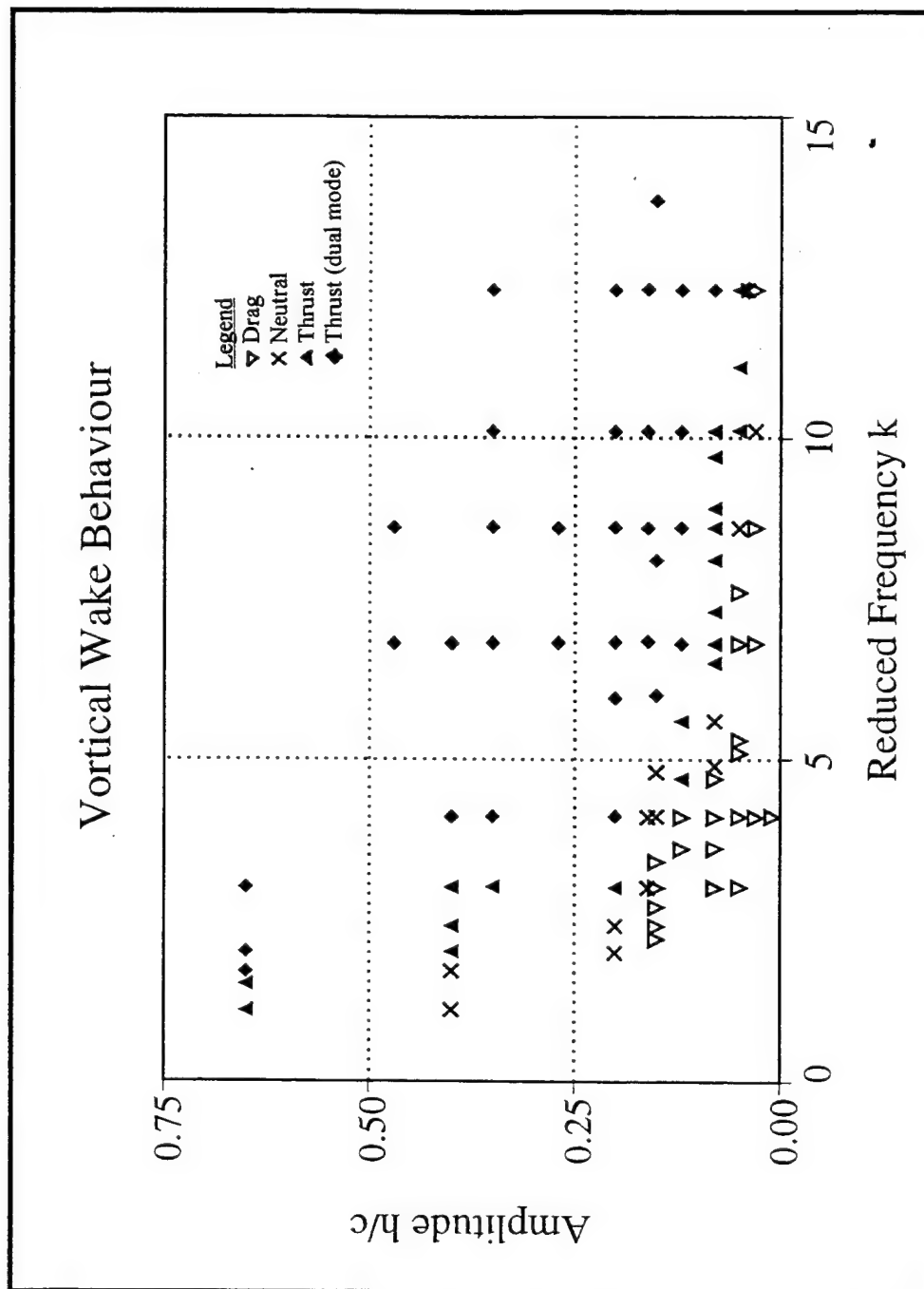


Figure 22. Vortical wake behavior of the flapping airfoil as function of reduced frequency and amplitude

extrapolated towards $h/c = 0$ it intersects the axis at $L/c = 2\pi/k$. This is in agreement with the results from section C. A comparison between calculated and experimental values of the vortical wavelength as function of the amplitude and the reduced frequency is shown in Figure 23 and 24. There is a good agreement between computed and measured values. This is surprising because the experiments were done at low Reynolds numbers ($Re=250...1000$). Obviously the vortical wake can be essentially treated as inviscid flow.

At low amplitudes and low frequencies the agreement between computed and measured values deteriorates and the experimental results show a shorter vortical wavelength than the computed results. With decreasing amplitude or decreasing frequency the thrust producing wake changes into a neutral wake and finally into a drag producing wake, where the wavelength becomes smaller than $2\pi/k$. However, the potential flow code assumes inviscid flow and cannot predict drag. Therefore it predicts a larger vortical wavelength.

A direct comparison between the photographs from the water tunnel experiments and the digital images from the panel code is shown in Figures 25 and 26 for $k = 3.0$ and $k = 6.8$ respectively and with $h/c = 0.2$.

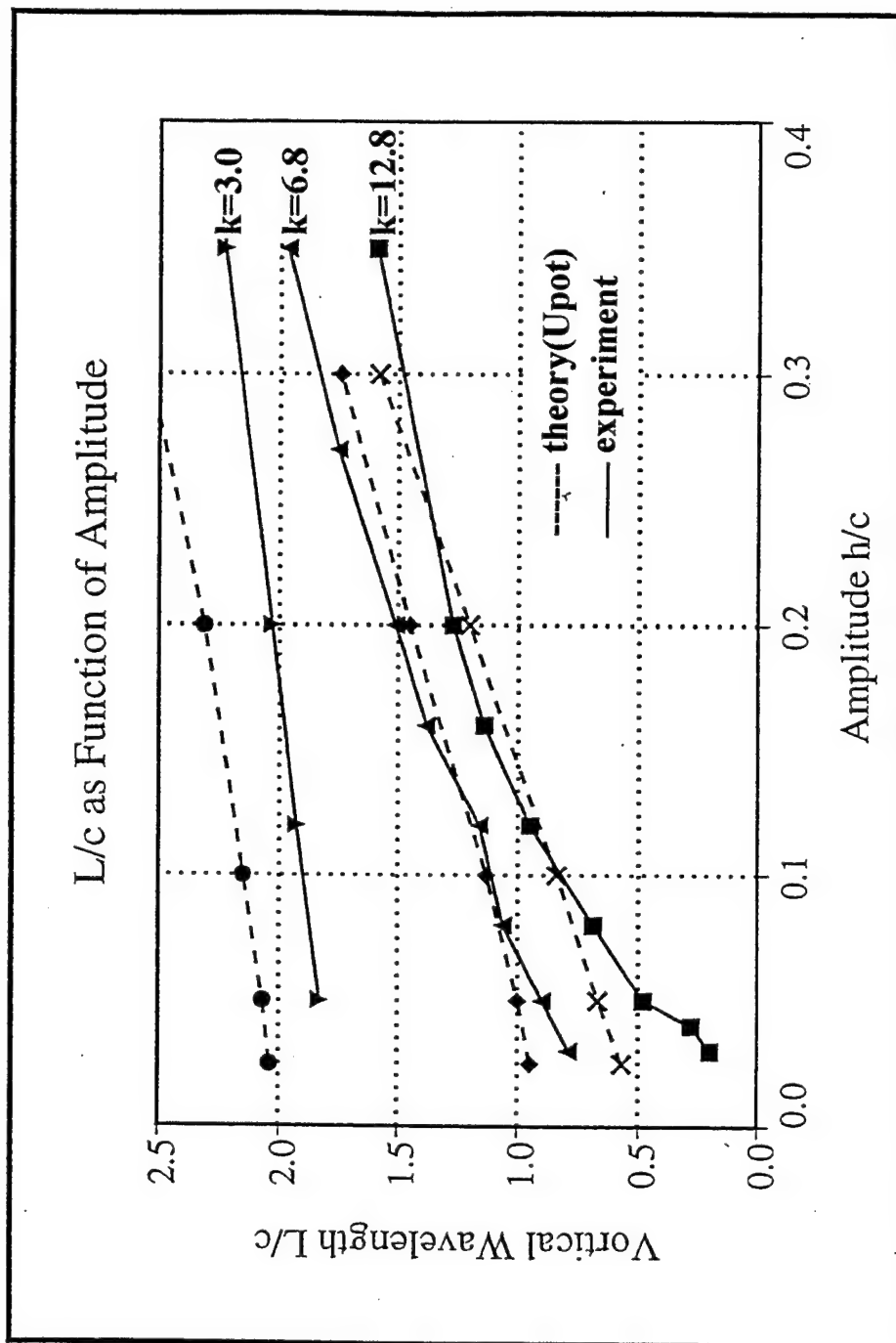


Figure 23. Vortical wavelength as function of the amplitude, comparison between measurements and theory

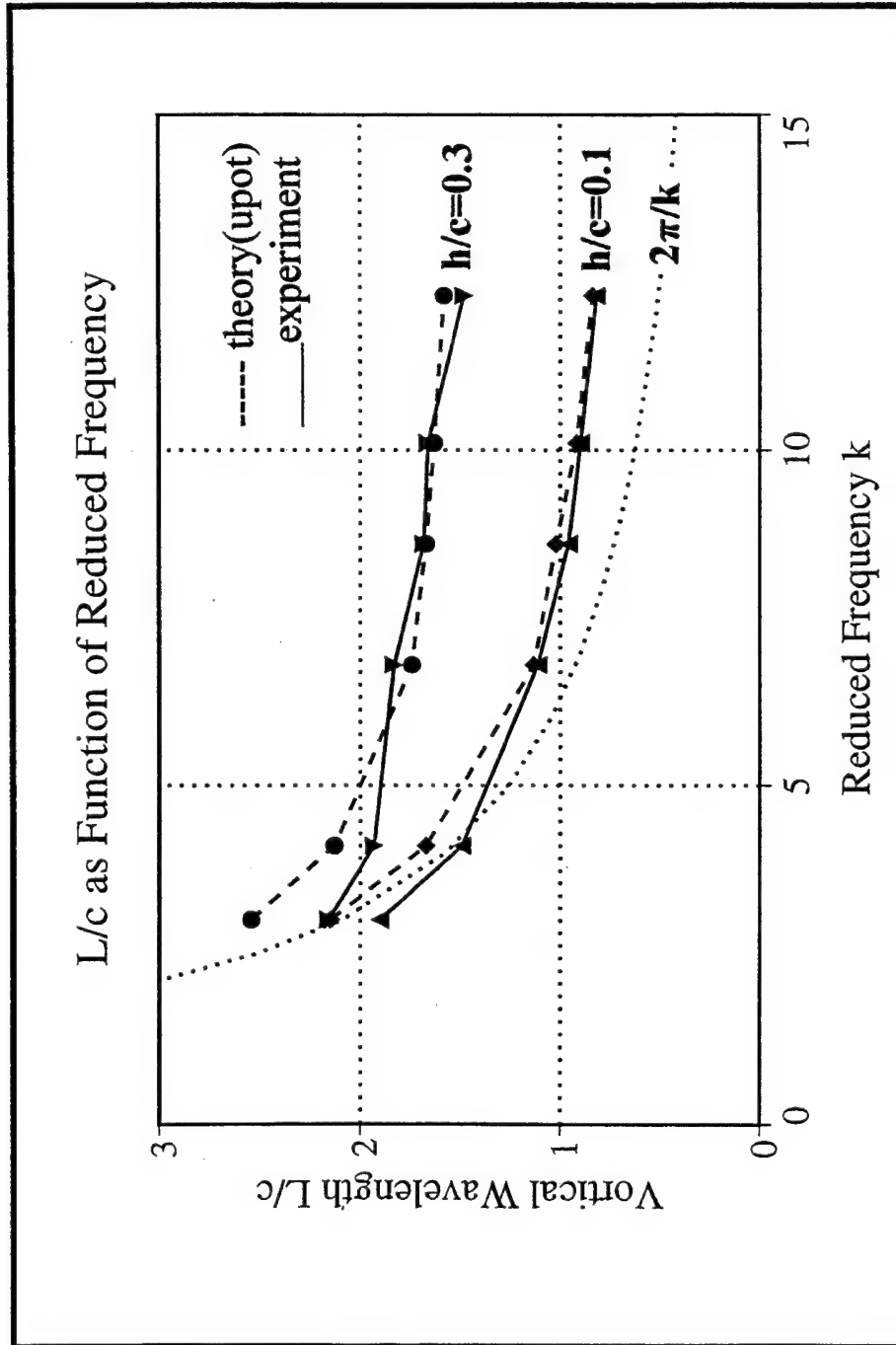


Figure 24. Vortical wavelength as function of the reduced frequency, comparison between measurements and theory

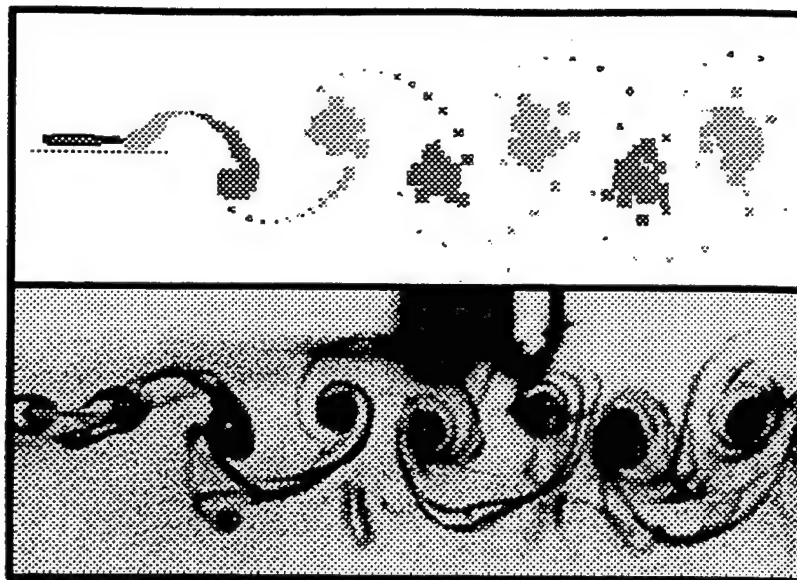


Figure 25. Wake comparison for $k=3.00$ and $h/c=0.2$

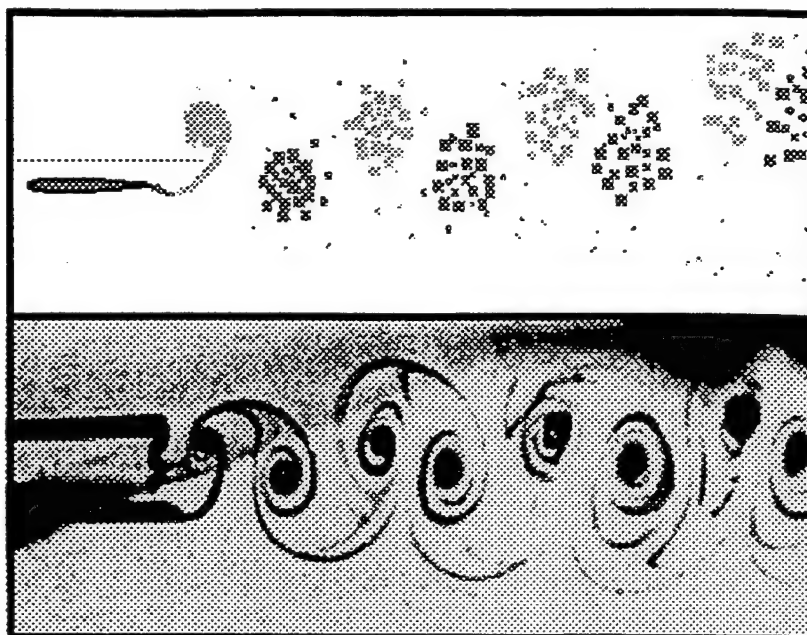


Figure 26. Wake comparison for $k=6.83$ and $h/c=0.2$

G. DUAL MODE BEHAVIOR

At low frequencies and low amplitudes the wake is symmetric about a horizontal centerline and the wake vortices are evenly spaced. As the frequency or the amplitude is increased the wake symmetry is lost. The vortices begin to form pairs and travel away from the centerline. As the vortex pairs travel up or down, small remnants of vorticity break off from the vortex pairs and travel down or up. Both upward and downward travel are observed. Figure 27 shows both modes for $k = 6.8$ and $h/c = 0.2$. The occurrence of both modes is observed randomly. It is possible to make the vortices switch from mode "up" to mode "down" and vice versa by generating a major upstream disturbance. According to Jones et al [Ref. 14] the dual mode behavior is also observed in the computed wake plots and the direction of travel is determined by the starting condition of the airfoil motion. All wake photographs are evaluated with respect to a dual mode behavior and the result is added to Tables 6 through 11 and 13 through 20 (Appendix B) and Figure 22. All wakes show a dual mode behavior at high values of $h \cdot k$, i.e. at high plunge velocities.

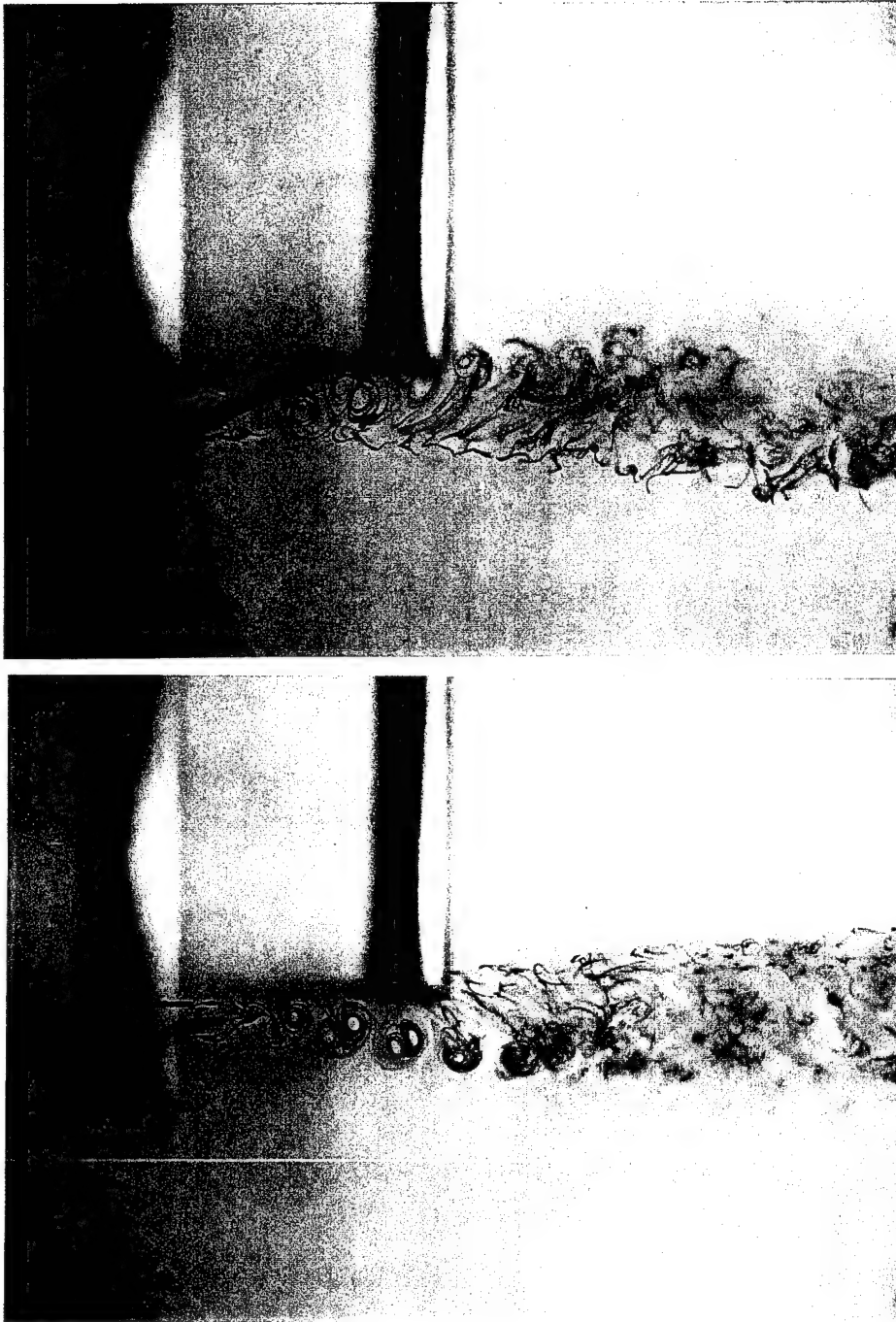


Figure 27. Dual mode behaviour of the vortical wake
top: mode "up", bottom: mode "down"

H. VELOCITY PROFILES

1. Small Airfoil (1 cm chord)

a. Measurement No 1 (upstream velocity profile)

Figure 28 shows the velocity profile 1 cm upstream of the leading edge of the flapping airfoil at $k = 35$, $h/c = 0.12$. and the free stream velocity measured without airfoil. It shows a peak ($u=1.5U$) as expected for a thrust producing airfoil, however it also shows a minimum of $0.7 U$ which was not expected. The location of the maximum and the minimum are displaced which may be due to the dual mode asymmetric wake behavior, which is to be expected at this frequency/ amplitude Since the maximum is located at $x = -15\text{mm}$ the mode is obviously "down".

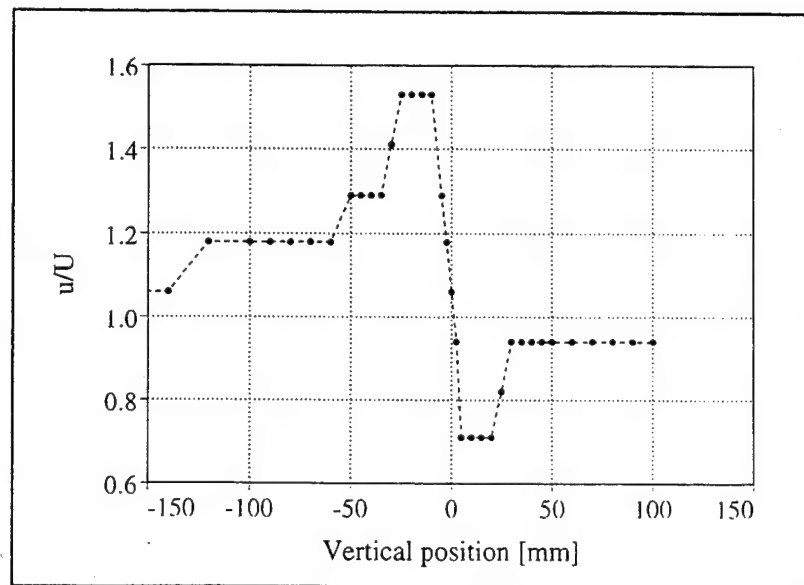


Figure 28. Velocity profile 10mm upstream of leading edge
 $c=10\text{mm}$, $h=\pm 0.12c$, $f=5\text{Hz}$, $k=35$, $U=8.5\text{mm/s}$

b. Measurement No 2 (velocity as function of the amplitude)

Figure 29 shows the velocity upstream of the airfoil as a function of the amplitude, measured at the location where the velocity showed a maximum in measurement No 1 ($x = -10$ mm, $y = -15$ mm). At $h/c = 0.35$ a maximum velocity of $2.44 U$ is attained. When the amplitude is further increased, the peak velocity drops again. The measurement was stopped at $h/c = 0.65$ because of airfoil bending vibration.

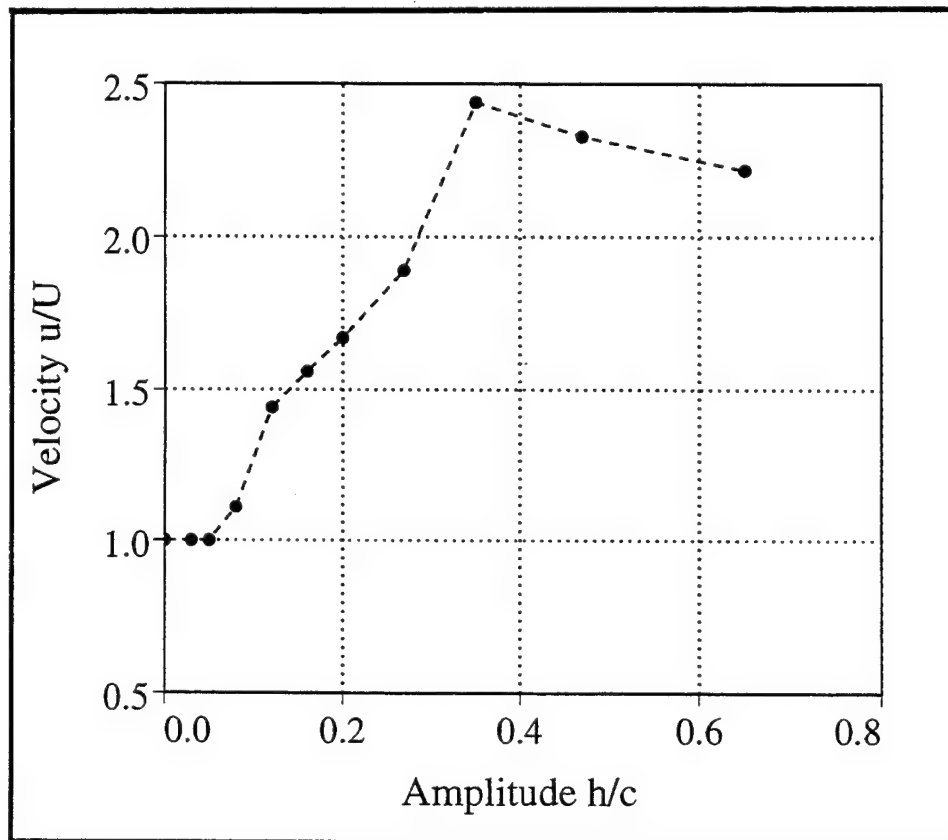


Figure 29. Velocity 10mm upstream of flapping airfoil leading edge as function of the amplitude h/c .

$c=10$ mm, $y=-15$ mm, $f=5$ Hz, $k=35$, $U=9$ mm/s

c. Measurement No 3 (velocity above and below of the airfoil)

Figure 30 shows the streamwise velocity distribution 4mm above and 4mm below the stationary airfoil. It shows a small increase in velocity above (1.05 U) and below (1.1 U) the airfoil. The difference between upper and lower surface may be due to a small negative angle of attack. It also shows a slight minimum of 0.98 U one chordlength upstream of the airfoil. Because of its small magnitude this minimum is not an explanation for the minimum velocity observed in measurement No 1.

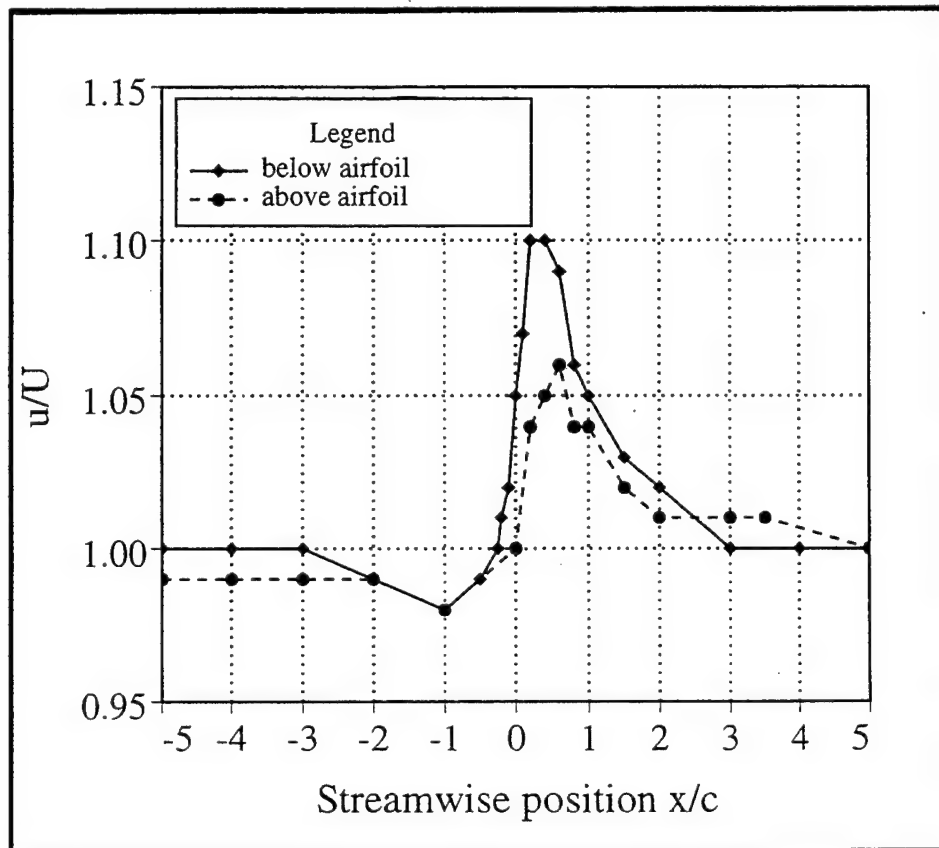


Figure 30. Streamwise velocity distribution above and below of the stationary airfoil, $c=10\text{mm}$, $y=\pm 4\text{mm}$, $U=10.5\text{cm/s}$.

d. Measurement No 4 (dual mode behavior)

Like in measurement No 1 the velocity profile was measured 1 cm upstream of the flapping airfoil, however the amplitude was increased to $h/c = 0.35$ which is according to measurement 2 the amplitude that produces maximum flow velocities. Figure 31 shows the data plotted from Table 27. The measurement started at $y = +100$ mm and the y-coordinate was decreased in 10 mm steps. There are two discontinuities in the graph: at $y = 80$ mm and at $y = -40$ mm. The wake structure has obviously switched from mode "down" to mode "up" and back again. In mode "down" the measurement was continued by increasing the y-coordinate again until it reached its original value $y = +100$ mm.

To verify the assumption of random mode switching the measurement was repeated with dye injection upstream of the airfoil. Figure 32 shows the data plotted from Table 28. Measurements started at $y = -100$ mm with positive increments. Again there is a discontinuity at $y = -40$ mm. The injected dye proved that the wake has switched from mode "up" to mode "down".

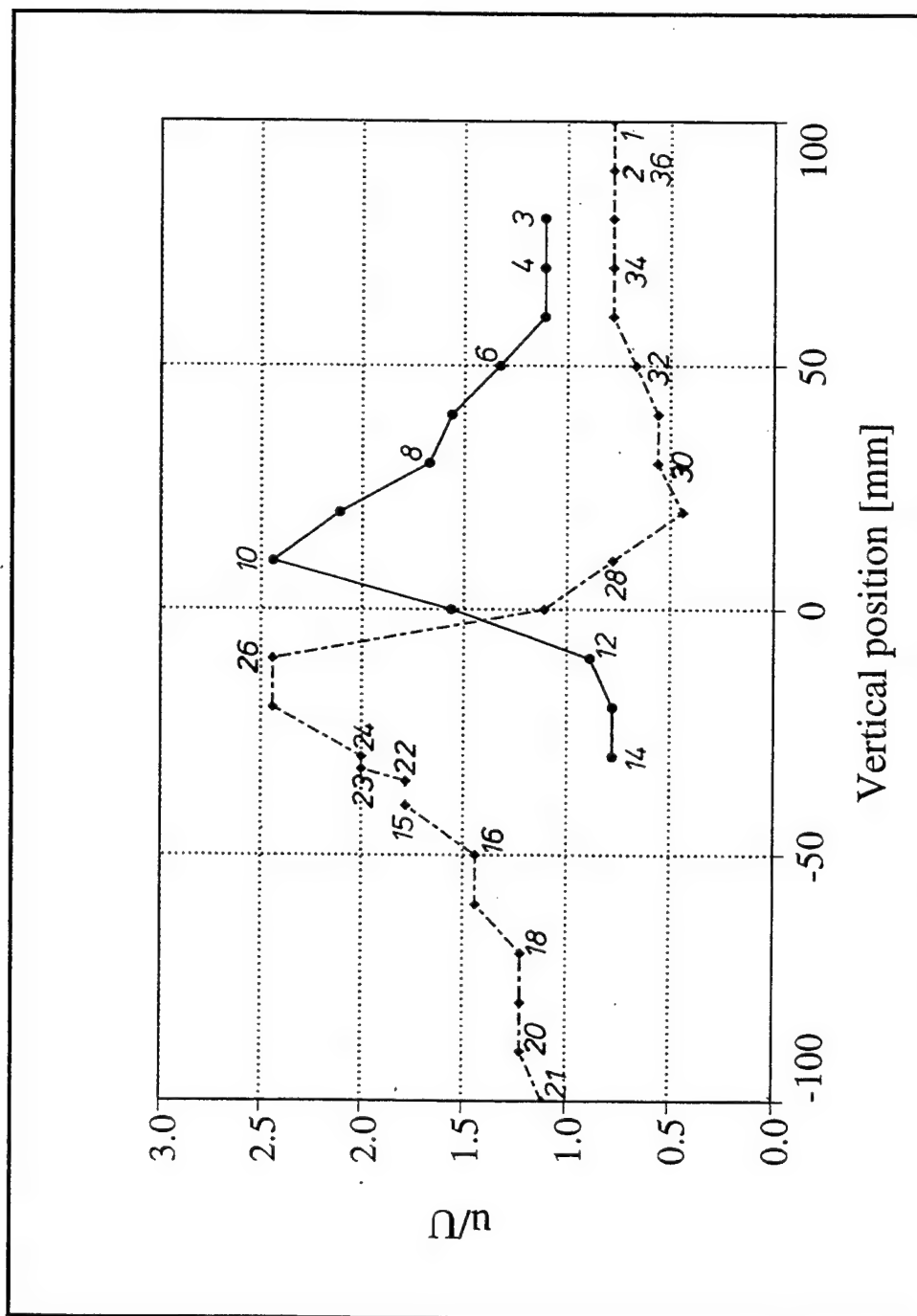


Figure 31. Velocity profile 10mm upstream of flapping airfoil leading edge, $c=10\text{mm}$, $h=0.35c$, $f=5\text{Hz}$, $k=35$, $U=9\text{mm/s}$,
 — = mode "up", ---- = mode "down", numbers indicate sequence of measurement

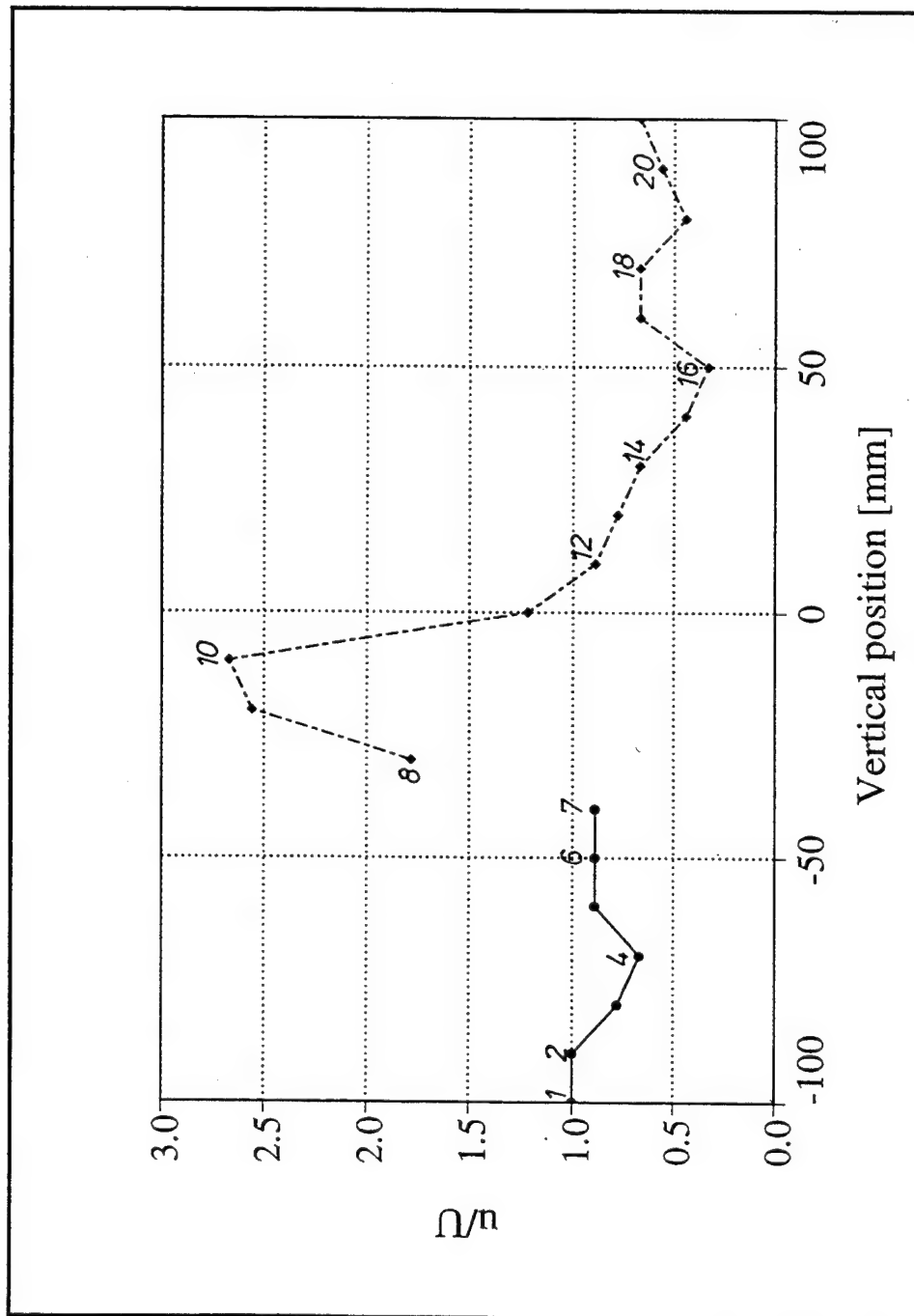


Figure 32. Velocity profile 10mm upstream of flapping airfoil leading edge, $c=10\text{mm}$, $h=0.35c$, $f=5\text{Hz}$, $k=35$, $U=9\text{mm/s}$,
 — = mode "up", - - - = mode "down", numbers indicate sequence of measurement

2. Large Airfoil (10 cm chord)

e. Measurements No 5 and No 6 (dual mode behavior)

Both measurements were made to confirm the observed dual mode upstream velocity profiles using a different airfoil. To obtain the same reduced frequency as in measurement No 4 the velocity was increased to 9.0 cm/s. The data from Table 29 through Table 32 are plotted in Figure 33. Again both modes can be clearly distinguished. (Mode "down" was measured at 8.6 cm/s due to a small drift of the free stream velocity.)

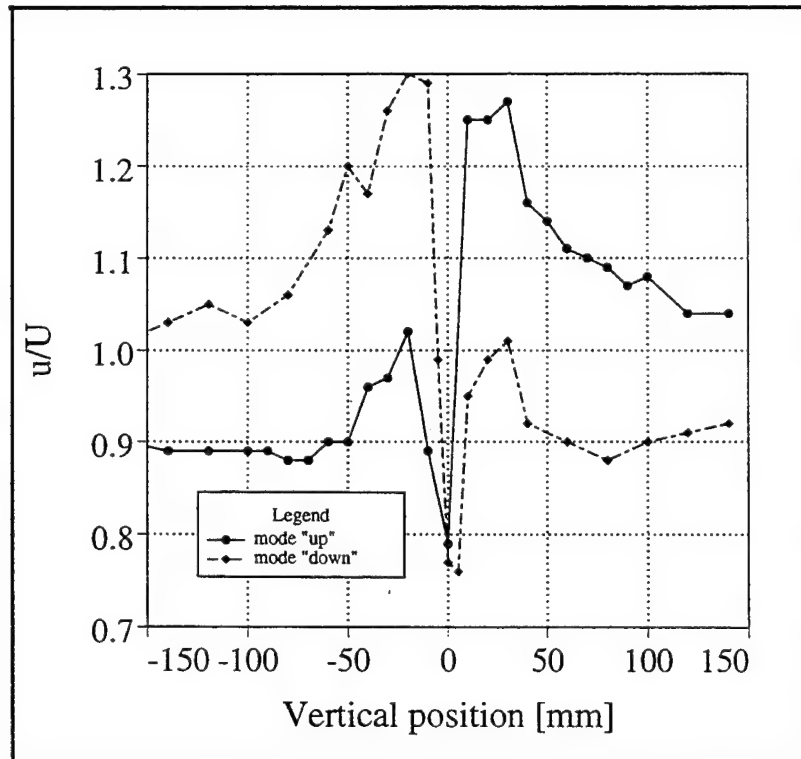


Figure 33. Velocity profiles 10mm upstream of airfoil leading edge, $c=100\text{mm}$, $h=0.04c$, $f=5\text{Hz}$, $k=35$ (36.5 for mode "down"), $U=9.0\text{cm/s}$ (8.6cm/s for mode "down")

f. Measurements No 7 and No 8 (symmetric wake)

Downstream velocity profiles were measured in addition to the upstream velocity profiles. The free stream velocity was increased to 21 cm/s to obtain a reduced frequency $k = 15$ which was small enough so that the wake no longer showed a dual mode behaviour. Figure 34 shows the upstream velocity profiles and Figure 35 shows the downstream velocity profiles both for the stationary and flapping airfoil. While there is only a small upstream effect, a jet velocity of $2U$ is observed in the wake.

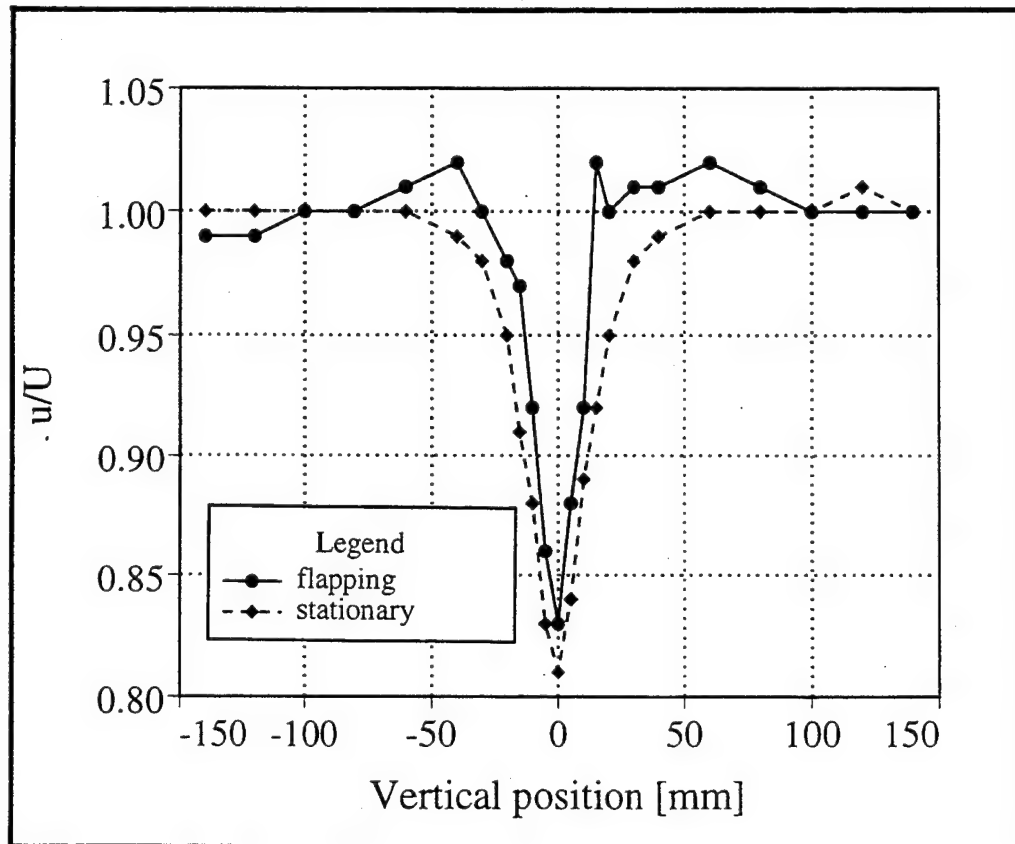


Figure 34. Velocity profiles 10mm upstream of airfoil leading edge,
 $c=100\text{mm}$, $h=0.04c$, $f=5\text{Hz}$, $k=15$, $U=21\text{cm/s}$

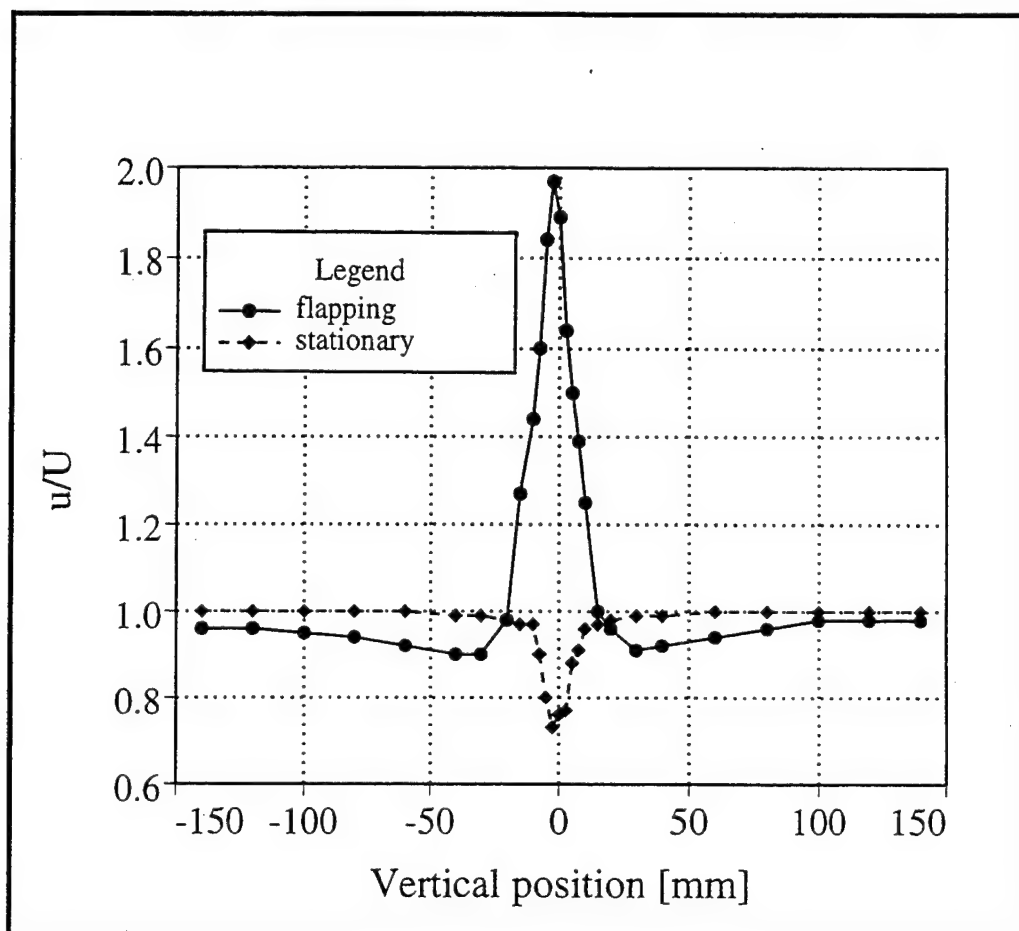


Figure 35. Velocity profiles 40mm downstream of airfoil trailing edge,
 $c=100\text{mm}$, $h=0.04c$, $f=5\text{Hz}$, $k=15$, $U=21\text{cm/s}$

g. Measurements No 9 and No 10 (airfoil with AOA)

Both measurements have the same parameters as measurements No 7 and No 8 except an angle of attack of 10° (pivot at $0.25c$). Figure 36 shows the upstream velocity profiles and Figure 37 the downstream velocity profiles both for the stationary and flapping airfoil. The flow is directed downward and the wake is displaced towards negative y coordinates (similar to mode "down") and the maximum in the upstream velocity profiles occurs at positive y -coordinates. The maximum jet velocity is $1.9 U$. It should be noted that the laser only measures the x -component of the velocity. So the total velocity may be larger since the velocity vector is directed downward.

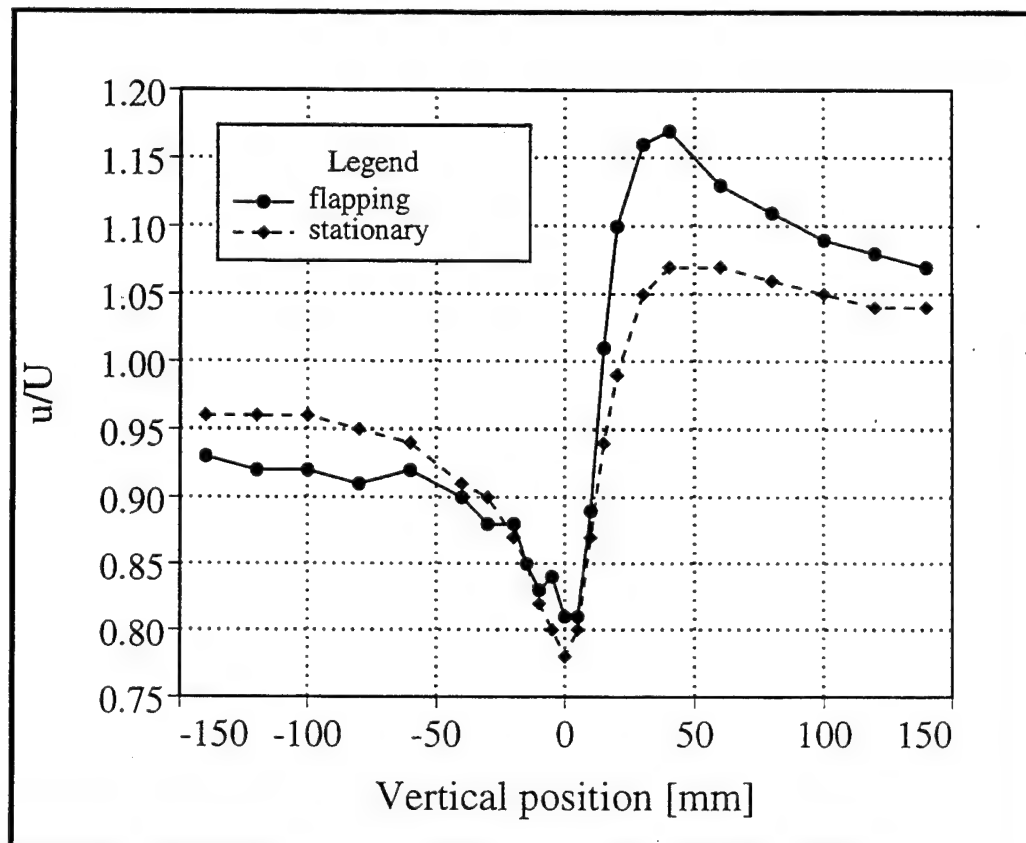


Figure 36. Velocity profiles 10mm upstream of airfoil leading edge,
AOA= 10° , $c=100\text{mm}$, $h=0.04c$, $f=5\text{Hz}$, $k=15$, $U=21\text{cm/s}$

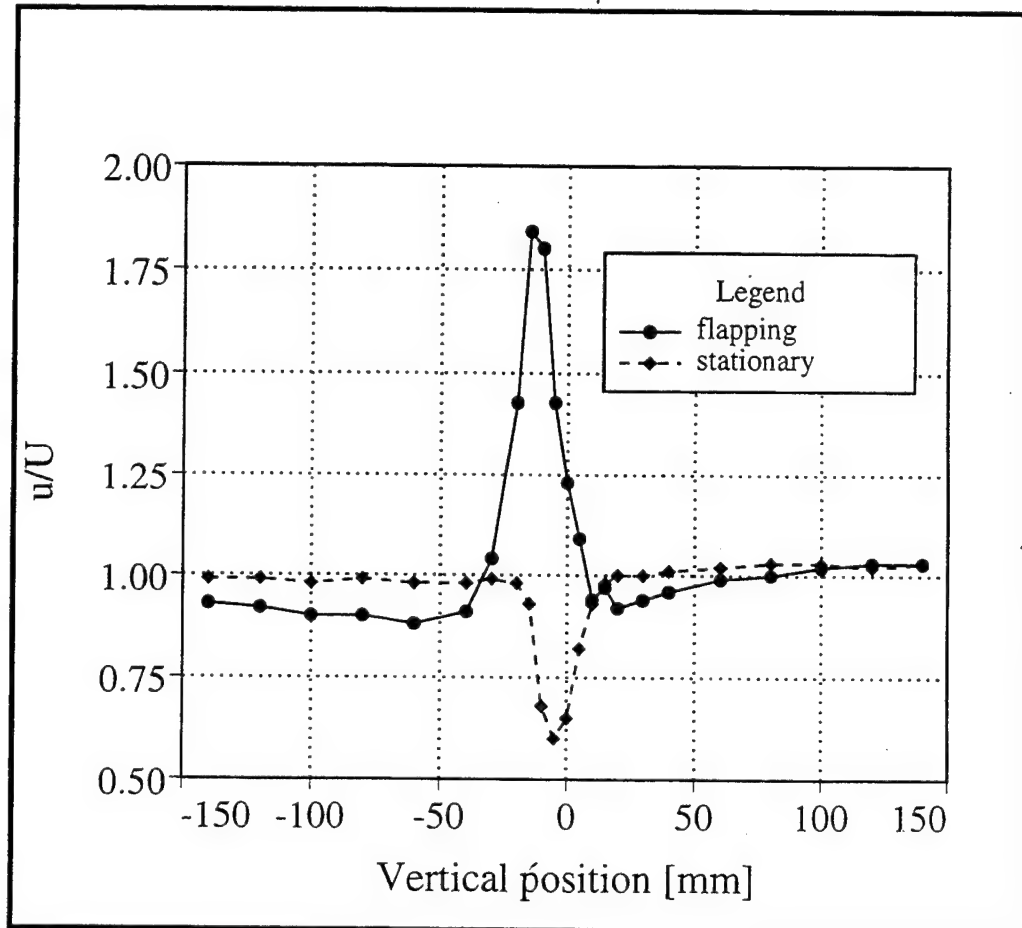


Figure 37. Velocity profiles 40mm downstream of airfoil trailing edge,
 $AOA=10^\circ$, $c=100\text{mm}$, $h=0.04c$, $f=5\text{Hz}$, $k=15$, $U=21\text{cm/s}$

V. CONCLUSIONS

The wake of a flapping airfoil has been examined in a water tunnel by means of flow visualization using colour dye injection. Laser velocimetry was used for measurements of the flowfield upstream and downstream of the flapping airfoil. The wake geometry was evaluated. Different vortical patterns for thrust or drag generating wakes can be clearly distinguished. At high reduced frequencies and high amplitudes the thrust generating wakes show a dual mode behavior. The thrust vector is deflected from the horizontal direction either upward or downward. There is some indication that the mode of deflection depends on the starting condition of the airfoil motion. However modes could also be manipulated by upstream disturbances and random mode switching has also been observed. Especially the 1cm airfoil tended to random switching while the 10cm airfoil showed a more stable behaviour. The regions of drag generation, thrust generation and dual mode behaviour were determined as function of the reduced frequency k and the amplitude h/c . They are separated by lines $(h/c) k = \text{const.}$ for a given airfoil.

Qualitative and quantitative comparisons were made between the observed wake pictures and the wake structure computed by the unsteady potential flow code UPOT. There is a good agreement between measured and computed wake geometries. The dual mode wake structure is also found in both approaches.

LDV measurements clearly showed the jet generated by a thrust producing flapping airfoil both upstream and downstream of the airfoil location. Mean streamwise velocity components of 2.5 times freestream velocity were observed at the upstream location ($h/c=0.35$, $k=35$) and of two times freestream velocity at the downstream location ($h/c=0.04$, $k=15$). The dual mode behaviour was also confirmed by the measured velocity profiles.

APPENDIX A.

WAKE PHOTOGRAPHS AND VORTICAL WAVELENGTH PLOTS

Figure 6A through 11A	Wake photographs from constant reduced frequency measurements
Figure 13A through 20A	Wake photographs from constant amplitude measurements
Figure 6B through 11B	Vortical wavelength plots from constant reduced frequency measurements
Figure 13B through 20B	Vortical wavelength plots from constant amplitude measurements

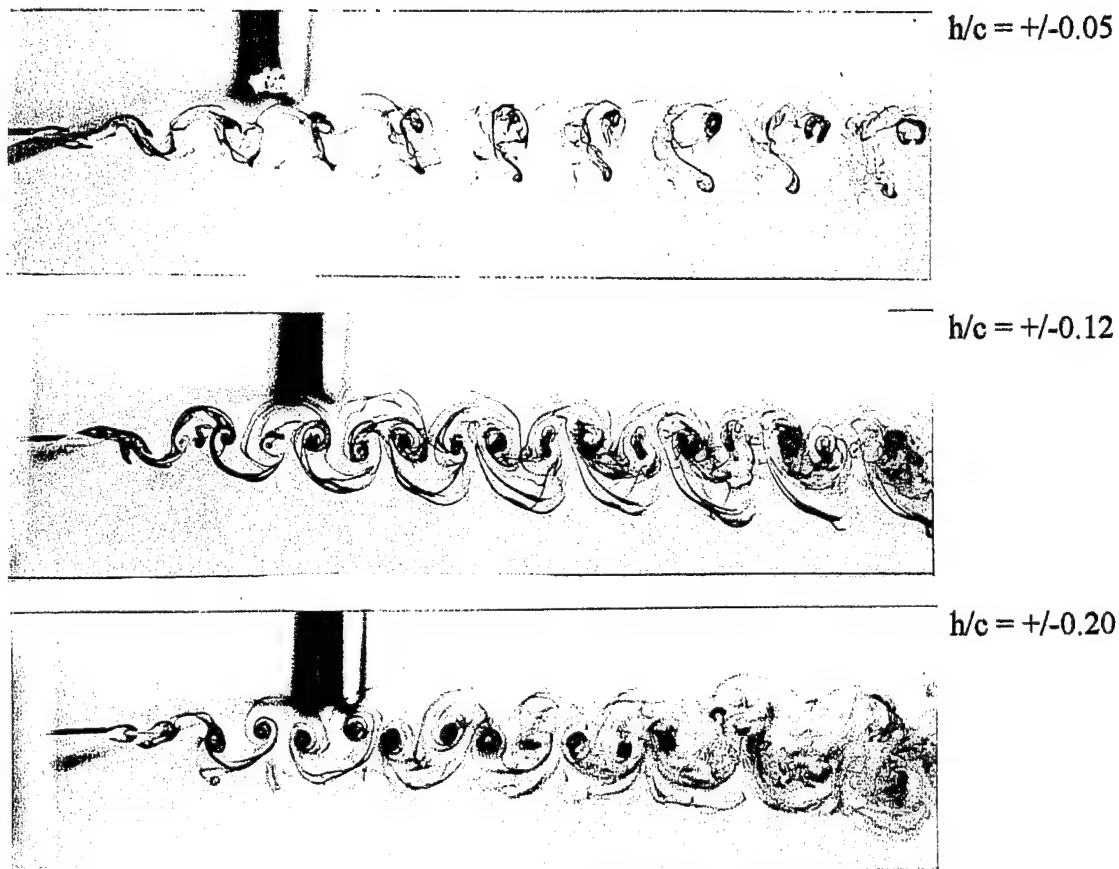


Figure 6A. Vortical Wake as Function of Amplitude h/c ,
 $f = 5\text{Hz}$, $u = 10.5\text{ cm/s}$, $k = 3.0$



$h/c = +/-0.35$



$h/c = +/-0.65$



$h/c = +/-0.65$

Figure 6A.(cont.) Vortical Wake as Function of Amplitude h/c
 $f = 5\text{Hz}$, $u = 10.5\text{ cm/s}$, $k = 3.0$

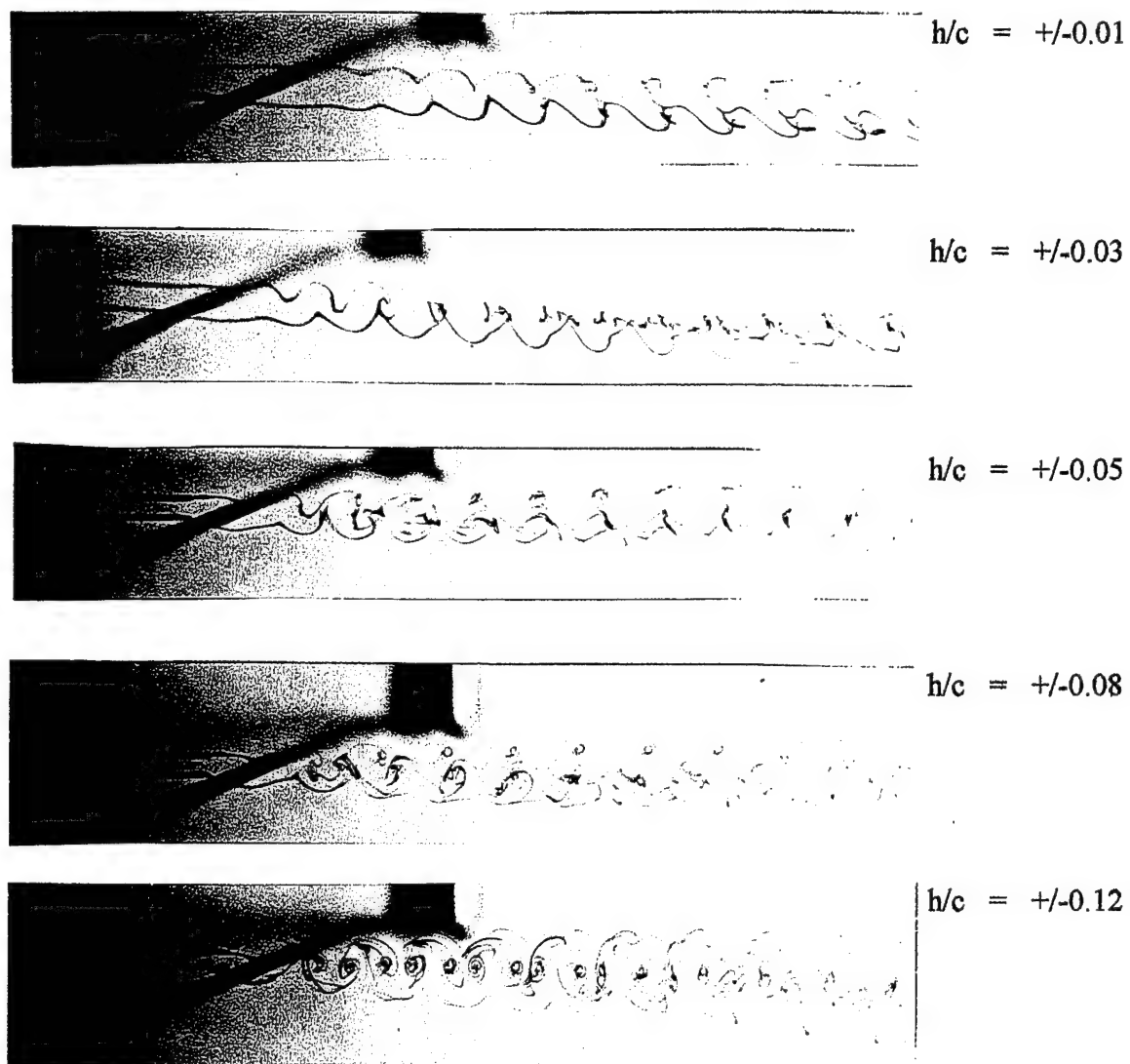
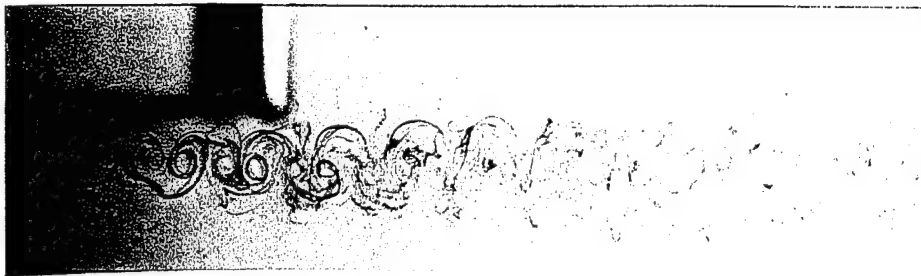


Figure 7A. Vortical Wake as Function of Amplitude h/c
 $f = 5\text{Hz}$, $u = 7.7\text{cm/s}$, $k = 4.1$



$h/c = \pm 0.16$



$h/c = \pm 0.20$



$h/c = \pm 0.35$

Figure 7A.(cont.) Vortical Wake as Function of Amplitude h/c
 $f = 5\text{Hz}$, $u = 7.7\text{cm/s}$, $k = 4.1$

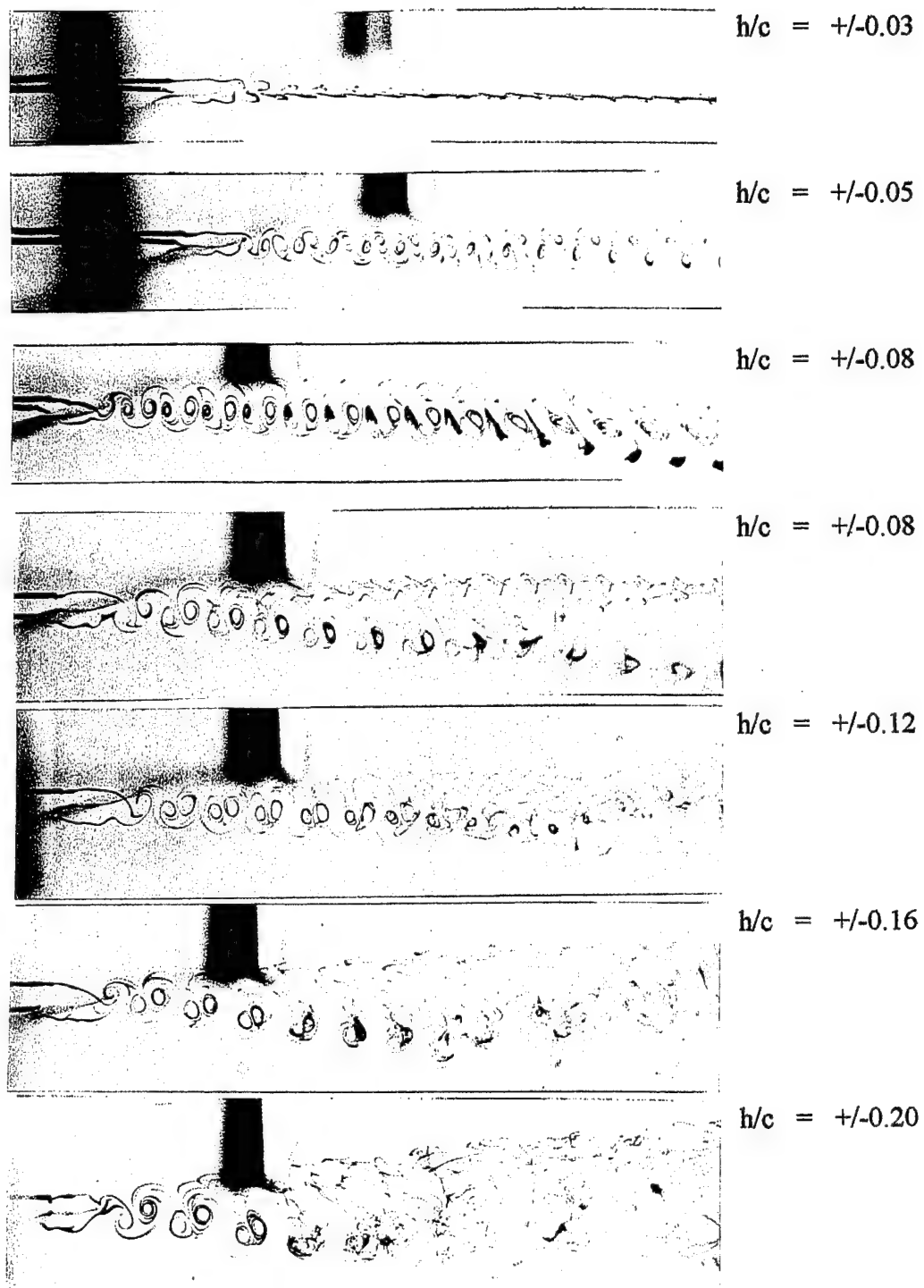


Figure 8A. Vortical Wake as Function of Amplitude h/c
 $f = 5\text{Hz}$, $u = 4.6\text{cm/s}$, $k = 6.8$

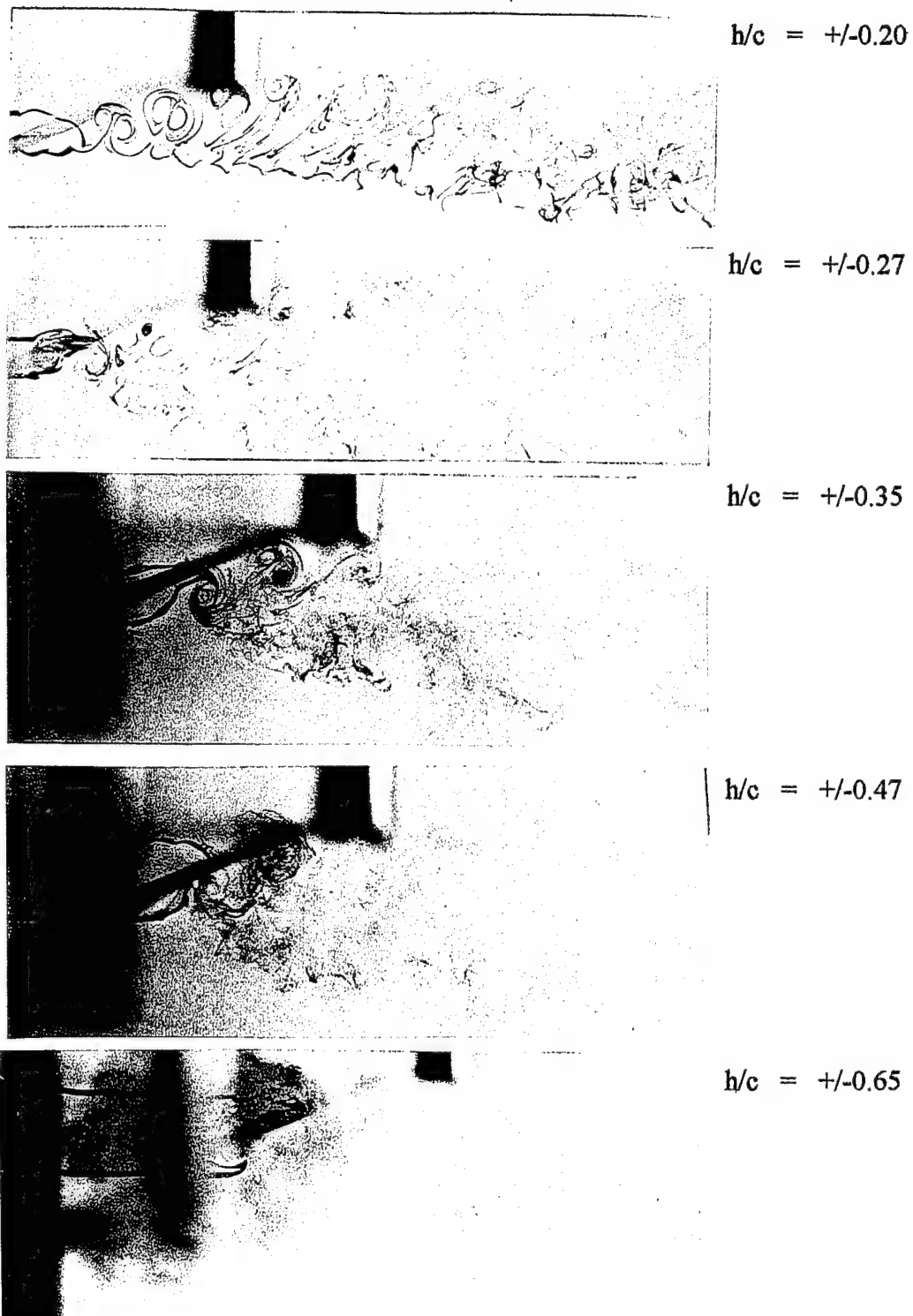


Figure 8A.(cont.) Vortical Wake as Function of Amplitude h/c
 $f = 5\text{Hz}$, $u = 4.6\text{cm/s}$, $k = 6.8$

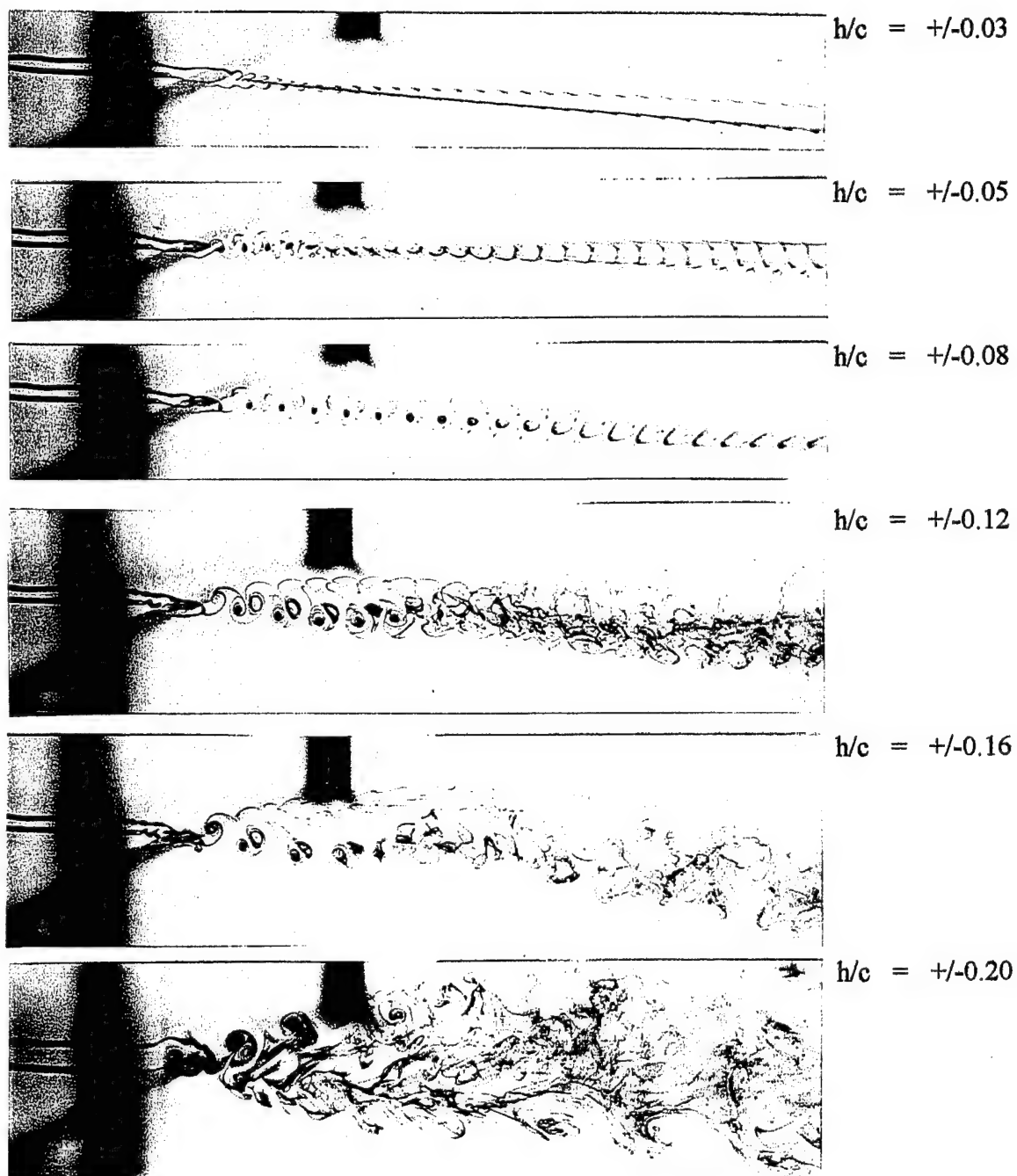
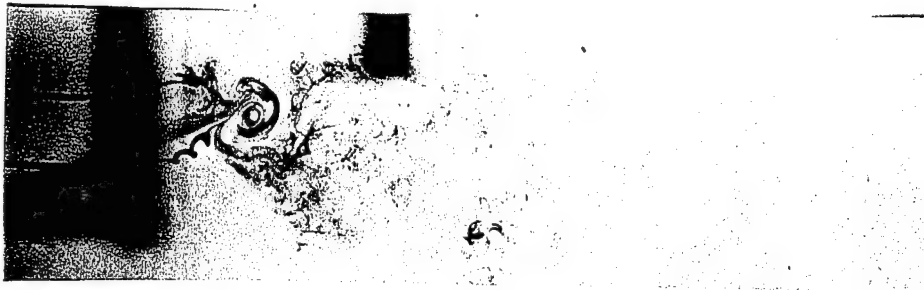


Figure 9A. Vortical Wake as Function of Amplitude h/c
 $f = 5\text{Hz}$, $u = 3.7\text{cm/s}$, $k = 8.6$



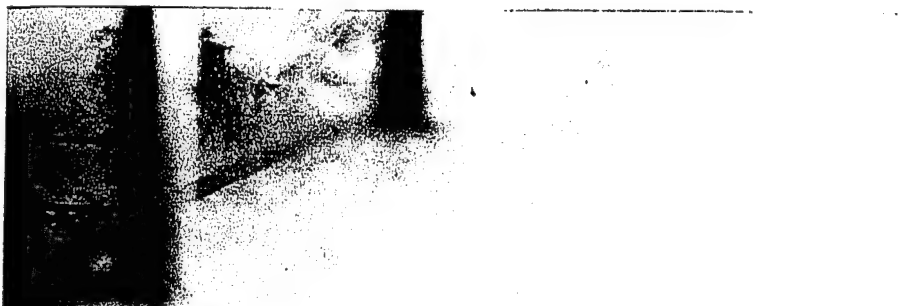
$h/c = +/-0.27$



$h/c = +/-0.35$



$h/c = +/-0.47$



$h/c = +/-0.65$

Figure 9A.(cont.) Vortical Wake as Function of Amplitude h/c
 $f = 5\text{Hz}$, $u = 3.7\text{ cm/s}$, $k = 8.6$

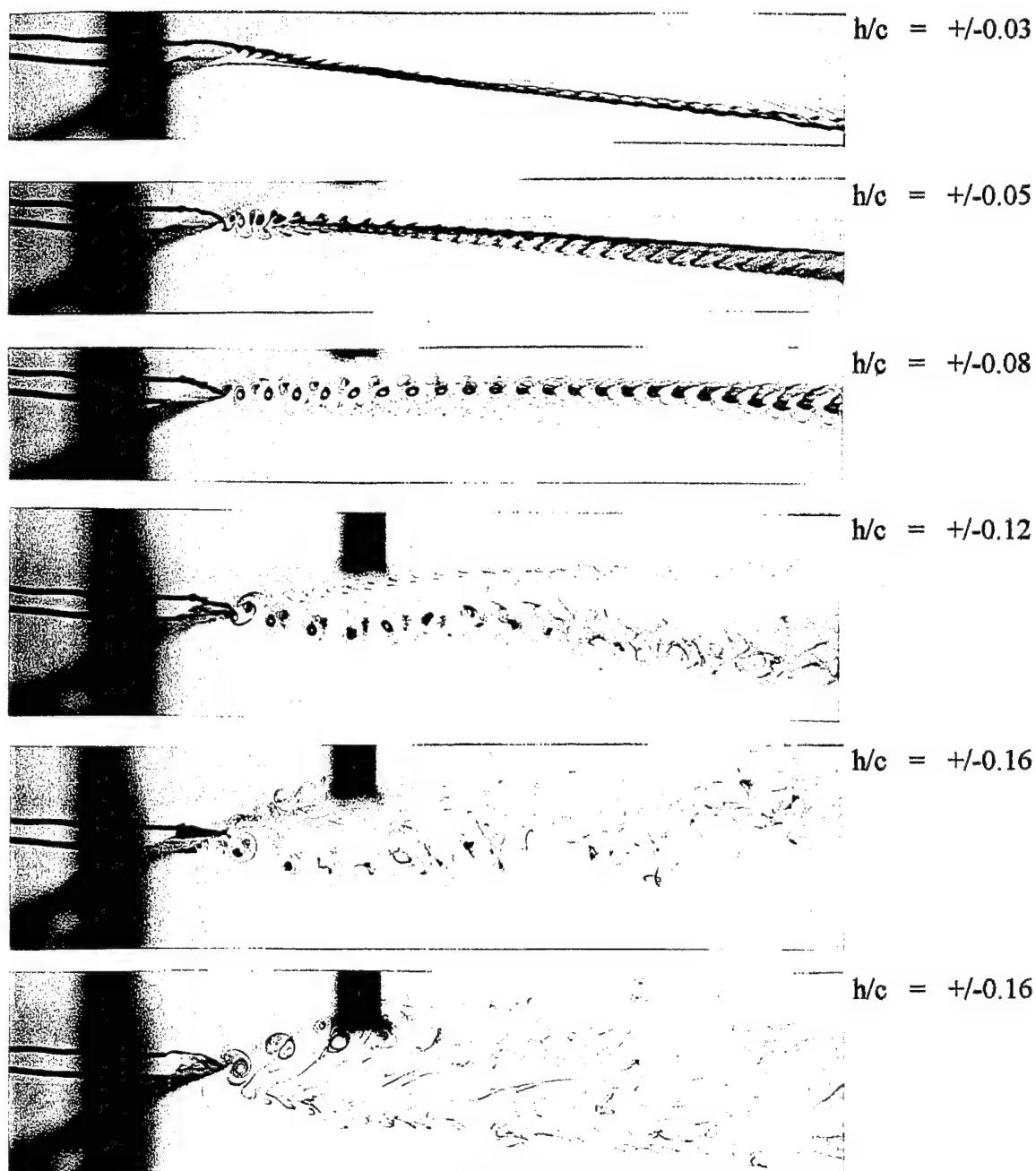
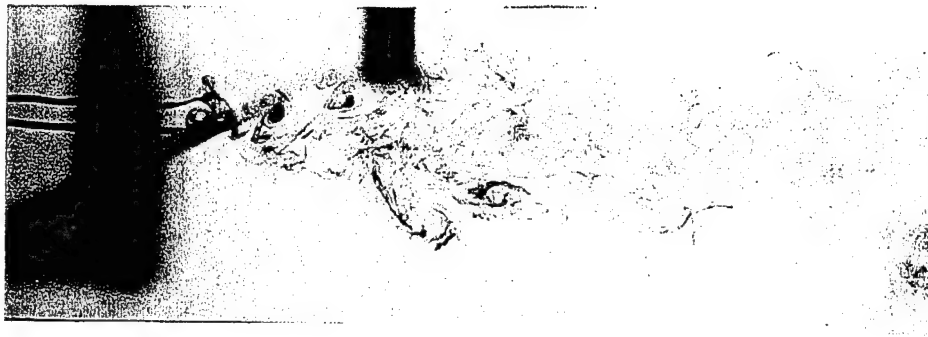
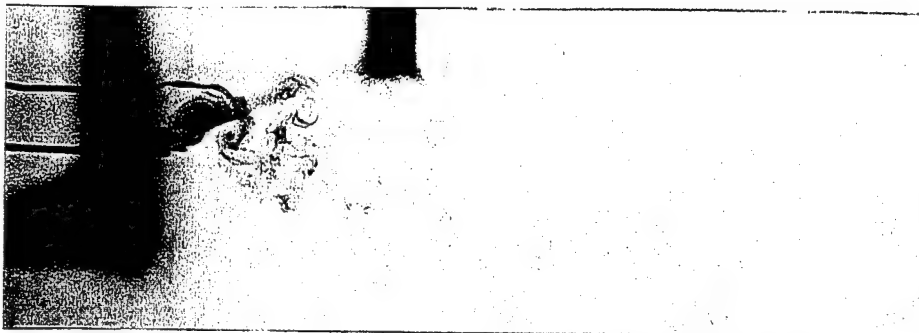


Figure 10A. Vortical Wake as Function of Amplitude h/c
 $f = 5\text{Hz}$, $u = 3.1\text{cm/s}$, $k = 10.1$



$h/c = +/-0.20$



$h/c = +/-0.35$



$h/c = +/-0.65$

Figure 10A.(cont.) Vortical Wake as Function of Amplitude h/c
 $f = 5\text{Hz}$, $u = 3.1\text{cm/s}$, $k = 10.1$

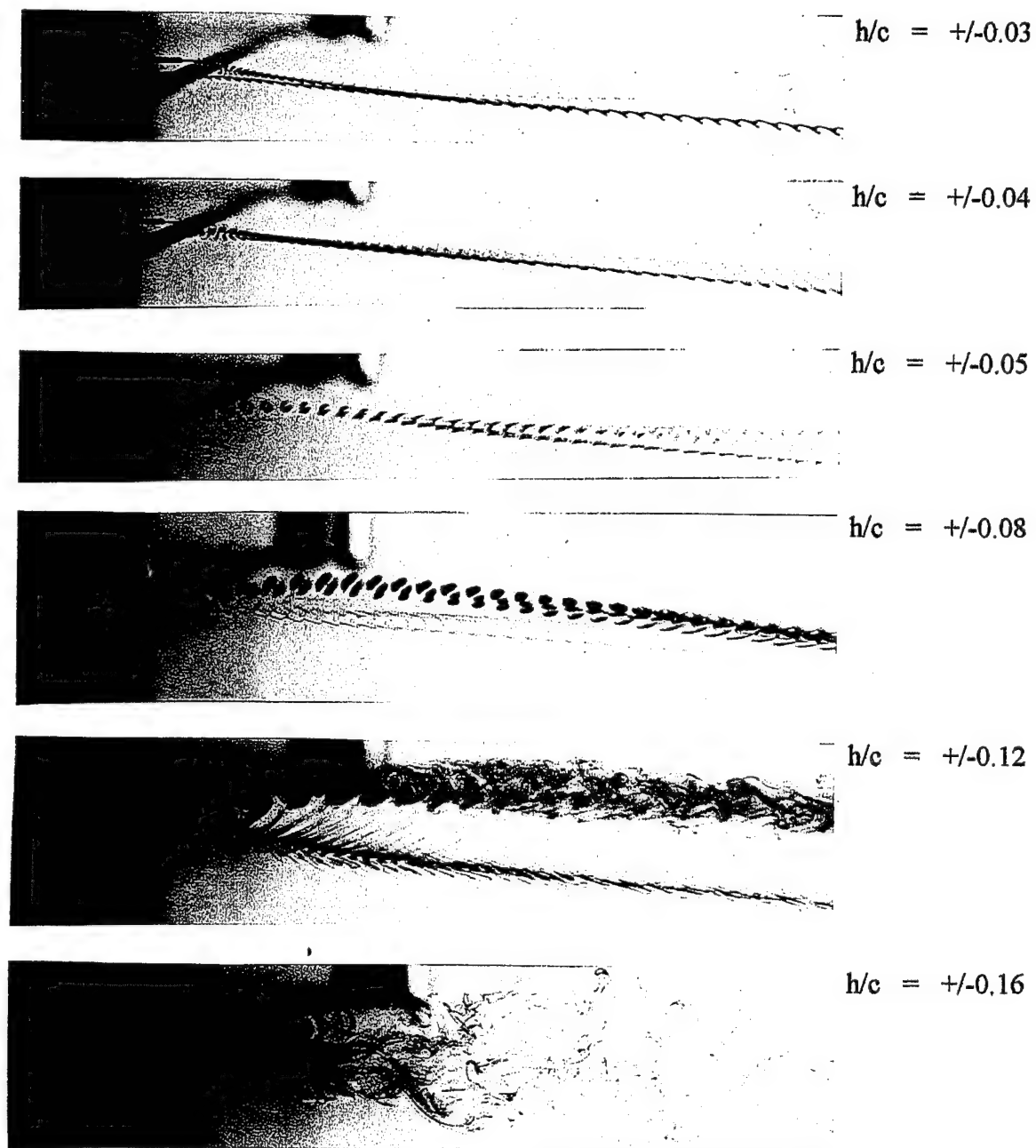
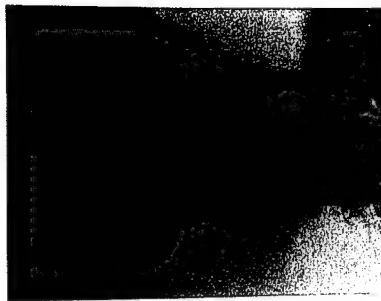
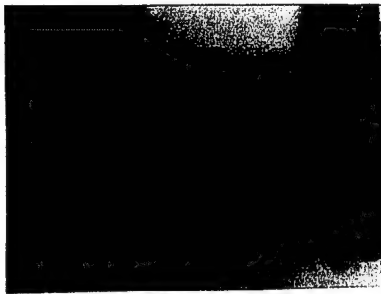


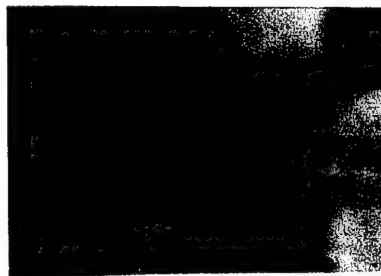
Figure 11A. Vortical Wake as Function of Amplitude h/c
 $f = 5\text{Hz}$, $u = 2.5\text{cm/s}$, $k = 12.3$



$h/c = +/-0.20$



$h/c = +/-0.35$



$h/c = +/-0.65$

Figure 11A.(cont.) Vortical Wake as Function of Amplitude h/c
 $f = 5\text{Hz}$, $u = 2.5\text{cm/s}$, $k = 12.3$

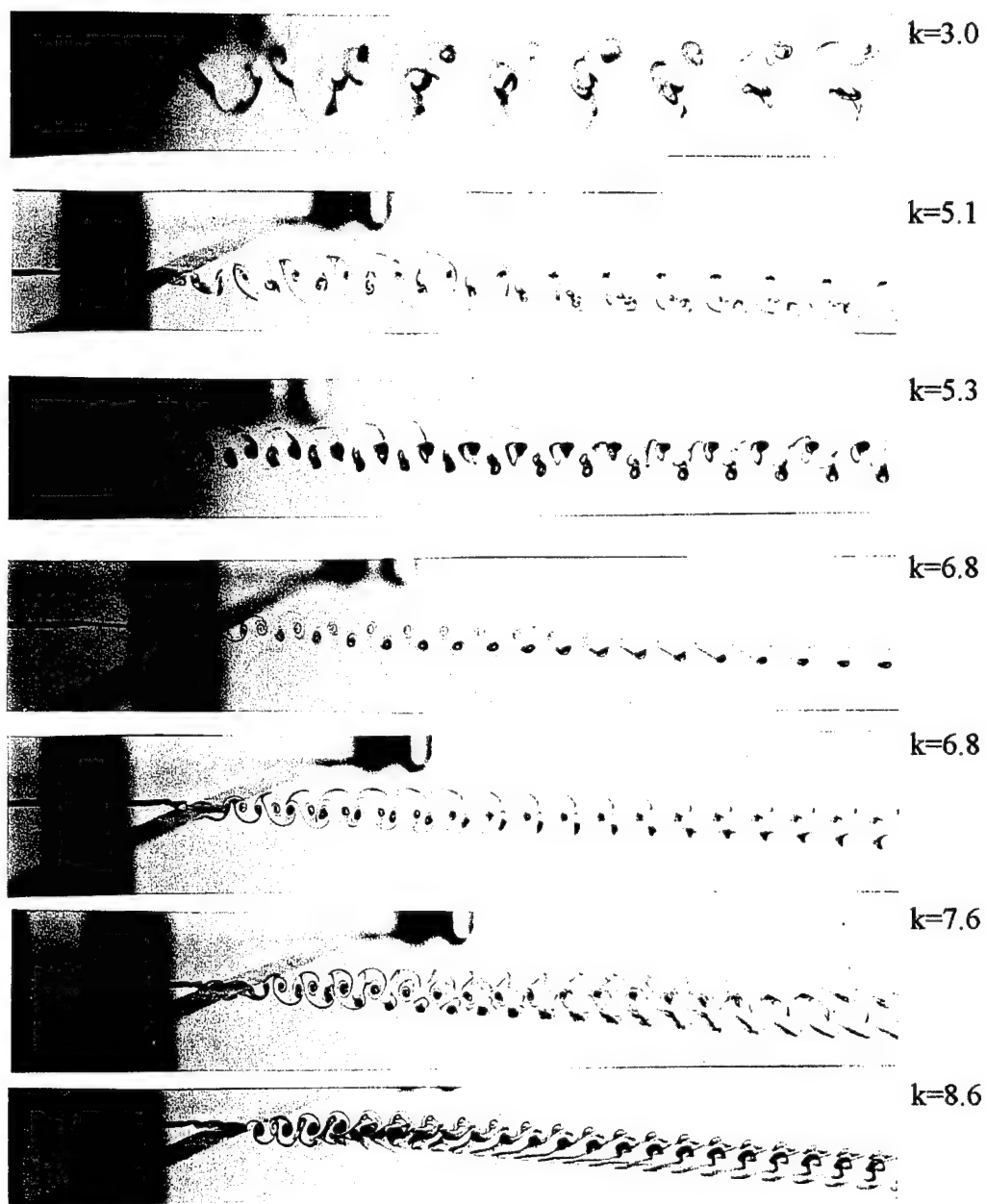


Figure 13A. Vortical Wake as Function of Reduced Frequency k
 Amplitude $h = \pm 0.05c$, Frequency $f = 5\text{Hz}$

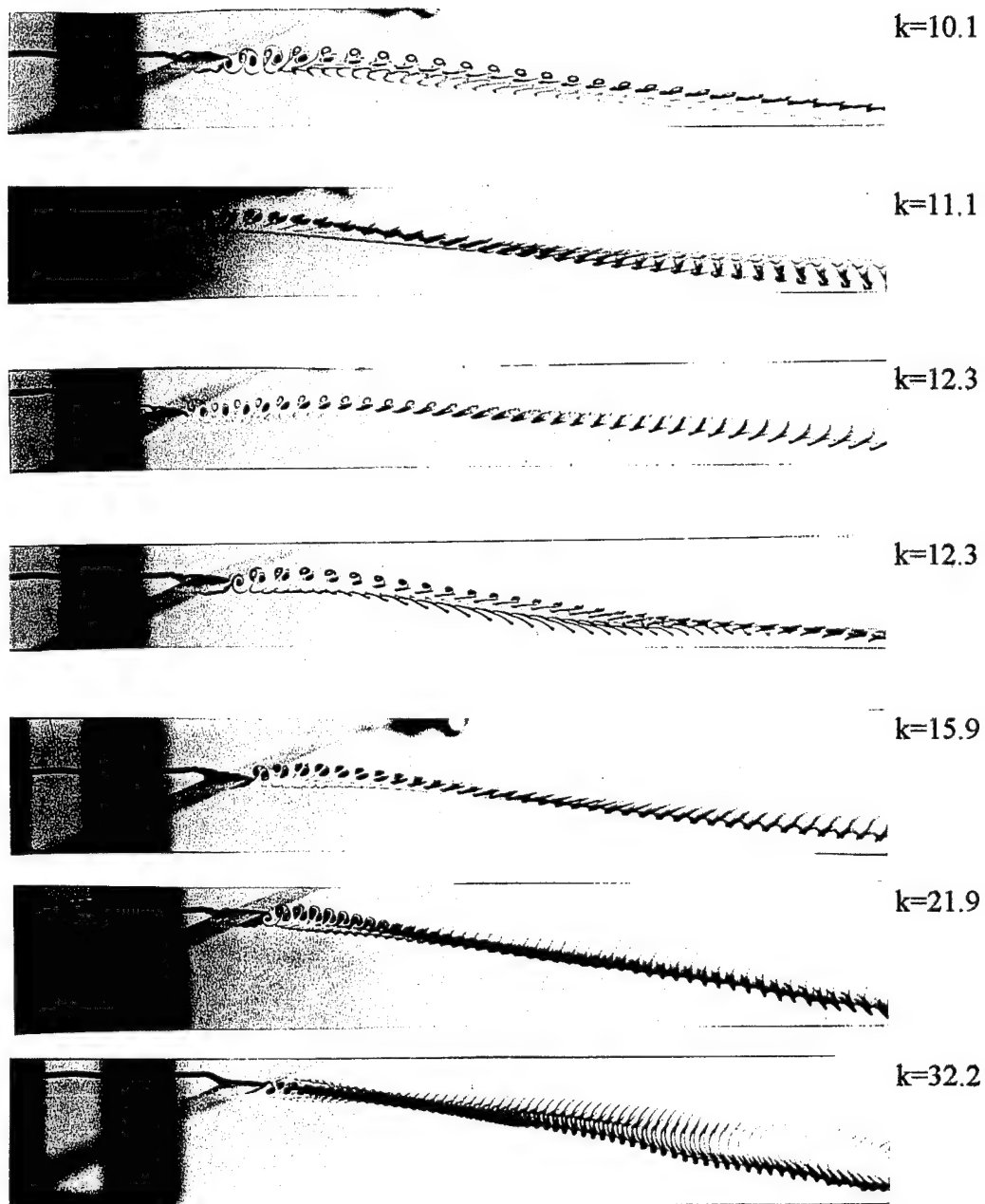


Figure 13A.(cont.) Vortical Wake as Function of Reduced Frequency k
 Amplitude $h = \pm 0.05c$, Frequency $f = 5\text{Hz}$

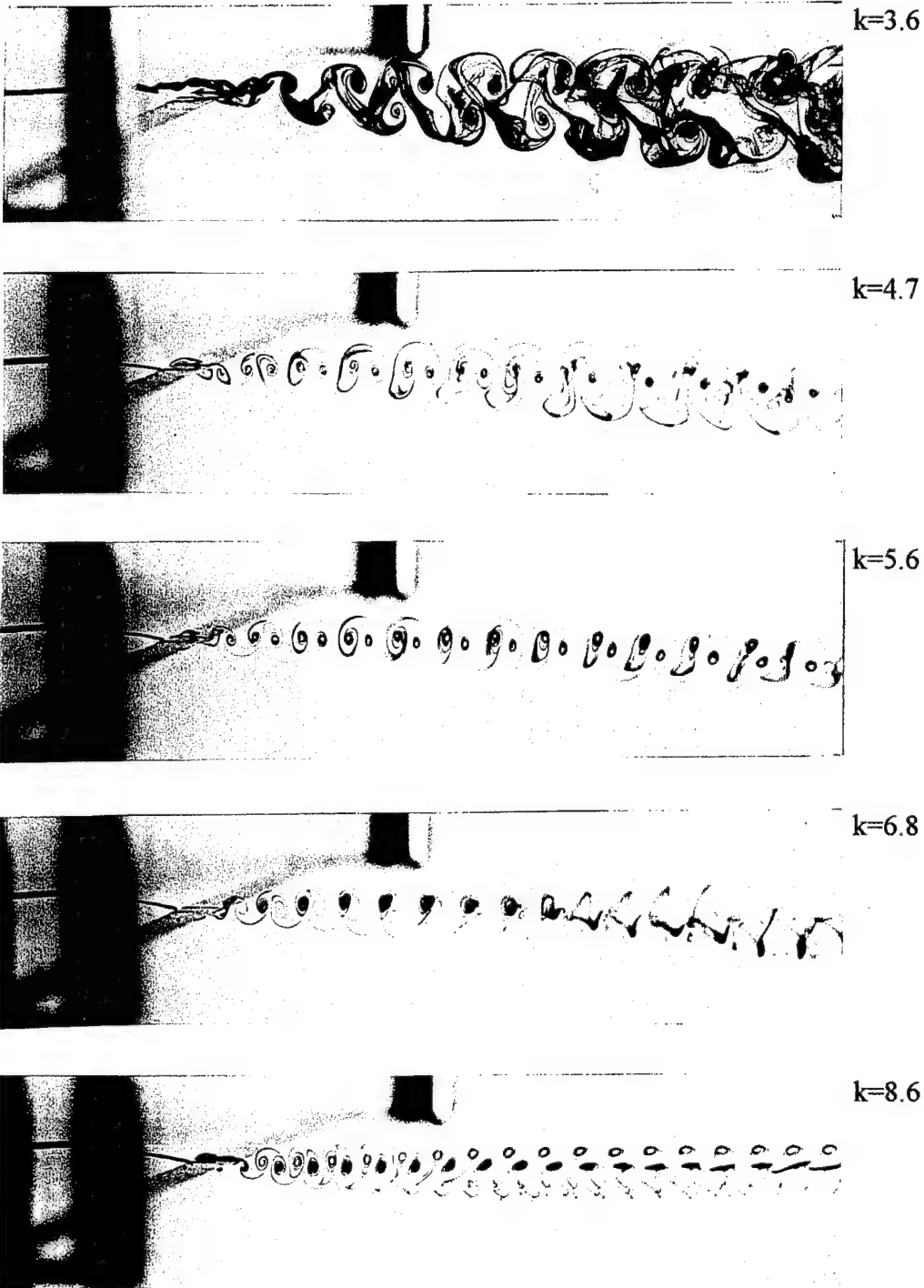


Figure 14A. Vortical Wake as Function of Reduced Frequency k
 Amplitude $h = \pm 0.08c$, Frequency $f = 5\text{Hz}$
 Chordlength $c = 1\text{cm}$

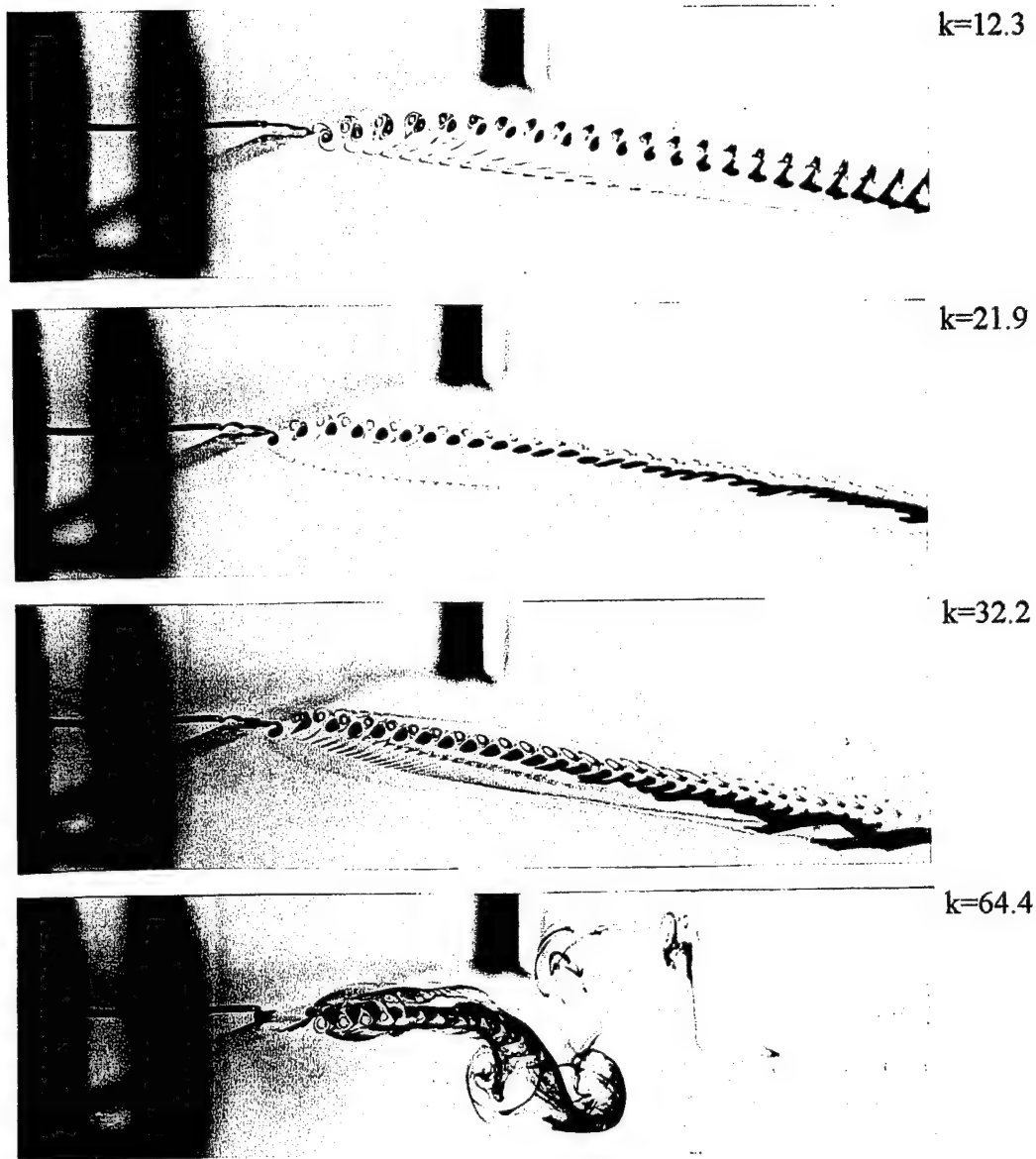


Figure 14A.(cont.) Vortical Wake as Function of Reduced Frequency k
 Amplitude $h = \pm 0.08c$, Frequency $f = 5\text{Hz}$
 Chord Length $c = 1\text{cm}$

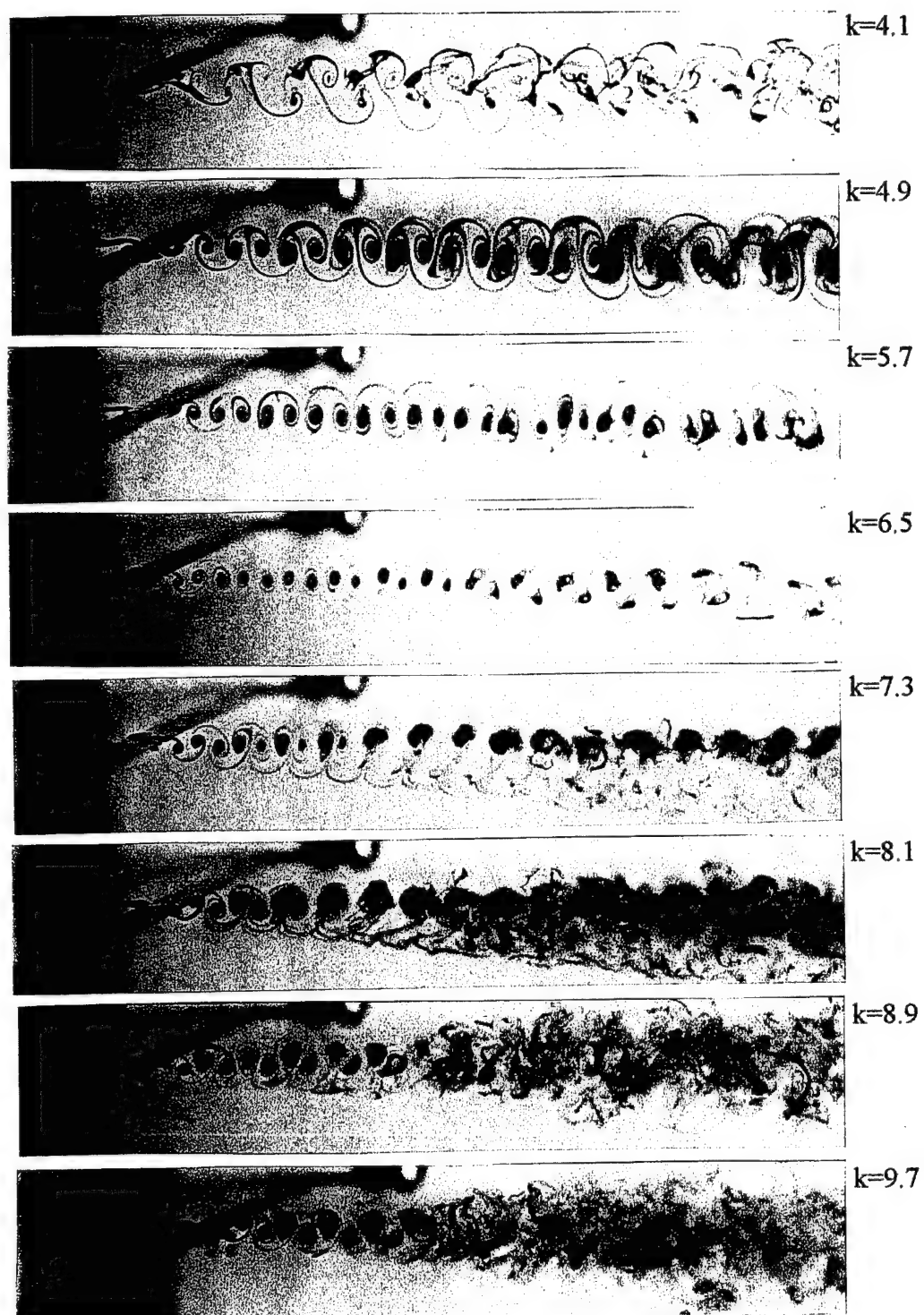


Figure 15A. Vortical Wake as Function of Reduced Frequency k
 Amplitude $h = \pm 0.08c$, $U = 7.7$ cm/s
 Chord Length $c = 1$ cm

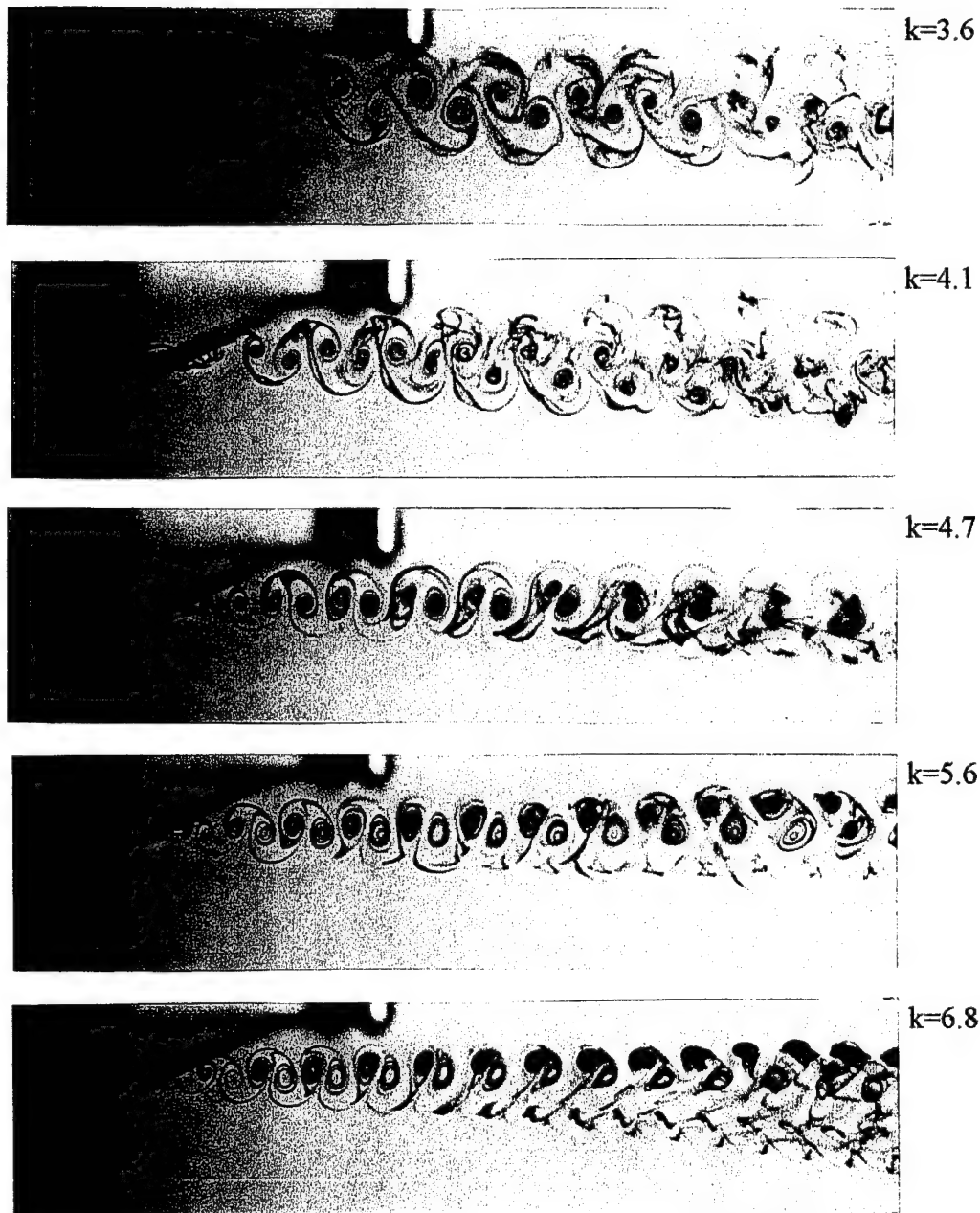


Figure 16A. Vortical Wake as Function of Reduced Frequency k
 Amplitude $h = \pm 0.12c$, Frequency $f = 5\text{Hz}$,
 Chord Length $c = 1\text{cm}$

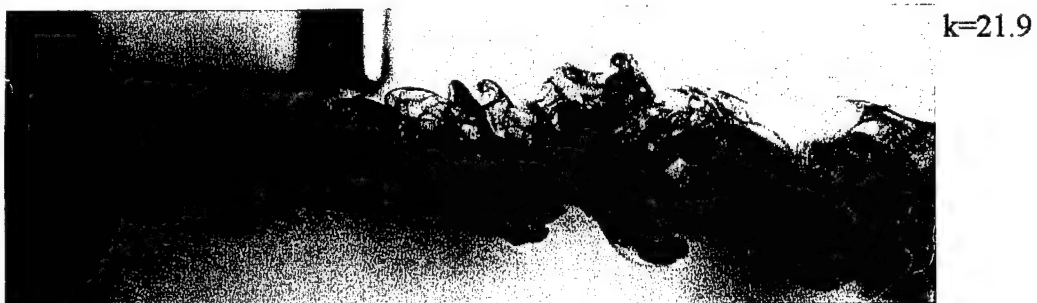
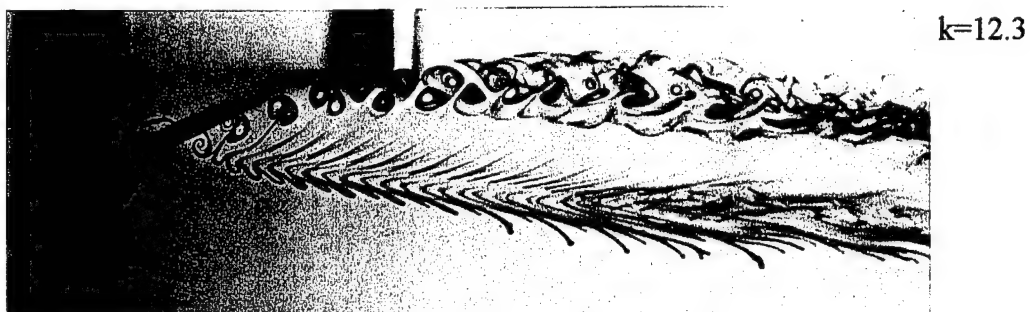
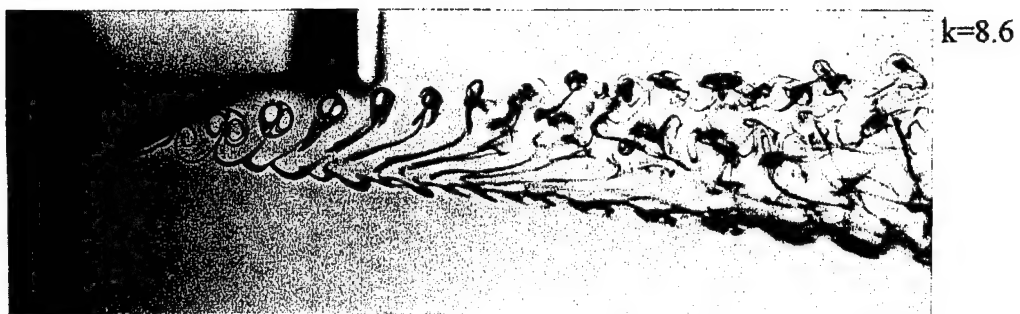


Figure 16A.(cont.) Vortical Wake as Function of Reduced Frequency k
 Amplitude $h = \pm 0.12c$, Frequency $f = 5\text{Hz}$,
 Chord Length $c = 1\text{cm}$

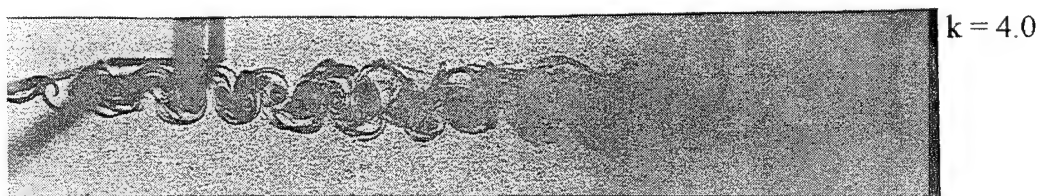
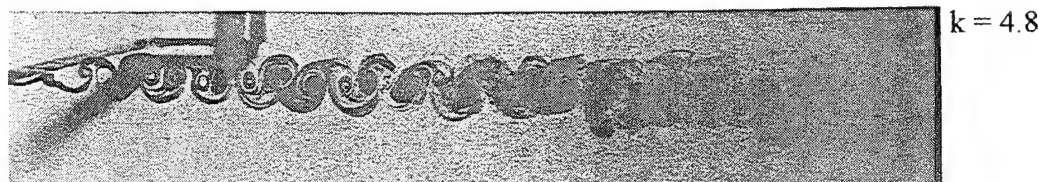
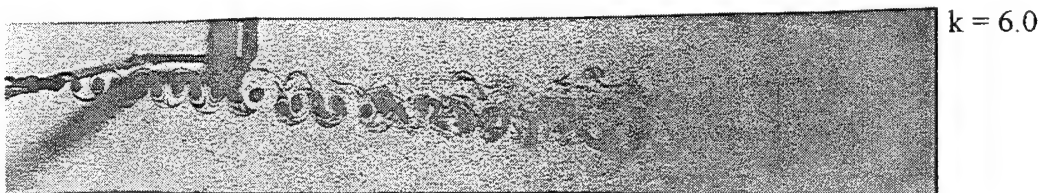
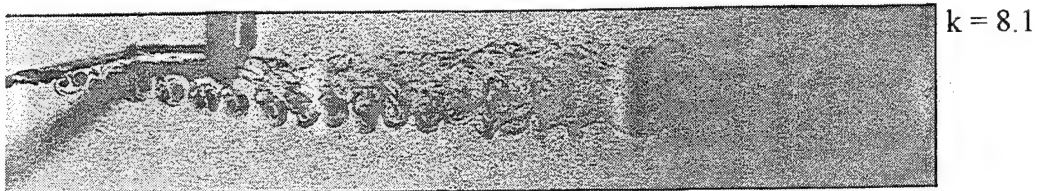
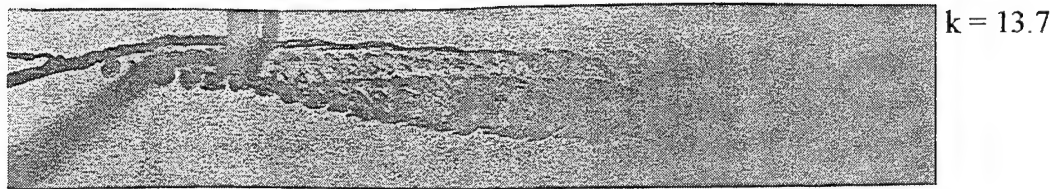
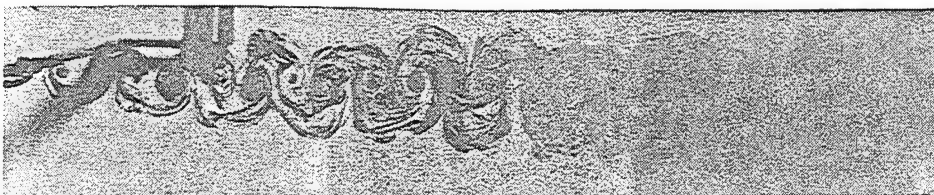


Figure 17A. Vortical Wake as Function of Reduced Frequency k
Amplitude $h = \pm 0.15c$, Frequency $f = 10$ Hz,
Chord Length $c = 1$ cm



$k = 3.4$



$k = 3.0$



$k = 2.7$



$k = 2.4$



$k = 2.2$

Figure 17A.(cont.) Vortical Wake as Function of Reduced Frequency k
 Amplitude $h = \pm 0.15c$, Frequency $f = 10\text{Hz}$
 Chord Length $c = 1\text{cm}$

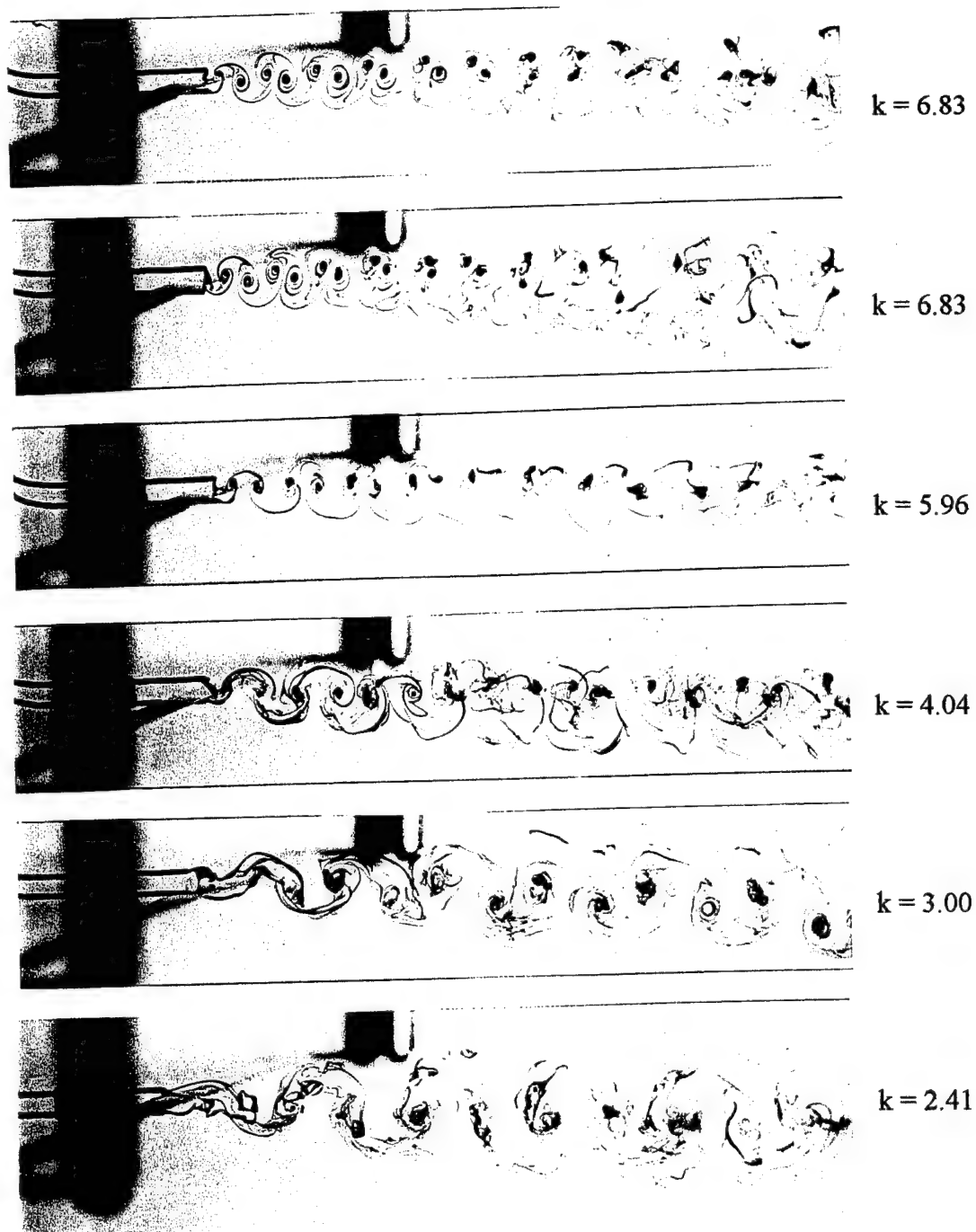


Figure 18A. Vortical Wake as Function of Reduced Frequency k ,
Amplitude $h = \pm 0.2c$, Frequency $f = 5\text{Hz}$,
Chord Length $c = 1\text{cm}$



Figure 18A.(cont.) Vortical Wake at Reduced Frequency $k = 1.99$
Amplitude $h = \pm 0.2c$, Frequency $f = 5\text{Hz}$,
Chord Length $c = 1\text{cm}$

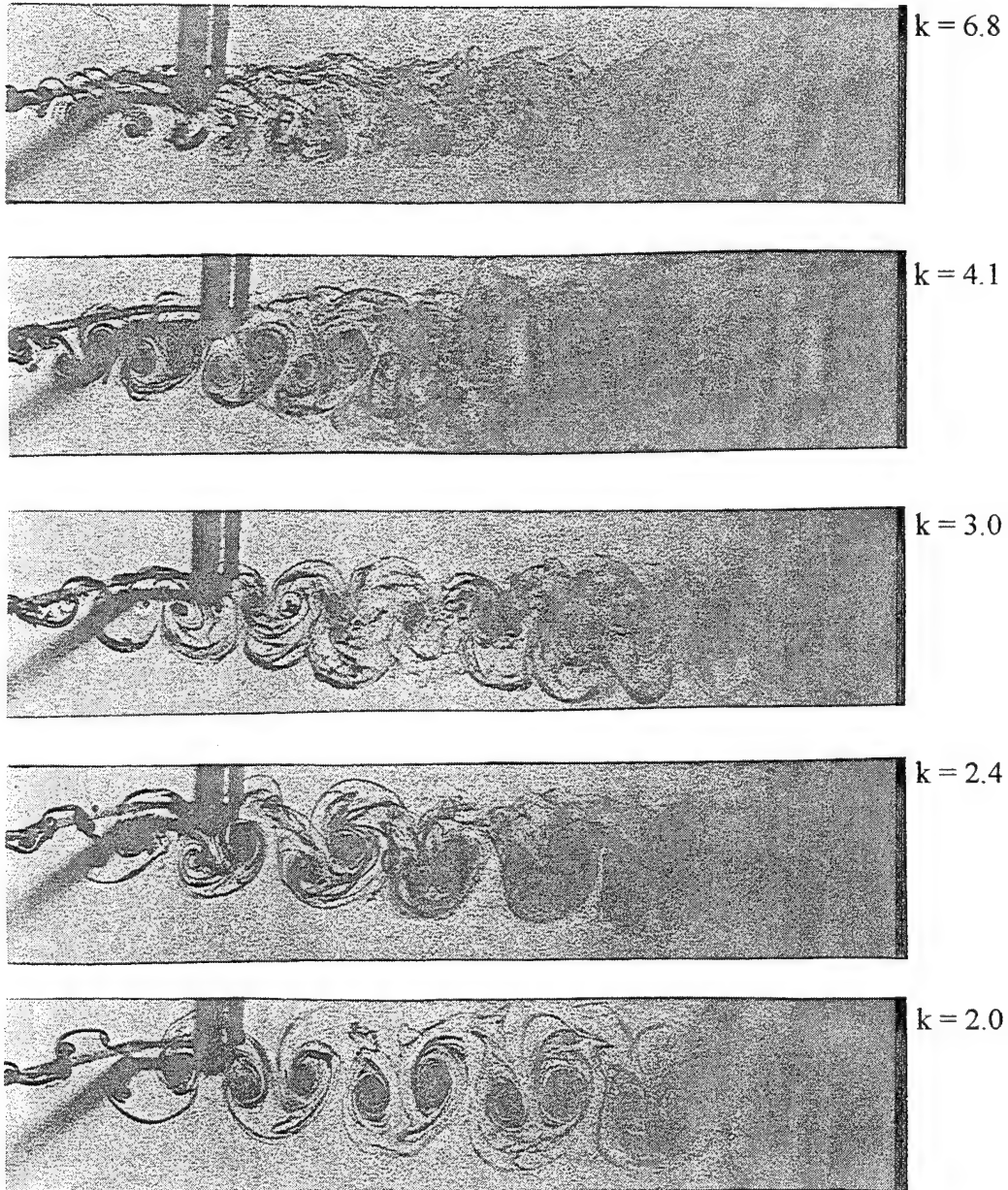


Figure 19A. Vortical Wake as Function of Reduced Frequency k
 Amplitude $h = \pm 0.4c$, Frequency $f = 5\text{Hz}$,
 Chord Length $c = 1\text{cm}$

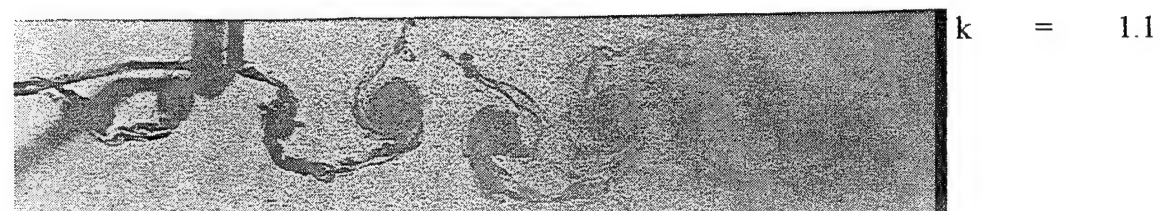
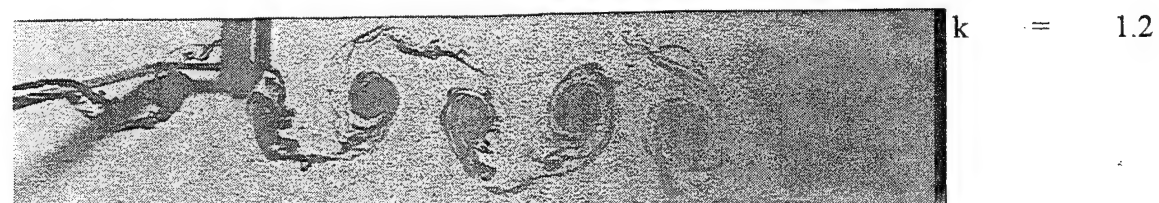
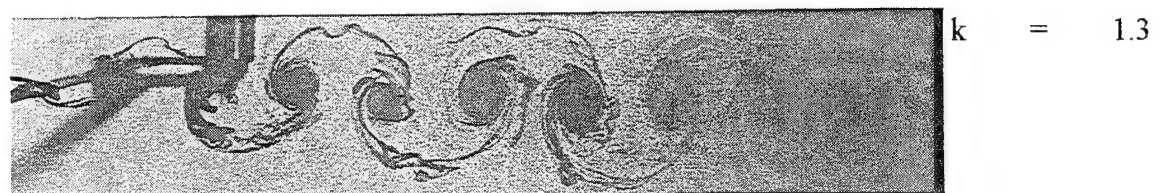
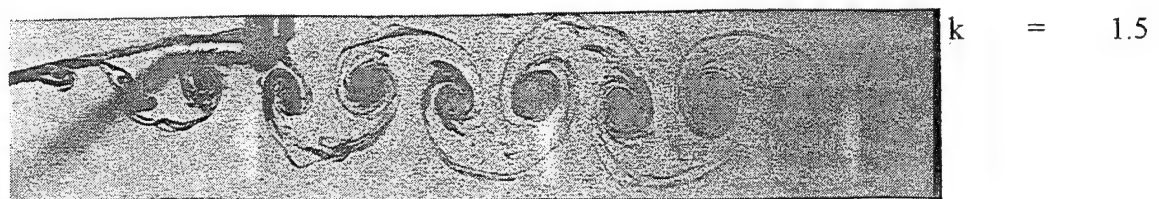
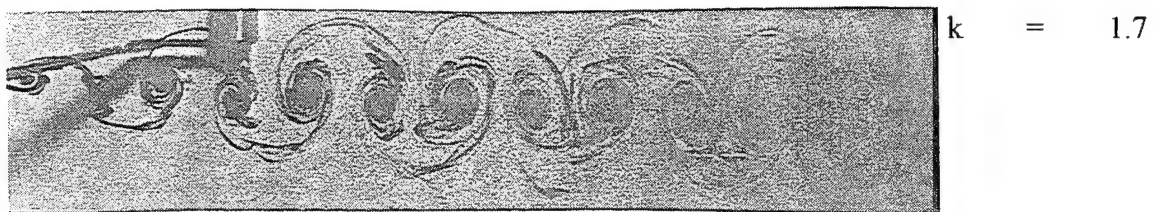
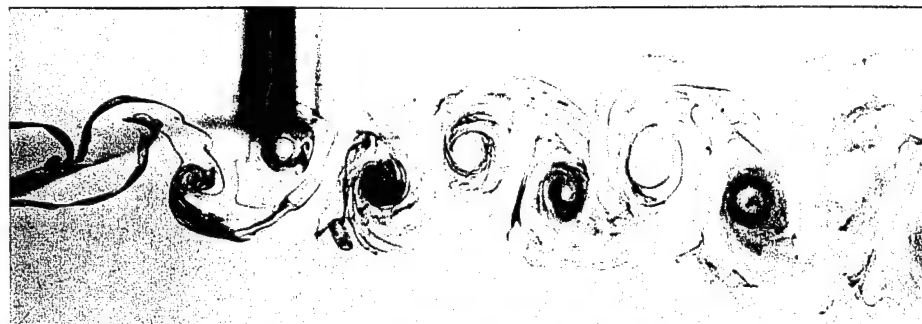


Figure 19A.(cont.) Vortical Wake as Function of Reduced Frequency k ,
 Amplitude $h = \pm 0.4c$, Frequency $f = 5\text{Hz}$,
 Chord Length $c = 1\text{cm}$



$k = 1.99$



$k = 1.69$



$k = 1.48$



$k = 1.33$

Figure 20A. Vortical Wake as Function of Reduced Frequency k ,
Amplitude $h = \pm 0.65c$, Frequency $f = 5\text{Hz}$
Chord Length $c = 1\text{cm}$

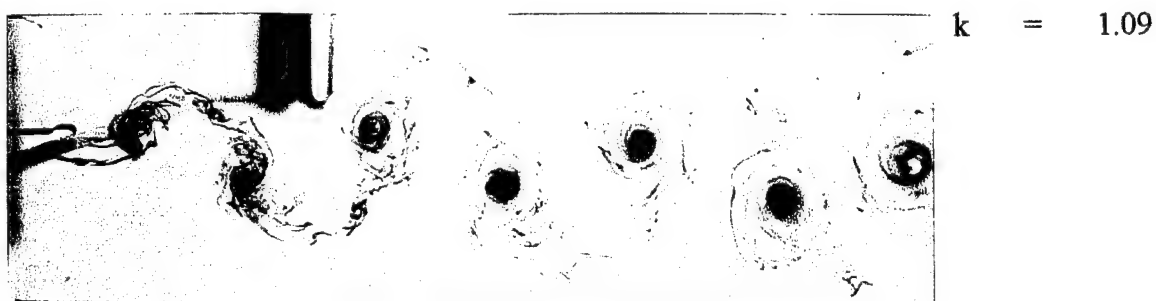
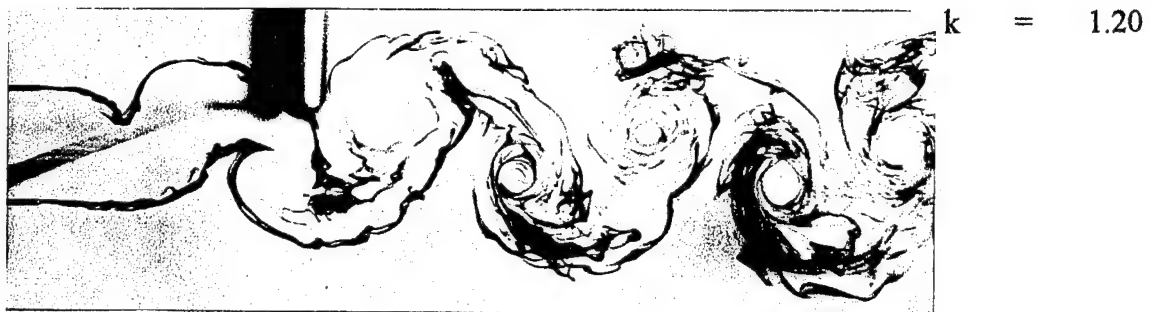


Figure 20A.(cont.) Vortical Wake as Function of Reduced Frequency k ,
 Amplitude $h = \pm 0.65c$, Frequency $f = 5\text{Hz}$,
 Chord Length $c = 1\text{cm}$

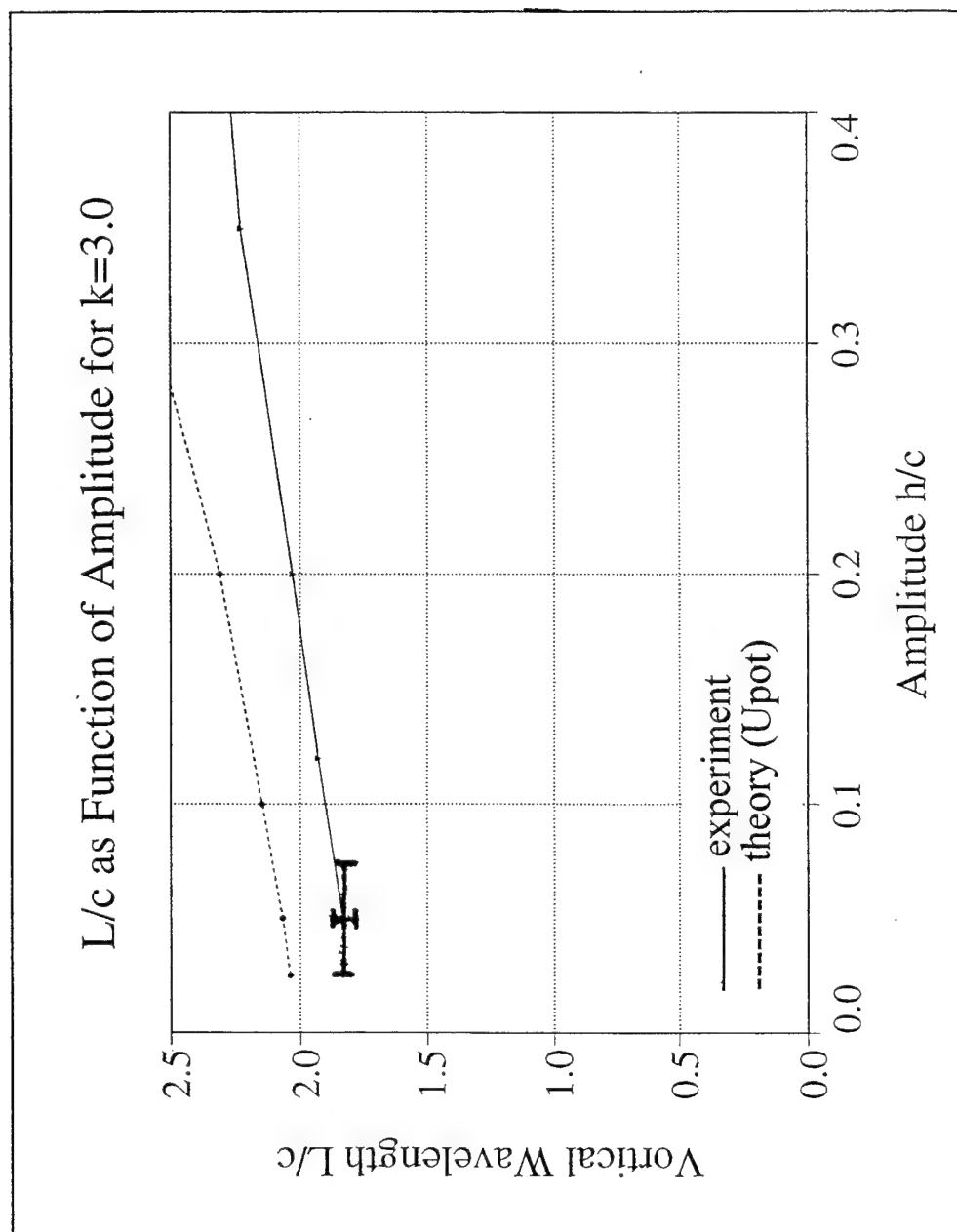


Figure 6B. Vortical wavelength as function of the amplitude, reduced frequency $k = 3.0$

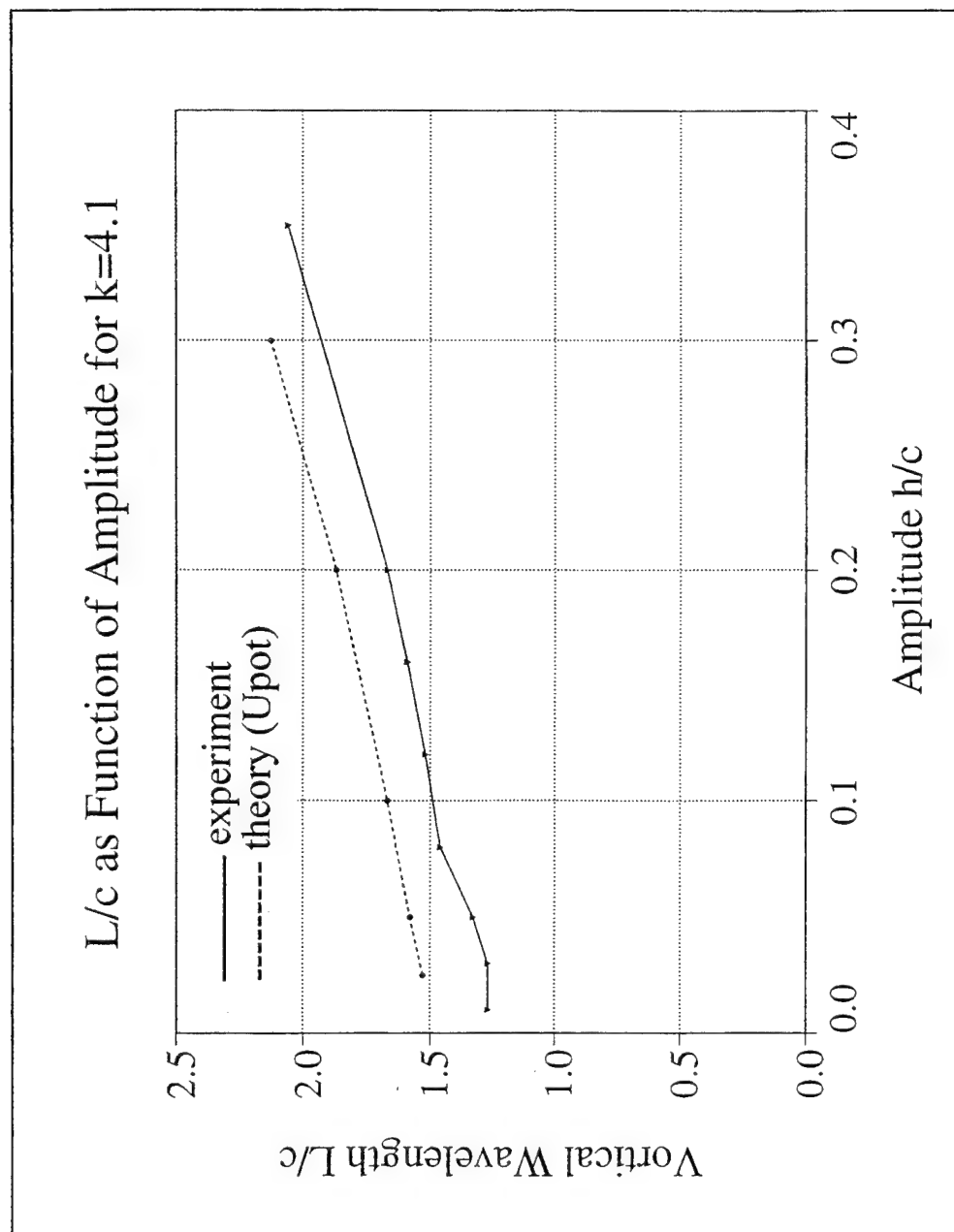


Figure 7B. Vortical wavelength as function of the amplitude, reduced frequency $k = 4.1$

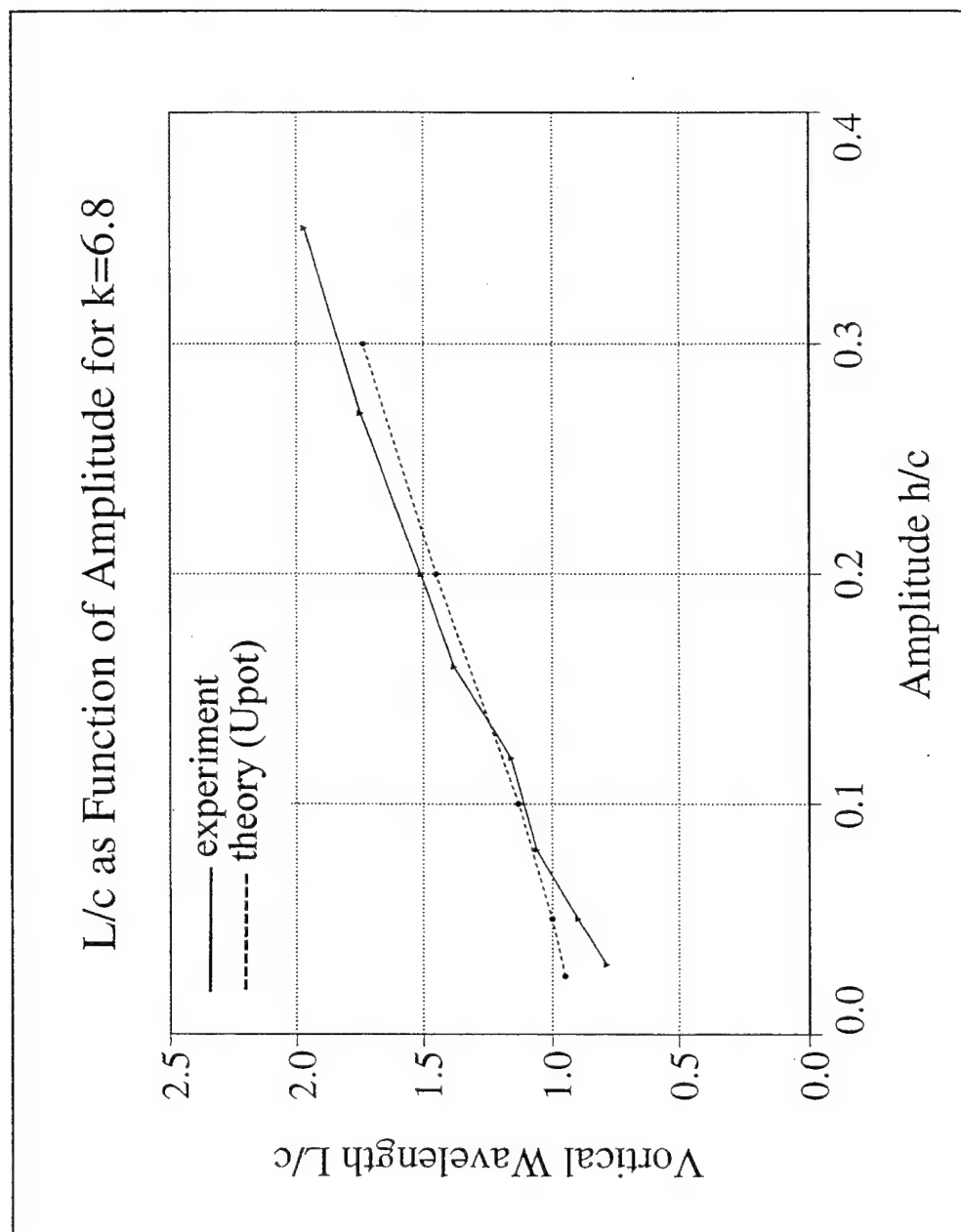


Figure 8B. Vortical wavelength as function of the amplitude, reduced frequency $k = 6.8$

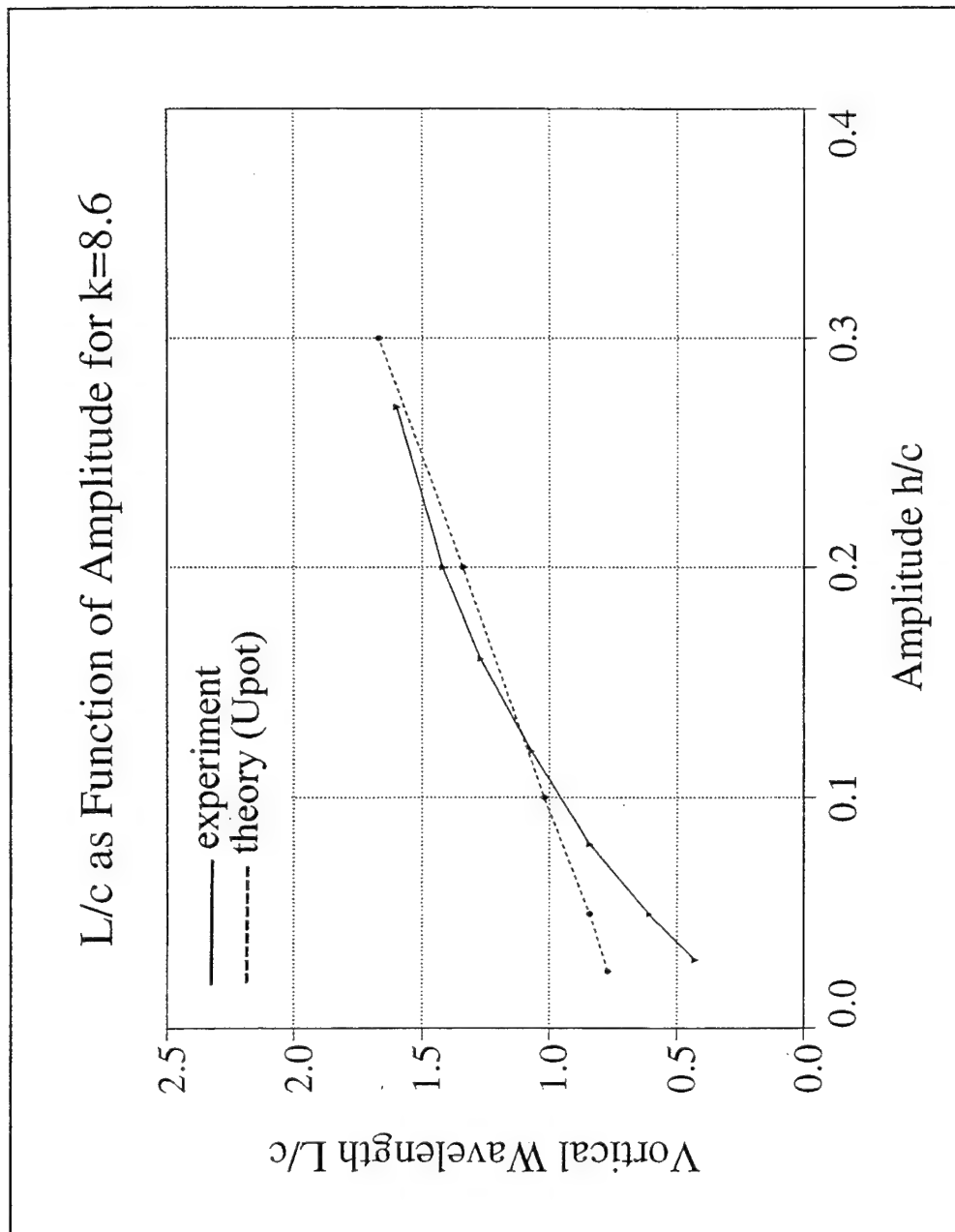


Figure 9B. Vortical wavelength as function of the amplitude, reduced frequency $k = 8.6$

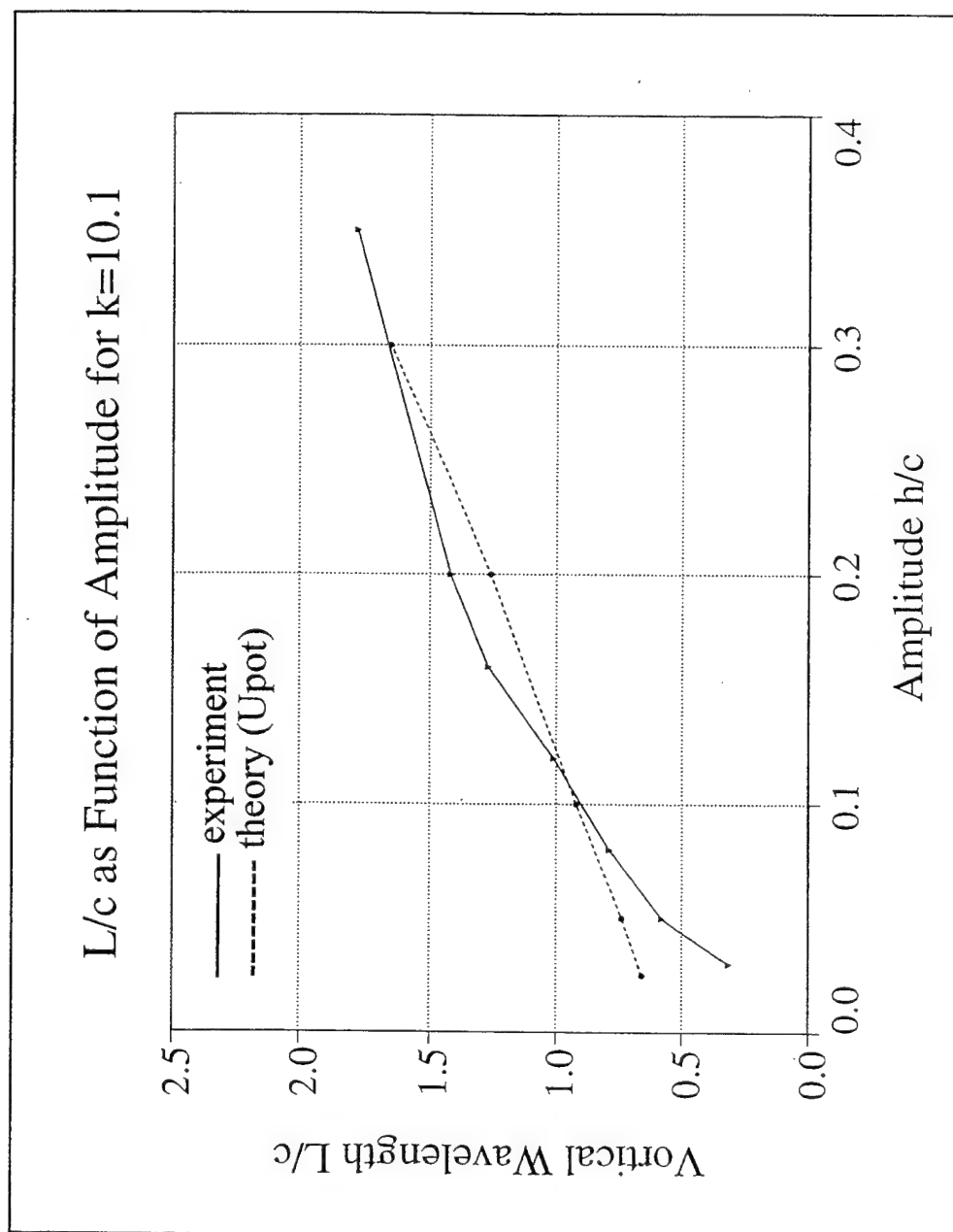


Figure 10B. Vortical wavelength as function of the amplitude, reduced frequency $k = 10.1$

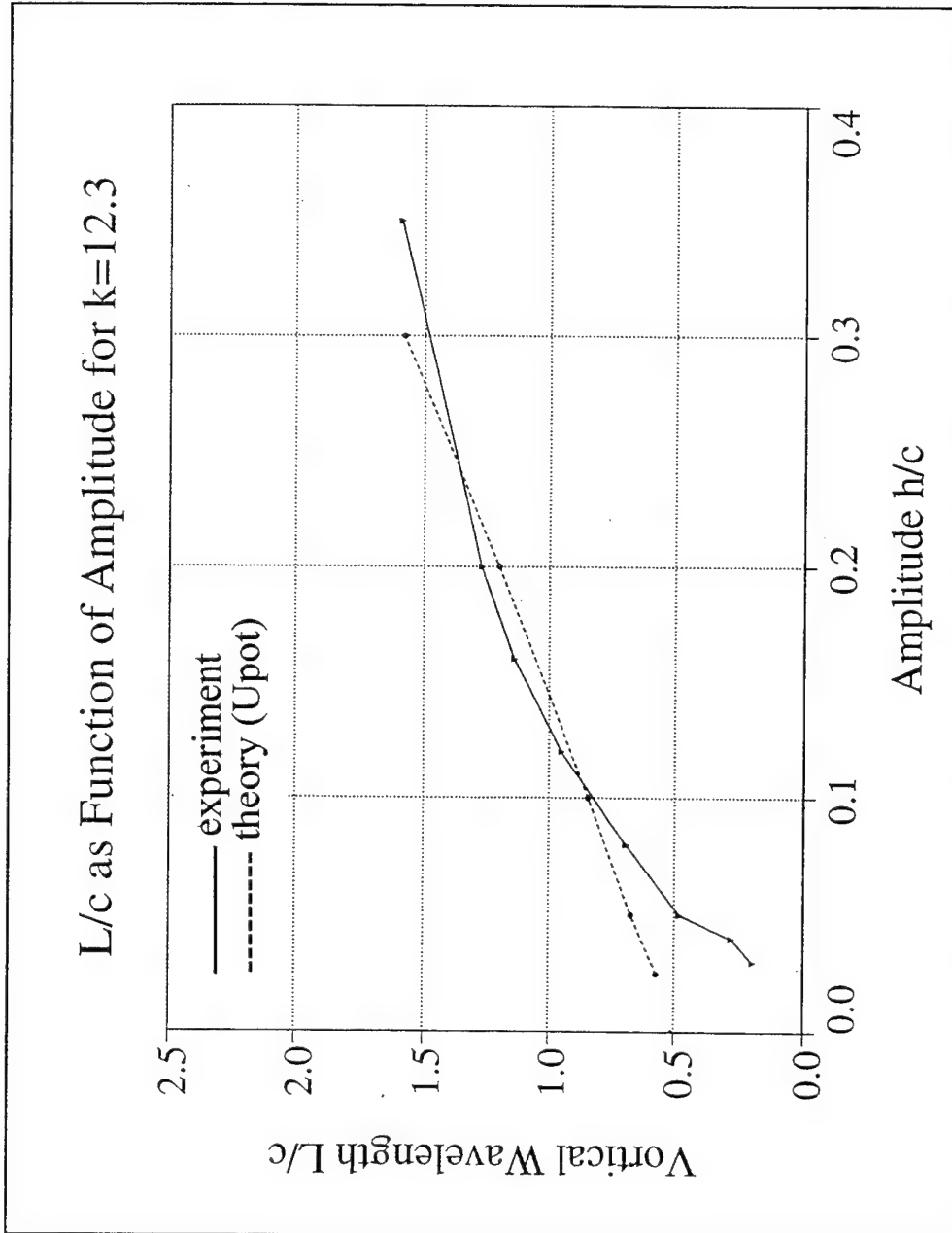


Figure 11B. Vortical wavelength as function of the amplitude, reduced frequency $k = 12.3$

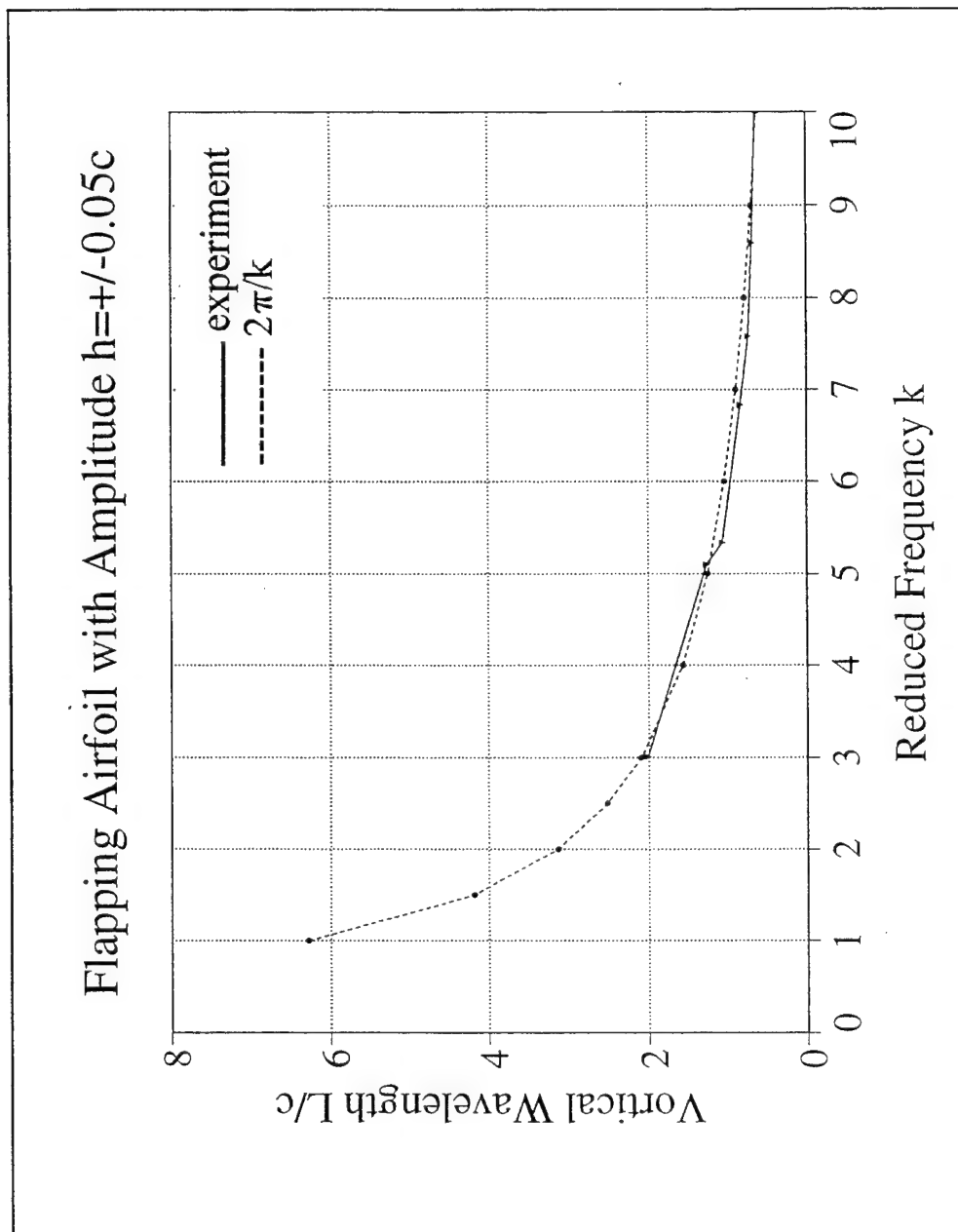


Figure 13B. Vortical wavelength as function of the reduced frequency, amplitude $h/c = 0.05$

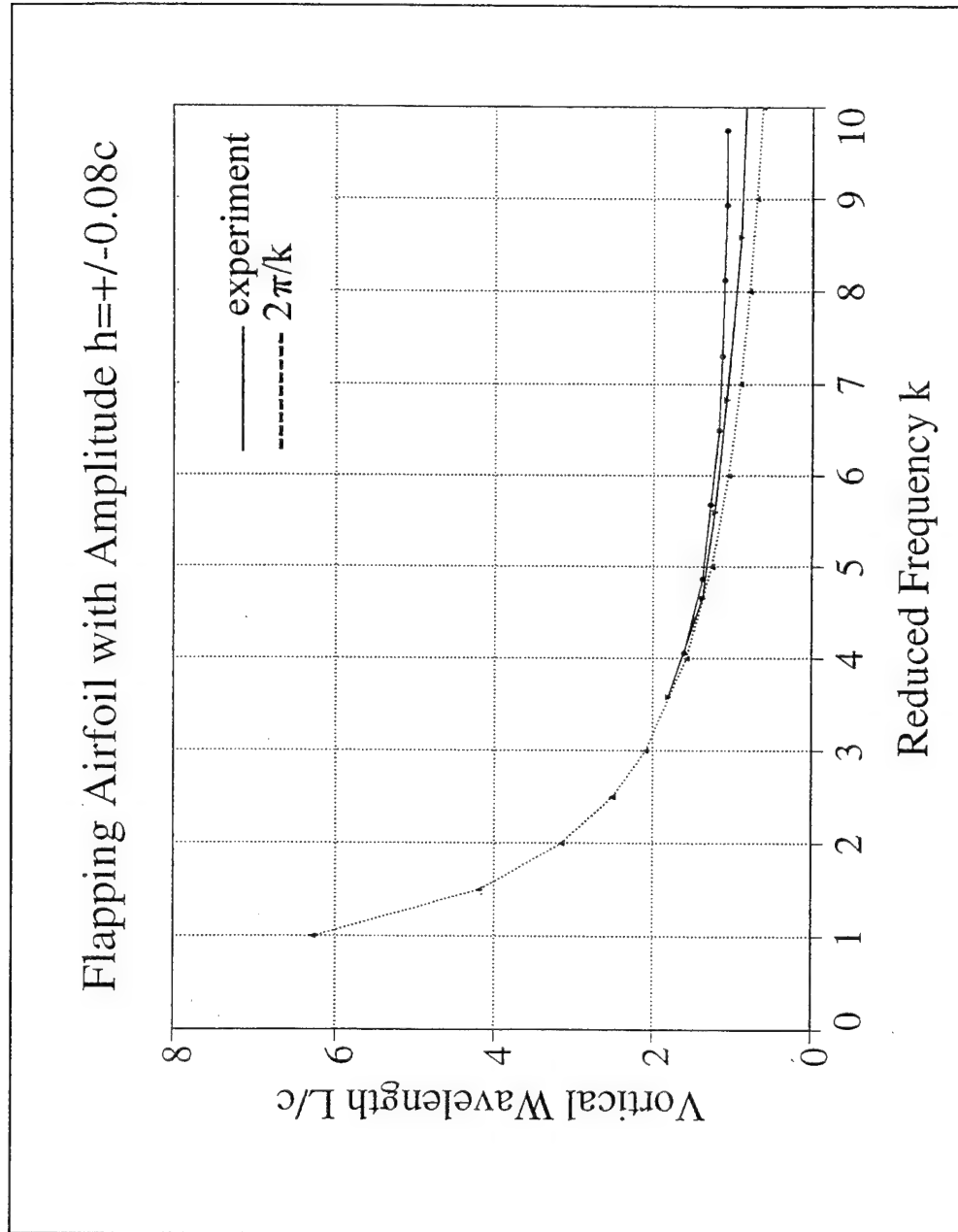


Figure 14B. Vortical wavelength as function of the reduced frequency, amplitude $h/c = 0.08$

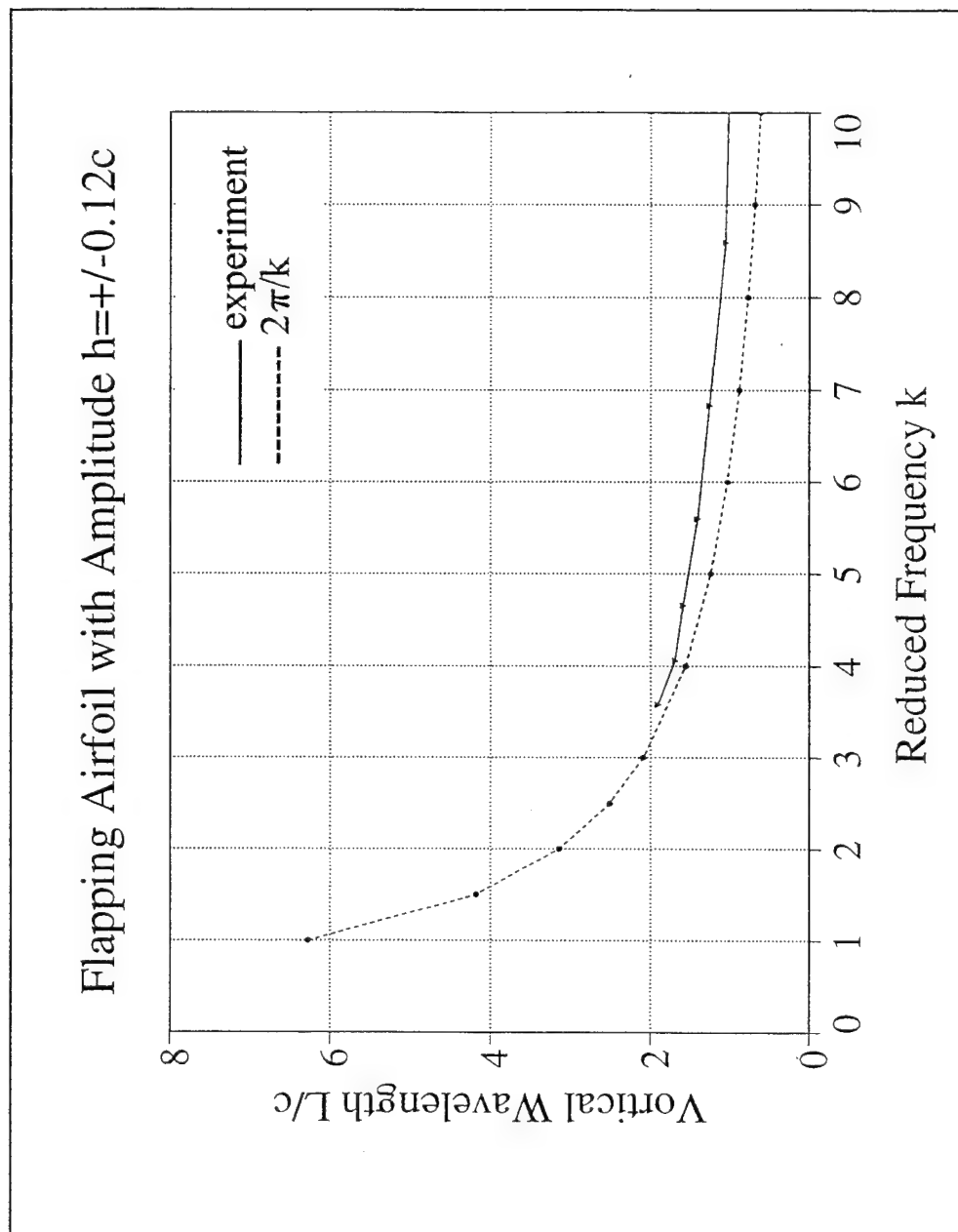


Figure 16B. Vortical wavelength as function of the reduced frequency, amplitude $h/c = 0.12$

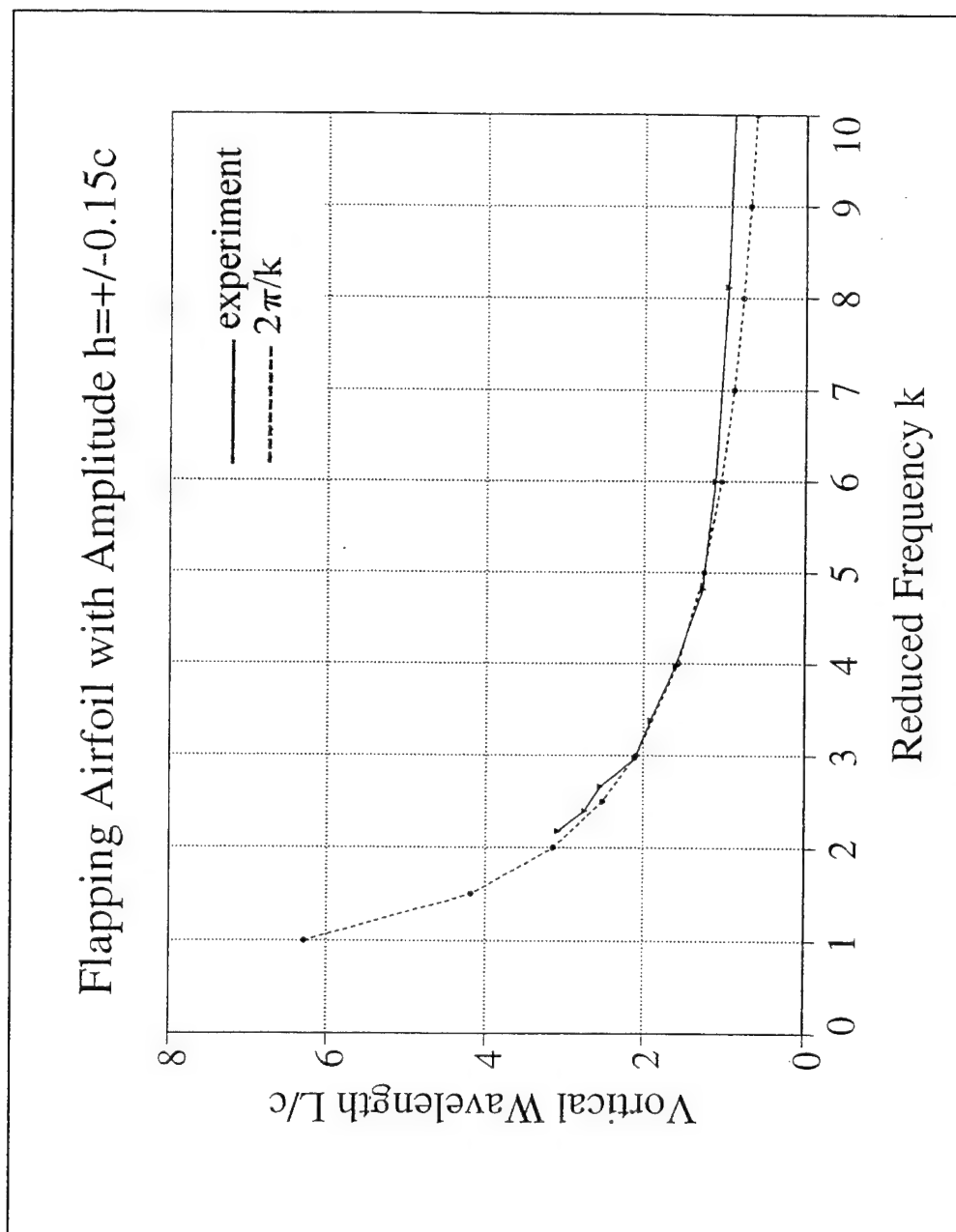


Figure 17B. Vortical wavelength as function of the reduced frequency, amplitude $h/c = 0.15$

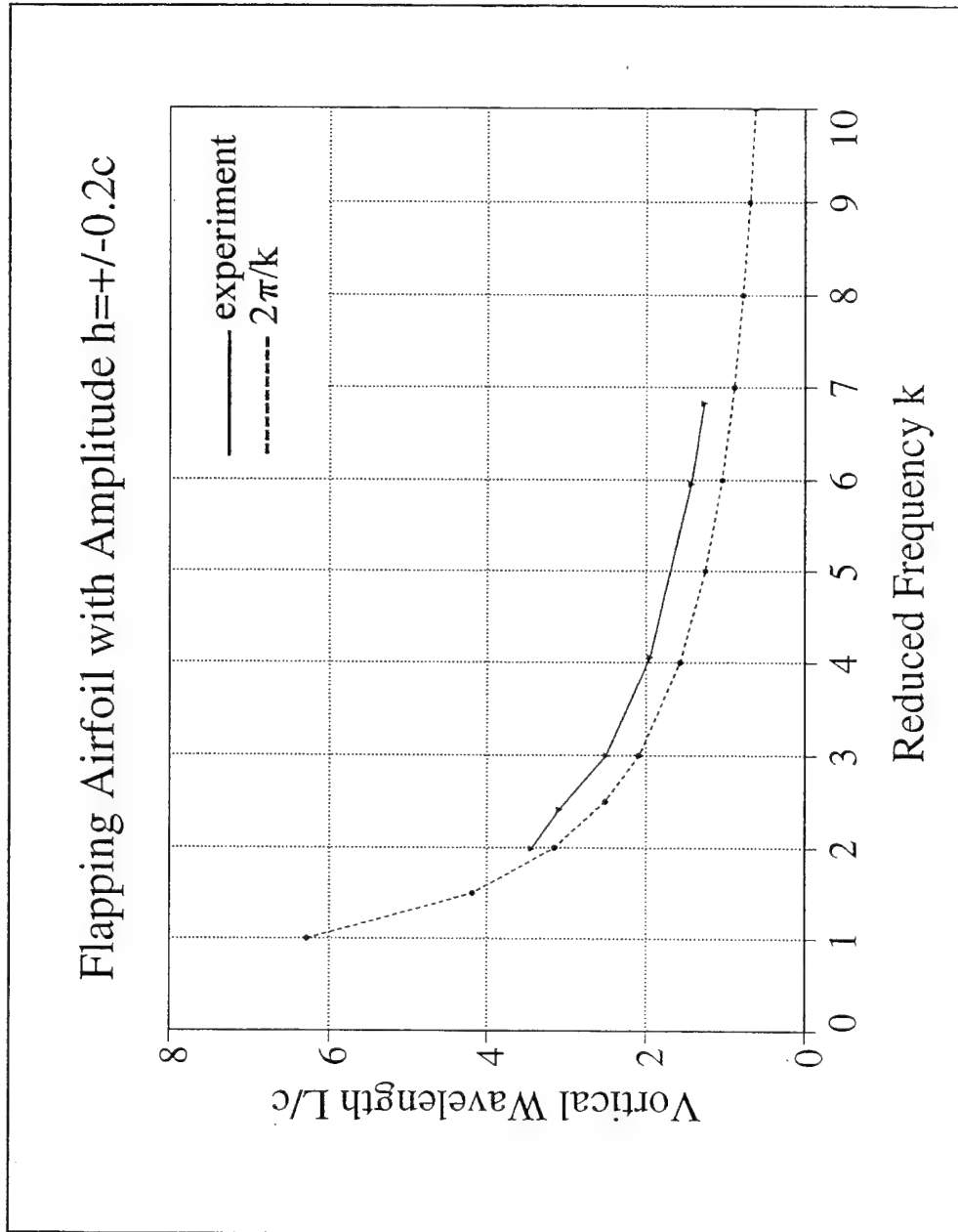


Figure 18B. Vortical wavelength as function of the reduced frequency, amplitude $h/c = 0.20$

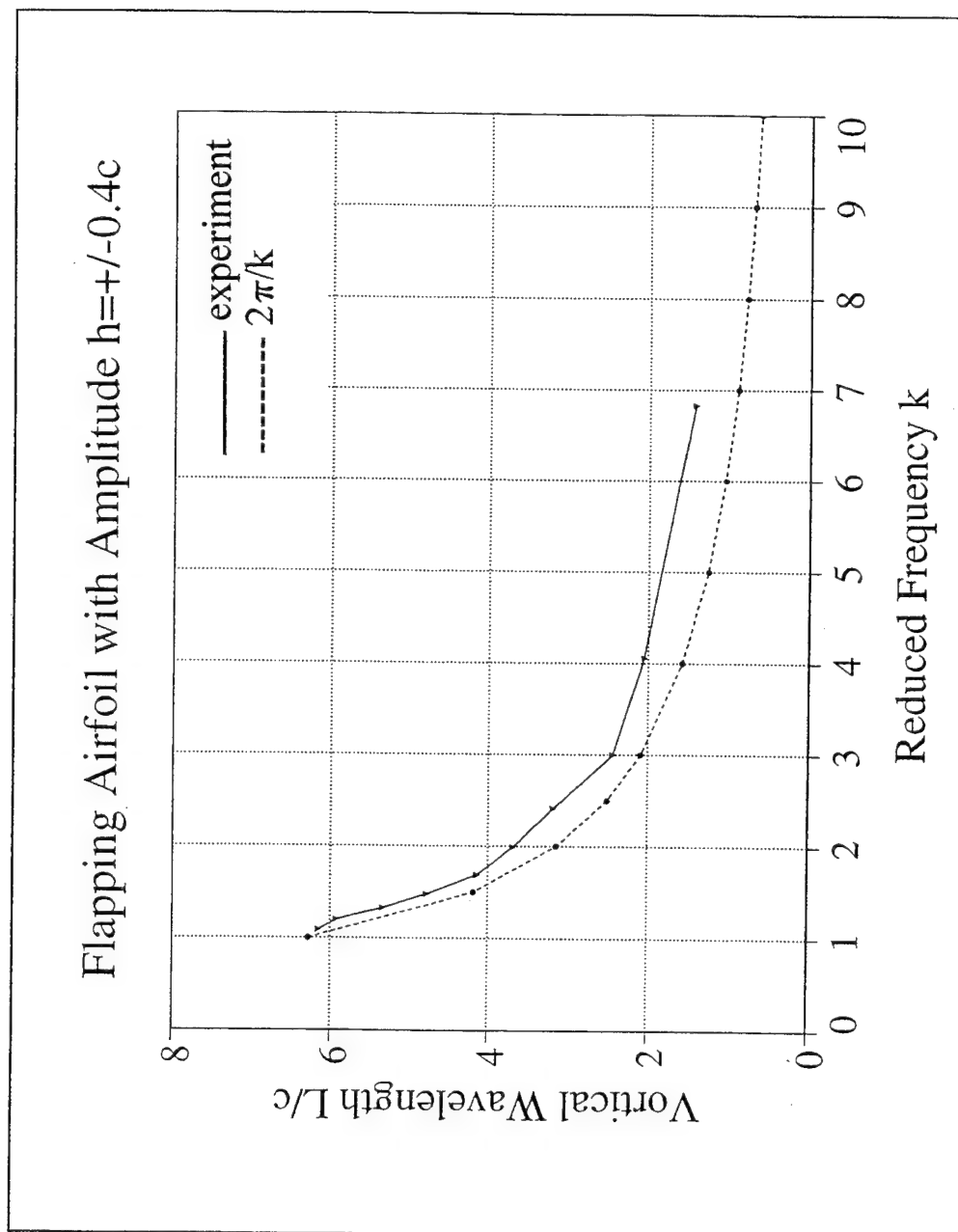


Figure 19B. Vortical wavelength as function of the reduced frequency, amplitude $h/c = 0.40$

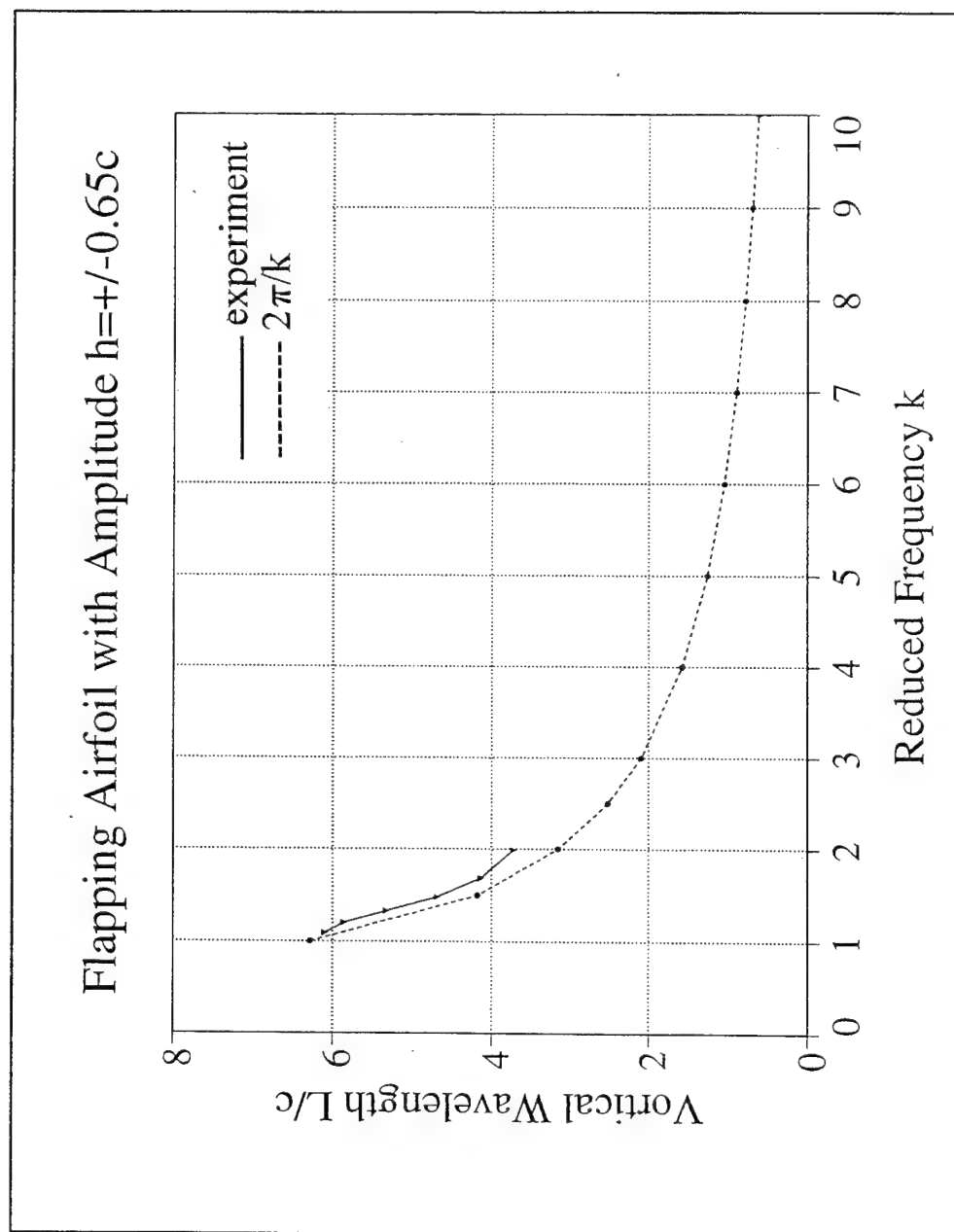


Figure 20B. Vortical wavelength as function of the reduced frequency, amplitude $h/c = 0.65$

APPENDIX B. TABLES

Table 6 through 11 Vortical wavelength from constant reduced frequency measurements

Table 13 through 20 Vortical wavelength from constant amplitude measurements

Table 23 through 36 LDV velocity data

amplitude setting	amplitude h/c	vortical wavelength L [in]	vortical wavelength L/c	wake signature
10	0.05	0.71	1.83	D
20	0.12	0.75	1.93	I
30	0.20	0.79	2.03	T
40	0.35	0.87	2.23	T
50	0.65	0.95	2.44	T2

Table 6. Vortical wavelength as function of amplitude
 chordlength of flapping airfoil = 1cm = 0.39in
 displayed velocity = 0.3ft/s
 actual velocity = 0.105m/s
 frequency = 5Hz
 reduced frequency $k = 3.005$
 $2\pi/k = 2.09$
 Reynolds number = 1037
 wake signature: D = drag
 I = indifferent
 T = thrust
 T2= thrust, dual mode

amplitude setting	amplitude h/c	vortical wavelength L [in]	vortical wavelength L/c	wake signature
0	0.01	0.50	1.27	D
5	0.03	0.50	1.27	D
10	0.05	0.53	1.33	D
15	0.08	0.58	1.46	D
20	0.12	0.60	1.52	I
25	0.16	0.63	1.59	I
30	0.20	0.66	1.67	I
40	0.35	0.81	2.06	T

Table 7. Vortical wavelength as function of amplitude
chordlength of flapping airfoil = 1cm = 0.39in
displayed velocity = 0.2ft/s
actual velocity = 0.077m/s
frequency = 5Hz
reduced frequency $k = 4.058$
 $2\pi/k = 1.55$
Reynolds number = 760
wake signature: D = drag
I = indifferent
T = thrust
T2= thrust, dual mode

amplitude setting	amplitude h/c	vortical wavelength L [in]	vortical wavelength L/c	wake signature
5	0.03	0.31	0.79	D
10	0.05	0.35	0.90	D
15	0.08	0.42	1.06	T
20	0.12	0.46	1.16	T
25	0.16	0.54	1.38	T2
30	0.20	0.59	1.51	T2
35	0.27	0.69	1.75	T2
40	0.35	0.77	1.97	T2
45	0.47			
50	0.65			

Table 8. Vortical wavelength as function of amplitude
chordlength of flapping airfoil = 1cm = 0.39in
displayed velocity = 0.1ft/s
actual velocity = 0.046m/s
frequency = 5Hz
reduced frequency $k = 6.828$
 $2\pi/k = 0.92$
Reynolds number = 454
wake signature: D = drag
I = indifferent
T = thrust
T2= thrust, dual mode

amplitude setting	amplitude h/c	vortical wavelength L [in]	vortical wavelength L/c	wake signature
5	0.03	0.17	0.43	D
10	0.05	0.24	0.61	I
15	0.08	0.33	0.84	T
20	0.12	0.42	1.07	T2
25	0.16	0.50	1.27	T2
30	0.20	0.56	1.42	T2
35	0.27	0.63	1.60	T2
40	0.35			
45	0.47			
50	0.65			

Table 9. Vortical wavelength as function of amplitude
chordlength of flapping airfoil = 1cm = 0.39in
displayed velocity = 0.06ft/s (velocity setting=80)
actual velocity = 0.037m/s
frequency = 5Hz
reduced frequency $k = 8.564$
 $2\pi/k = 0.73$
Reynolds number = 365
wake signature: D = drag
I = indifferent
T = thrust
T2= thrust, dual mode

amplitude setting	amplitude h/c	vortical wavelength L [in]	vortical wavelength L/c	wake signature
5	0.03	0.13	0.32	D
10	0.05	0.23	0.58	T
15	0.08	0.31	0.79	T
20	0.12	0.40	1.01	T2
25	0.16	0.50	1.27	T2
30	0.20	0.60	1.42	T2
40	0.35	0.70	1.78	T2

Table 10. Vortical wavelength as function of amplitude
 chordlength of flapping airfoil = 1cm = 0.39in
 displayed velocity = 0.04ft/s (velocity setting = 70)
 actual velocity = 0.031 m/s
 frequency = 5Hz
 reduced frequency $k = 10.105$
 $2\pi/k = 0.62$
 Reynolds number = 306
 wake signature: D = drag
 I = indifferent
 T = thrust
 T2= thrust, dual mode

amplitude setting	amplitude h/c	vortical wavelength L [in]	vortical wavelength L/c	wake signature
5	0.03	0.08	0.20	D
8	0.04	0.11	0.28	I
10	0.05	0.19	0.48	T
15	0.08	0.27	0.69	T2
20	0.12	0.40	0.95	T2
25	0.16	0.45	1.14	T2
30	0.20	0.50	1.27	T2
40	0.35	0.63	1.59	T2
50	0.65			

Table 11. Vortical wavelength as function of amplitude
 chordlength of flapping airfoil = 1cm = 0.39in
 displayed velocity = 0.02ft/s
 actual velocity = 0.025m/s
 frequency = 5Hz
 reduced frequency $k = 12.323$
 $2\pi/k = 0.51$
 Reynolds number = 247
 wake signature: D = drag
 I = indifferent
 T = thrust
 T2= thrust, dual mode

setting	Velocity u		Reduced Frequency k	Vortical Wave- length L [in]	Vortical Wave- length L/c	Wake Signature
	displayed [ft/s]	actual [m/s]				
	0.30	0.105	3.01	0.79	2.01	D
1.30	0.15	0.062	5.10	0.50	1.27	D
	0.14	0.059	5.34	0.42	1.07	D
1.00	0.10	0.046	6.83	0.33	0.84	D
0.90	0.08	0.041	7.58	0.29	0.74	D
0.80	0.06	0.037	8.59	0.27	0.69	T
0.70	0.04	0.031	10.11	0.25	0.64	T
	0.03	0.028	11.08	0.23	0.58	T
0.60	0.02	0.026	12.27	0.21	0.53	T
0.50	0	0.020	15.86	0.19	0.49	T2
0.40	0	0.014	21.93	0.16	0.41	T2
0.30	0	0.010	32.21	0.13	0.32	T2

Table 13. Vortical wavelength as function of reduced frequency
 chordlength of flapping airfoil = 1cm = 0.39in
 amplitude = 0.5mm = 0.05c
 frequency = 5Hz
 Reynolds number = 99...1037
 wake signature: D = drag
 I = indifferent
 T = thrust
 T2= thrust, dual mode

setting	Velocity u		Reduced Frequency k	Vortical Wave- length L [in]	Vortical Wave- length L/c	Wake Signature
	displayed [ft/s]	actual [m/s]				
1.80	0.24	0.088	3.58	0.71	1.80	D
1.40	0.17	0.067	4.66	0.54	1.37	I
1.20	0.13	0.056	5.60	0.48	1.22	T
1.00	0.10	0.046	6.83	0.42	1.07	T
0.80	0.06	0.037	8.59	0.35	0.89	T
0.60	0.02	0.026	12.27	0.29	0.74	T2
0.40	0	0.014	21.93	0.25	0.64	T2
0.30	0	0.010	32.21	0.22	0.56	T2
0.20	0	0.005	64.42	0.19	0.48	T

Table 14. Vortical wavelength as function of reduced frequency
 chordlength of flapping airfoil = 1cm = 0.39in
 amplitude = 0.8mm = 0.08c
 frequency = 5Hz
 Reynolds number = 49...869
 wake signature: D = drag
 I = indifferent
 T = thrust
 T2= thrust, dual mode

Frequency f [Hz]	Reduced Frequency k	Vortical Wavelength L [in]	Vortical Wavelength L/c	Wake Signature
5	4.06	0.63	1.60	D
6	4.87	0.54	1.37	I
7	5.68	0.50	1.27	I
8	6.49	0.46	1.17	T
9	7.30	0.44	1.13	T
10	8.12	0.43	1.10	T
11	8.93	0.42	1.07	T
12	9.74	0.42	1.07	T

Table 15. Vortical wavelength as function of reduced frequency
 chordlength of flapping airfoil = 1cm = 0.39in
 amplitude = 0.8mm = 0.08c
 velocity setting 1.60
 displayed 0.20ft/s
 actual 0.077m/s
 Reynolds number = 760
 wake signature: D = drag
 I = indifferent
 T = thrust
 T2= thrust, dual mode

setting	Velocity u		Reduced Frequency k	Vortical Wave- length L [in]	Vortical Wave- length L/c	Wake Signature
	displayed [ft/s]	actual [m/s]				
1.80	0.24	0.088	3.58	0.75	1.91	D
1.60	0.20	0.077	4.06	0.67	1.70	D
1.40	0.17	0.067	4.66	0.63	1.60	I
1.20	0.13	0.056	5.60	0.56	1.42	T
1.00	0.10	0.046	6.83	0.50	1.27	T
0.80	0.06	0.037	8.59	0.42	1.07	T2
0.60	0.02	0.026	12.27	0.38	0.97	T2
0.40	0	0.014	21.93	0.35	0.90	T2

Table 16. Vortical wavelength as function of reduced frequency
 chordlength of flapping airfoil = 1cm = 0.39in
 amplitude = 1.2mm = 0.12c
 frequency = 5Hz
 Reynolds number = 138...869
 wake signature: D = drag
 I = indifferent
 T = thrust
 T2= thrust, dual mode

setting	Velocity u		Reduced Frequency k	Vortical Wave- length L [in]	Vortical Wave- length L/c	Wake Signature
	displayed [ft/s]	actual [m/s]				
	1.0	0.288	2.18	1.20	3.08	D
	0.9	0.262	2.40	1.08	2.74	D
	0.8	0.237	2.66	1.00	2.54	I
	0.7	0.212	2.96	0.83	2.11	I
	0.6	0.186	3.38	0.75	1.91	I
	0.5	0.158	3.98	0.63	1.60	I
	0.4	0.130	4.82	0.50	1.27	I
	0.3	0.105	6.00	0.44	1.12	T
	0.2	0.077	8.12	0.38	0.97	T2
	0.1	0.046	13.66	0.29	0.74	T2

Table 17. Vortical wavelength as function of reduced frequency
 chordlength of flapping airfoil = 1cm = 0.39in
 amplitude = 1.5mm = 0.15c
 frequency = 10Hz
 Reynolds number = 454...2844
 wake signature: D = drag
 I = indifferent
 T = thrust
 T2= thrust, dual mode

setting	Velocity u		Reduced Frequency k	Vortical Wave- length L [in]	Vortical Wave- length L/c	Wake Signature
	displayed [ft/s]	actual [m/s]				
	0.50	0.158	1.99	1.34	3.43	I
	0.40	0.130	2.41	1.20	3.08	I
	0.30	0.105	3.00	0.98	2.50	T
	0.20	0.077	4.06	0.76	1.95	I
	0.12	0.052	5.96	0.56	1.43	T
	0.10	0.046	6.83	0.50	1.27	T2

Table 18. Vortical wavelength as function of reduced frequency
 chordlength of flapping airfoil = 1cm = 0.39in
 amplitude = 2mm = 0.2c
 frequency = 5Hz
 Reynolds number = 454...1560
 wake signature: D = drag
 I = indifferent
 T = thrust
 T2= thrust, dual mode

setting	Velocity u		Reduced Frequency k	Vortical Wave-length L [in]	Vortical Wave-length L/c	Wake Signature
	displayed [ft/s]	actual [m/s]				
	1.0	0.288	1.09	2.42	6.15	I
	0.9	0.262	1.20	2.33	5.92	I
	0.8	0.237	1.33	2.10	5.33	I
	0.7	0.212	1.48	1.88	4.78	I
	0.6	0.186	1.69	1.63	4.14	I
	0.5	0.158	1.99	1.45	3.68	T
	0.4	0.130	2.41	1.25	3.18	T
	0.3	0.105	3.00	0.95	2.44	T
	0.2	0.077	4.06	0.80	2.05	T
	0.1	0.046	6.83	0.56	1.42	T2

Table 19. Vortical wavelength as function of reduced frequency
 chordlength of flapping airfoil = 1cm = 0.39in
 amplitude = 4mm = 0.4c
 frequency = 5Hz
 Reynolds number = 454...2844
 wake signature: D = drag
 I = indifferent
 T = thrust
 T2= thrust, dual mode

setting	Velocity u		Reduced Frequency k	Vortical Wave- length L [in]	Vortical Wave- length L/c	Wake Signature
	displayed [ft/s]	actual [m/s]				
	1.0	0.288	1.09	2.38	6.10	T
	0.9	0.262	1.20	2.29	5.86	T
	0.8	0.237	1.33	2.08	5.33	T
	0.7	0.212	1.48	1.83	4.70	T
	0.6	0.186	1.69	1.61	4.14	T
	0.5	0.158	1.99	1.45	3.72	T

Table 20. Vortical wavelength as function of reduced frequency
 chordlength of flapping airfoil = 1cm = 0.39in
 amplitude = 6.5mm = 0.65c
 frequency = 5Hz
 Reynolds number = 1560...2844
 wake signature: D = drag
 I = indifferent
 T = thrust
 T2= thrust, dual mode

y-position [mm]	velocity [m/s]	stand. dev. [m/s]	turb. intensity [%]
-160	0.009	0.004	41
-140	0.009	0.004	39
-120	0.010	0.004	39
-100	0.010	0.004	37
-90	0.009	0.004	41
-80	0.010	0.003	32
-70	0.010	0.004	40
-60	0.010	0.004	38
-50	0.011	0.004	33
-45	0.011	0.004	33
-40	0.011	0.004	33
-35	0.011	0.004	32
-30	0.012	0.003	27
-25	0.013	0.004	29
-20	0.012	0.004	33
-15	0.013	0.004	29
-10	0.013	0.004	31
-5	0.011	0.004	38
-2.5	0.010	0.004	38
0	0.009	0.004	40
2.5	0.008	0.003	44
5	0.006	0.004	60
10	0.006	0.004	55
15	0.006	0.003	52
20	0.006	0.004	58
25	0.007	0.004	54
30	0.008	0.003	46
35	0.007	0.004	52
40	0.008	0.004	47
45	0.009	0.004	44
50	0.008	0.004	45
60	0.008	0.004	47
70	0.008	0.004	47
80	0.008	0.004	49
90	0.009	0.004	44
100	0.008	0.004	51

Table 23. Velocity profile 10mm upstream of flapping airfoil leading edge, $c=10\text{mm}$, $h=\pm 0.12c$, $f=5\text{Hz}$, $k=35$, sample size = 200

y-position [mm]	velocity [m/s]	stand. dev. [m/s]	turb. intensity [%]
-100	0.008	0.004	44
-90	0.009	0.003	36
-80	0.009	0.004	43
-70	0.009	0.003	38
-60	0.009	0.004	43
-50	0.008	0.004	47
-40	0.008	0.004	42
-30	0.008	0.004	47
-20	0.009	0.004	38
-10	0.009	0.004	39
0	0.009	0.004	46
10	0.009	0.004	39
20	0.009	0.004	43
30	0.009	0.003	40
40	0.009	0.004	40
50	0.009	0.004	40
60	0.009	0.003	37
70	0.008	0.003	38
80	0.008	0.004	49
90	0.008	0.004	47
100	0.009	0.004	42

Table 24. Water tunnel free stream velocity profile
(same x-coordinate as in Table 23, without airfoil)
sample size = 200

Amplitude h/c	Velocity [m/s]	Stand. Dev. [m/s]	Turb.Intensity [%]
0	0.009	0.004	40
0.03	0.009	0.004	44
0.05	0.009	0.004	41
0.08	0.010	0.004	40
0.12	0.013	0.004	29
0.16	0.014	0.004	28
0.20	0.015	0.005	32
0.27	0.017	0.005	26
0.35	0.022	0.006	26
0.47	0.021	0.011	50
0.65	0.020	0.020	102

Table 25. Velocity 10mm upstream of flapping airfoil leading edge as function of the amplitude h/c, c=10mm, y=-15mm, f= 5Hz, U=9mm/s, k=35, sample size = 200.

Streamwise position x/c	Velocity [mm/s]	
	upper surface	lower surface
-5.00	104	105
-4.00	104	105
-3.00	104	105
-2.00	104	104
-1.00	103	103
-0.50		104
-0.25		105
-0.20		106
-0.10		107
0	105	110
0.10		112
0.20	109	115
0.40	110	115
0.60	111	114
0.80	109	111
1.00	109	110
1.50	107	108
2.00	106	107
3.00	106	105
3.50	106	
4.00		105
5.00	105	105

Table 26. Streamwise velocity distribution above and below of the stationary airfoil, $c=10\text{mm}$, $y=\pm 4\text{mm}$, $U=105\text{mm/s}$

y-position [mm]	velocity [m/s]	stand. dev. [m/s]	turb. intensity [%]	sample size
100	0.007	0.003	47	200
90	0.006	0.004	58	198
80	0.010	0.004	38	198
70	0.010	0.004	37	200
60	0.010	0.004	36	200
50	0.012	0.004	33	200
40	0.014	0.004	29	200
30	0.015	0.004	26	198
20	0.019	0.004	23	200
10	0.022	0.006	29	200
0	0.014	0.006	42	200
-10	0.008	0.008	96	200
-20	0.007	0.004	55	195
-30	0.007	0.004	61	199
-40	0.016	0.004	24	200
-50	0.013	0.004	30	200
-60	0.013	0.004	30	200
-70	0.011	0.005	40	200
-80	0.011	0.004	38	200
-90	0.011	0.004	40	200
-100	0.010	0.004	37	200
-35	0.016	0.005	30	200
-32.5	0.018	0.004	24	200
-30	0.018	0.004	21	200
-20	0.022	0.005	25	199
-10	0.022	0.007	33	200
0	0.010	0.004	40	198
10	0.007	0.007	102	200
20	0.004	0.004	100	198
30	0.005	0.004	88	169
40	0.005	0.004	81	199
50	0.006	0.004	65	200
60	0.007	0.004	52	187
70	0.007	0.004	62	199
80	0.007	0.004	60	199
90	0.007	0.004	55	200
100	0.007	0.004	57	198
110	0.008	0.004	47	200

Table 27. Velocity profile 10mm upstream of flapping airfoil leading edge, $c=10\text{mm}$, $h=\pm 0.35c$, $f=5\text{Hz}$, $k=35$, $U=9\text{mm/s}$

y position [mm]	velocity [m/s]	stand.dev. [m/s]	turb.intensity [%]	sample size
-100	0.009	0.004	42	147
-90	0.009	0.004	47	120
-80	0.007	0.005	72	167
-70	0.006	0.004	69	99
-60	0.008	0.004	53	123
-50	0.008	0.004	47	117
-40	0.008	0.004	54	154
-30	0.016	0.006	39	159
-20	0.023	0.005	23	159
-10	0.024	0.007	29	159
0	0.011	0.005	49	155
10	0.008	0.007	94	177
20	0.007	0.005	77	190
30	0.006	0.004	65	102
40	0.004	0.004	111	104
50	0.003	0.004	151	184
60	0.006	0.004	70	142
70	0.006	0.004	64	194
80	0.004	0.004	98	104
90	0.005	0.004	79	78
100	0.006	0.004	65	71

Table 28. Velocity profile 10mm upstream of flapping airfoil leading edge, $c=10\text{mm}$, $h=\pm 0.35c$, $f=5\text{Hz}$, $k=35$, $U=9\text{mm/s}$

y-position [mm]	velocity [m/s]	stand. dev. [m/s]	turb. intensity [%]
-180	0.081	0.005	6
-160	0.082	0.006	7
-140	0.081	0.006	8
-120	0.081	0.007	9
-100	0.081	0.009	12
-90	0.081	0.011	13
-80	0.080	0.013	16
-70	0.080	0.015	19
-60	0.082	0.018	22
-50	0.082	0.022	26
-40	0.087	0.025	29
-30	0.088	0.033	37
-20	0.093	0.044	47
-15			
-10	0.081	0.046	58
-5			
0	0.072	0.019	26
5			
10	0.114	0.046	41
15			
20	0.114	0.046	44
30	0.116	0.030	26
40	0.106	0.028	26
50	0.104	0.023	22
60	0.101	0.018	18
70	0.100	0.015	15
80	0.099	0.012	12
90	0.097	0.010	10
100	0.098	0.008	8
120	0.095	0.007	7
140	0.095	0.006	6

Table 29. Velocity Profile 10mm upstream of flapping airfoil leading edge, mode "up", $c=100\text{mm}$, $h=\pm 0.04c$, $f=5\text{Hz}$, $k=35$, $U=9\text{cm/s}$, sample size = 400

y-position [mm]	velocity [m/s]	stand. dev. [m/s]	turb. intensity [%]
-180			
-160			
-140	0.091	0.004	5
-120	0.091	0.005	6
-100	0.091	0.004	5
-90	0.091	0.005	5
-80	0.091	0.005	6
-70	0.091	0.004	5
-60	0.091	0.005	6
-50	0.091	0.005	5
-40	0.091	0.004	5
-30	0.089	0.005	6
-20	0.088	0.005	6
-15	0.083	0.004	5
-10	0.080	0.005	6
-5	0.071	0.004	5
0	0.067	0.004	6
5	0.069	0.004	6
10	0.075	0.004	6
15	0.080	0.005	6
20	0.085	0.005	5
30	0.087	0.005	5
40	0.089	0.005	6
50	0.091	0.006	6
60	0.090	0.005	5
70	0.091	0.005	5
80	0.091	0.005	6
90	0.090	0.005	5
100	0.091	0.005	6
120	0.091	0.005	6
140	0.090	0.005	6

Table 30. Velocity profile 10mm upstream of stationary airfoil leading edge, $c=100\text{mm}$, $U=9\text{cm/s}$, sample size = 200

y-position [mm]	velocity [m/s]	stand. dev. [m/s]	turb. intensity [%]
-180	0.087	0.006	7
-160	0.087	0.006	7
-140	0.089	0.006	7
-120	0.090	0.008	9
-100	0.089	0.009	10
-90			
-80	0.091	0.013	14
-70			
-60	0.097	0.018	18
-50	0.103	0.021	20
-40	0.101	0.028	28
-30	0.108	0.036	33
-20	0.112	0.044	40
-15			
-10	0.111	0.045	40
-5	0.085	0.040	47
0	0.066	0.019	28
5	0.065	0.040	62
10	0.082	0.048	59
15			
20	0.085	0.046	54
30	0.087	0.033	38
40	0.079	0.028	36
50			
60	0.077	0.018	23
70			
80	0.076	0.011	15
90			
100	0.077	0.008	11
120	0.078	0.007	9
140	0.079	0.005	7

Table 31. Velocity profile 10mm upstream of flapping airfoil leading edge, mode "down", $c=100\text{mm}$, $h=\pm 0.04c$, $f=5\text{Hz}$, $k=36.5$, $U=8.6\text{cm/s}$, sample size = 400

y-position [mm]	velocity [m/s]	stand. dev. [m/s]	turb. intensity [%]
-180			
-160			
-140	0.085	0.005	6
-120	0.085	0.005	6
-100	0.085	0.005	6
-90			
-80	0.085	0.005	6
-70			
-60	0.085	0.005	6
-50			
-40	0.084	0.005	6
-30	0.082	0.005	6
-20	0.079	0.005	6
-15	0.077	0.005	6
-10	0.072	0.004	6
-5	0.067	0.005	7
0	0.064	0.005	7
5	0.066	0.005	7
10	0.072	0.004	6
15	0.077	0.005	6
20	0.081	0.005	6
30	0.083	0.005	6
40	0.085	0.005	6
50			
60	0.086	0.005	6
70			
80	0.086	0.005	6
90			
100	0.086	0.005	6
120	0.086	0.005	6
140	0.086	0.005	6

Table 32. Velocity profile 10mm upstream of stationary airfoil leading edge, $c=100\text{mm}$, $U=8.6\text{cm/s}$, sample size = 400

y-position [mm]	Stationary Airfoil			Flapping Airfoil		
	velocity [m/s]	stand. dev. [m/s]	turb. intens. [%]	velocity [m/s]	stand. dev. [m/s]	turb. intens. [%]
-140	0.211	0.006	3	0.207	0.009	5
-120	0.211	0.007	3	0.208	0.009	4
-100	0.210	0.007	3	0.210	0.010	5
-80	0.210	0.008	4	0.210	0.013	6
-60	0.210	0.007	4	0.213	0.018	9
-40	0.207	0.007	3	0.214	0.026	12
-30	0.205	0.006	3	0.209	0.035	17
-20	0.199	0.007	3	0.205	0.039	19
-15	0.192	0.006	3	0.203	0.038	18
-10	0.184	0.006	3	0.194	0.036	18
-7.5						
-5	0.175	0.007	4	0.180	0.023	13
-2.5						
0	0.171	0.006	4	0.175	0.011	6
2.5						
5	0.176	0.006	3	0.185	0.026	14
7.5						
10	0.186	0.007	4	0.193	0.037	19
15	0.193	0.008	4	0.214	0.037	17
20	0.200	0.008	4	0.211	0.037	17
30	0.206	0.006	3	0.212	0.033	15
40	0.207	0.007	3	0.212	0.027	13
60	0.211	0.006	3	0.214	0.017	8
80	0.211	0.006	3	0.212	0.013	6
100	0.211	0.008	4	0.211	0.009	4
120	0.212	0.008	4	0.210	0.008	4
140	0.209	0.007	3	0.210	0.007	3

Table 33. Velocity profiles 10mm upstream of airfoil leading edge, $c=100\text{mm}$, $h=\pm 0.04c$, $f=5\text{Hz}$, $k=15$, $U=21\text{cm/s}$, sample size = 400

y-position [mm]	Stationary Airfoil			Flapping Airfoil		
	velocity [m/s]	stand. dev. [m/s]	turb. intens. [%]	velocity [m/s]	stand. dev. [m/s]	turb. intens. [%]
-140	0.210	0.007	3	0.202	0.008	4
-120	0.211	0.007	3	0.202	0.009	4
-100	0.211	0.007	4	0.200	0.010	5
-80	0.210	0.006	3	0.198	0.011	5
-60	0.210	0.008	4	0.194	0.012	6
-40	0.208	0.007	3	0.189	0.016	8
-30	0.208	0.007	3	0.190	0.024	13
-20	0.205	0.008	4	0.206	0.069	33
-15	0.204	0.008	4	0.266	0.054	20
-10	0.204	0.011	5	0.303	0.062	21
-7.5	0.190	0.018	10	0.335	0.047	14
-5	0.169	0.024	14	0.387	0.056	14
-2.5	0.153	0.024	15	0.414	0.075	18
0	0.160	0.026	16	0.396	0.068	17
2.5	0.162	0.023	14	0.345	0.051	15
5	0.184	0.022	12	0.315	0.069	22
7.5	0.191	0.021	11	0.292	0.059	20
10	0.202	0.010	5	0.263	0.059	22
15	0.204	0.007	3	0.210	0.063	30
20	0.205	0.007	4	0.202	0.039	19
30	0.207	0.007	3	0.192	0.018	10
40	0.207	0.007	3	0.193	0.012	6
60	0.209	0.007	4	0.198	0.012	6
80	0.211	0.007	3	0.201	0.010	5
100	0.210	0.008	4	0.205	0.009	4
120	0.211	0.007	3	0.205	0.008	4
140	0.210	0.006	3	0.205	0.007	4

Table 34. Velocity profiles 40mm downstream of airfoil trailing edge, $c=100\text{mm}$, $h=\pm 0.04c$, $f=5\text{Hz}$, $k=15$, $U=21\text{cm/s}$, sample size = 400

y-position [mm]	Stationary Airfoil			Flapping Airfoil		
	velocity [m/s]	stand. dev. [m/s]	turb. intens. [%]	velocity [m/s]	stand. dev. [m/s]	turb. intens. [%]
-140	0.202	0.007	4	0.195	0.008	4
-120	0.201	0.007	3	0.194	0.008	4
-100	0.202	0.007	4	0.194	0.009	5
-80	0.199	0.007	3	0.192	0.013	7
-60	0.197	0.006	3	0.193	0.015	8
-40	0.192	0.007	4	0.188	0.026	14
-30	0.188	0.006	3	0.185	0.031	17
-20	0.182	0.006	3	0.184	0.035	19
-15	0.178	0.007	4	0.178	0.040	22
-10	0.173	0.006	4	0.175	0.039	22
-7.5						
-5	0.168	0.006	3	0.176	0.039	22
-2.5						
0	0.164	0.006	4	0.170	0.031	18
2.5						
5	0.168	0.006	4	0.171	0.017	10
7.5						
10	0.182	0.006	3	0.187	0.019	10
15	0.197	0.007	3	0.212	0.032	15
20	0.208	0.007	3	0.230	0.041	18
30	0.220	0.008	4	0.243	0.037	15
40	0.224	0.007	3	0.245	0.028	12
60	0.224	0.007	3	0.237	0.020	8
80	0.223	0.007	3	0.233	0.013	6
100	0.220	0.007	3	0.229	0.010	4
120	0.219	0.008	4	0.227	0.009	4
140	0.219	0.008	3	0.225	0.008	4

Table 35. Velocity profiles 10mm upstream of airfoil leading edge, $AoA=10^\circ$, $c=100\text{mm}$, $h=\pm 0.04c$, $f=5\text{Hz}$, $k=15$, $U=21\text{cm/s}$, sample size = 400

y-position [mm]	Stationary Airfoil			Flapping Airfoil		
	velocity [m/s]	stand. dev. [m/s]	turb. intens. [%]	velocity [m/s]	stand. dev. [m/s]	turb. intens. [%]
-140	0.207	0.007	3	0.195	0.009	5
-120	0.207	0.007	3	0.193	0.009	5
-100	0.206	0.007	3	0.190	0.010	5
-80	0.207	0.007	3	0.190	0.010	5
-60	0.206	0.007	4	0.185	0.013	7
-40	0.206	0.007	4	0.191	0.028	14
-30	0.207	0.008	4	0.218	0.058	26
-20	0.206	0.012	6	0.301	0.070	23
-15	0.196	0.025	13	0.387	0.072	19
-10	0.143	0.030	21	0.378	0.065	17
-7.5						
-5	0.127	0.030	23	0.300	0.074	25
-2.5						
0	0.137	0.041	30	0.258	0.069	27
2.5						
5	0.173	0.034	19	0.229	0.053	23
7.5						
10	0.196	0.018	9	0.197	0.046	23
15	0.205	0.012	6	0.203	0.025	12
20	0.209	0.009	4	0.193	0.017	9
30	0.210	0.007	3	0.197	0.012	6
40	0.212	0.006	3	0.201	0.012	6
60	0.215	0.007	3	0.208	0.011	5
80	0.217	0.008	4	0.211	0.010	5
100	0.216	0.007	3	0.215	0.009	4
120	0.215	0.008	4	0.216	0.008	4
140	0.216	0.008	4	0.217	0.007	3

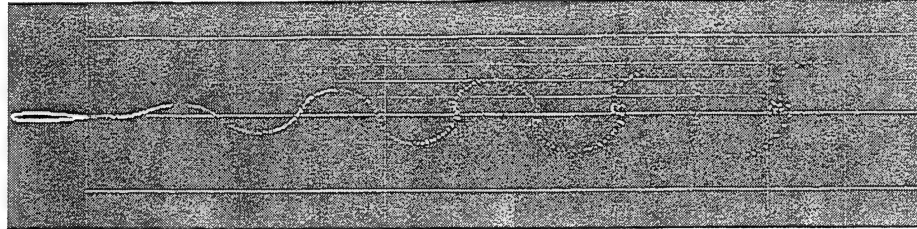
Table 36. Velocity profiles 40mm downstream of airfoil trailing edge, $AoA=10^\circ$, $c=100\text{mm}$, $h=\pm 0.04c$, $f=5\text{Hz}$, $k=15$, $U=21\text{cm/s}$, sample size = 400

APPENDIX C. COMPUTED WAKES

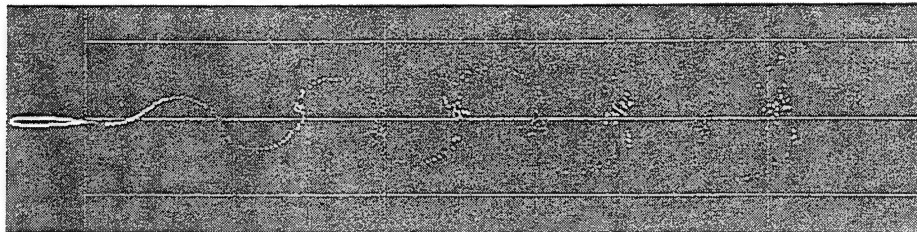
Figure 38 through 43 Wake plots from Ref. [7]

Table 22 Vortical wavelength measured from the wake plots

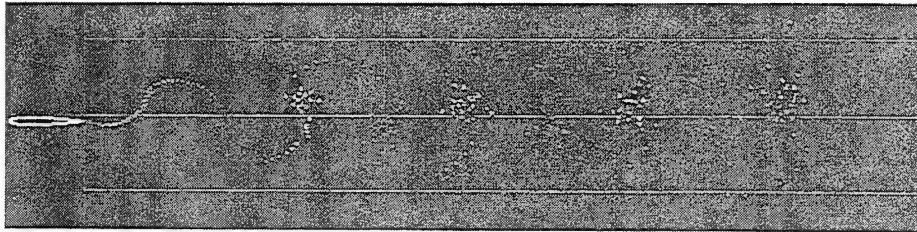
UPOTG wake geometry; $k = 3.00$, 60 time-steps/cycle, NACA 0010 airfoil defined by 100 points.



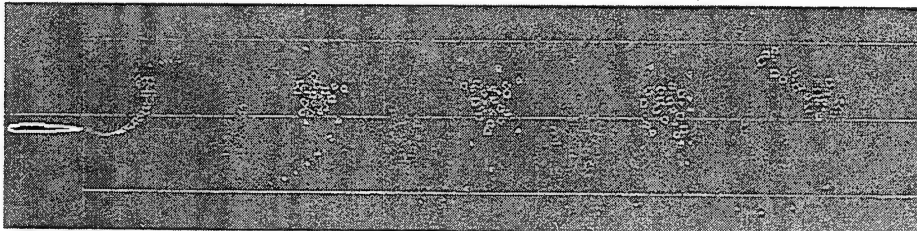
$h = \pm 0.025c$



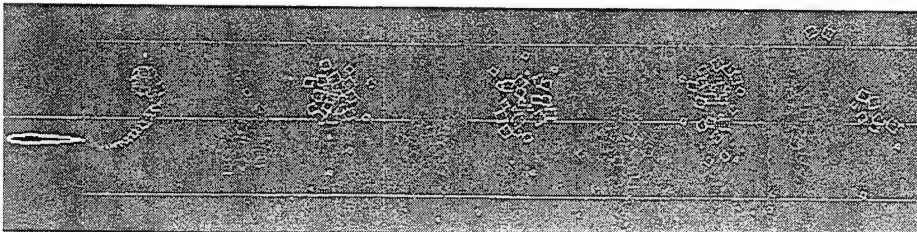
$h = \pm 0.050c$



$h = \pm 0.100c$



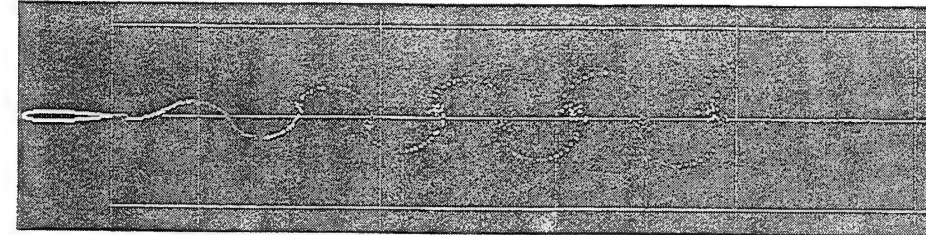
$h = \pm 0.200c$



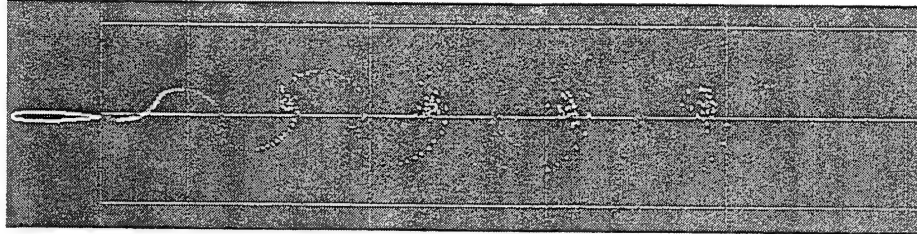
$h = \pm 0.300c$

Figure 38. Wake geometry for $k=3.00$

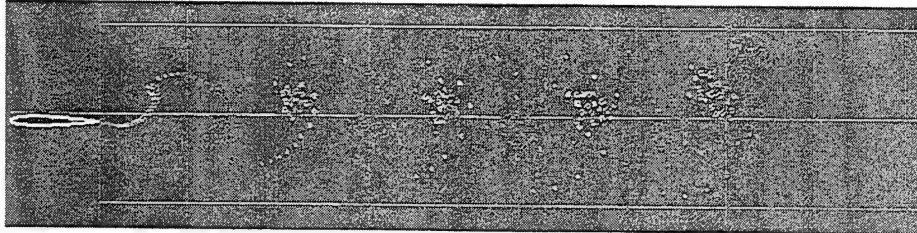
UPOTG wake geometry; $k = 4.06$, 60 time-steps/cycle, NACA 0010 airfoil defined by 100 points.



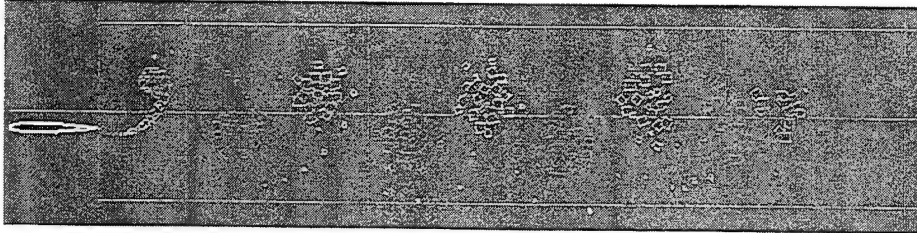
$h = \pm 0.025c$



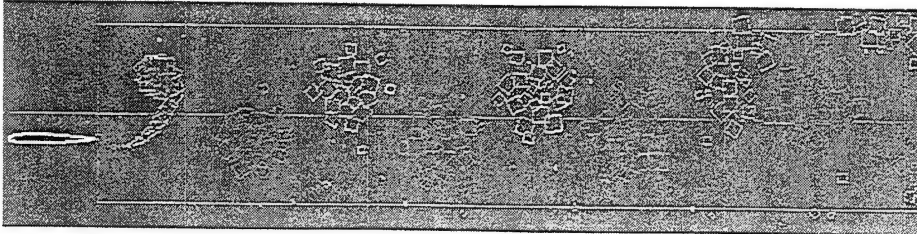
$h = \pm 0.050c$



$h = \pm 0.100c$



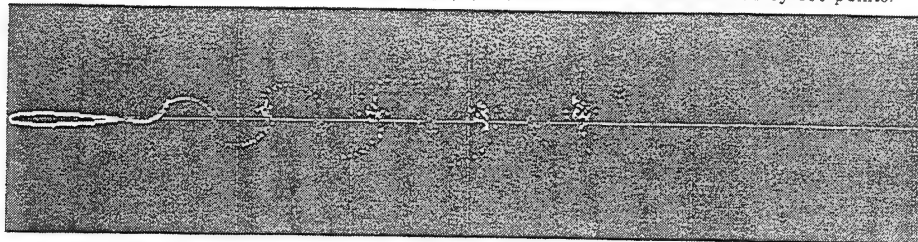
$h = \pm 0.200c$



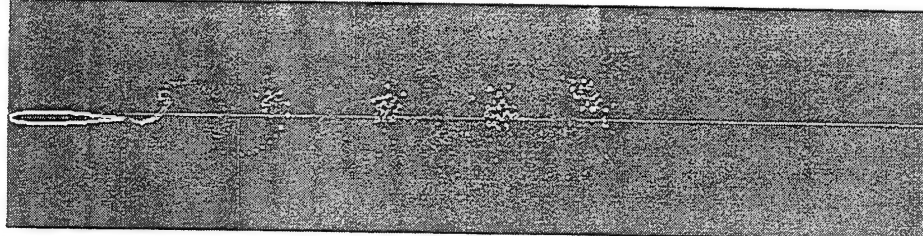
$h = \pm 0.300c$

Figure 39. Wake geometry for $k=4.06$

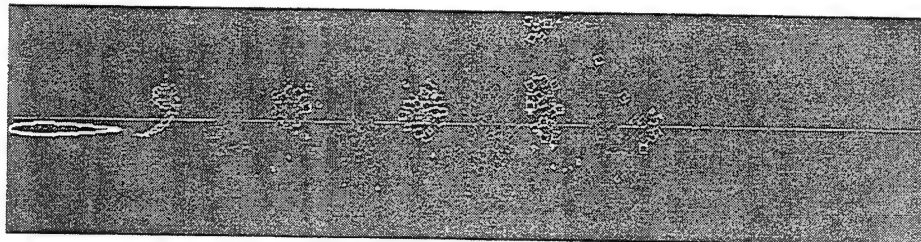
UPOTG wake geometry; $k = 6.83$, 60 time-steps/cycle, NACA 0010 airfoil defined by 100 points.



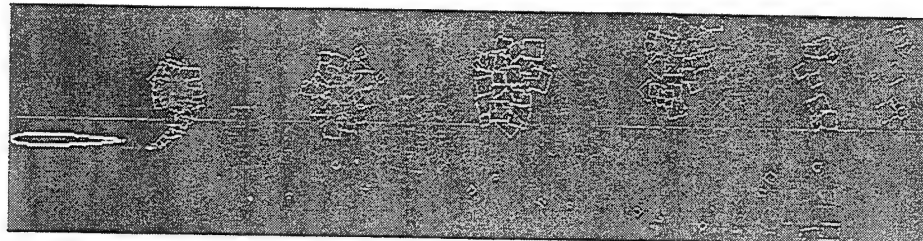
$h = \pm 0.025c$



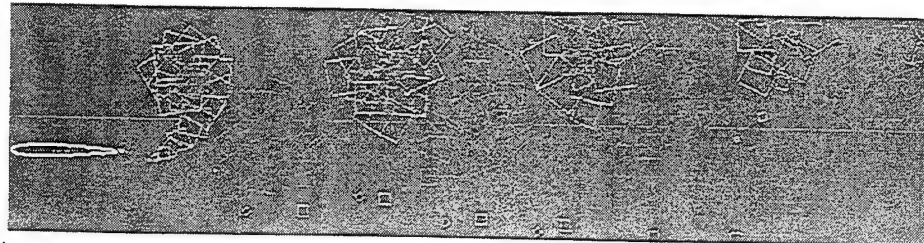
$h = \pm 0.050c$



$h = \pm 0.100c$



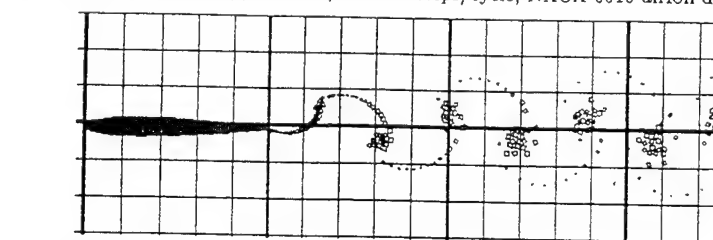
$h = \pm 0.200c$



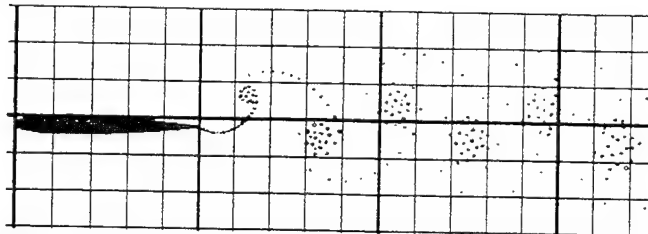
$h = \pm 0.300c$

Figure 40. Wake geometry for $k=6.83$

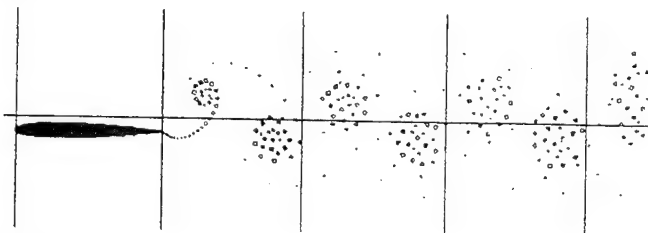
UPOTG wake geometry; $k = 8.56$, 60 time-steps/cycle, NACA 0010 airfoil defined by 100 points.



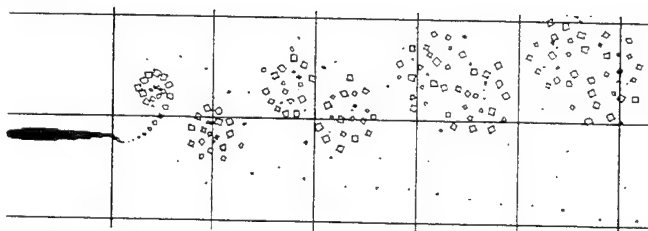
$h = \pm 0.025c$



$h = \pm 0.050c$



$h = \pm 0.100c$



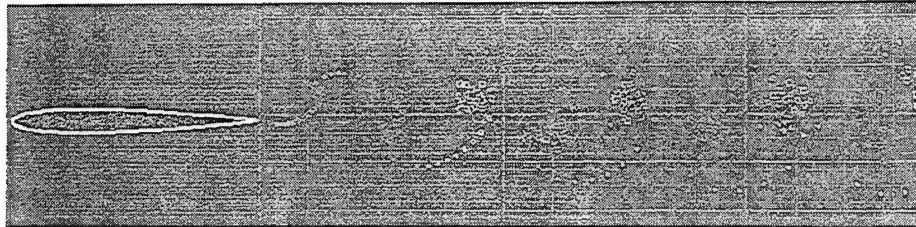
$h = \pm 0.200c$



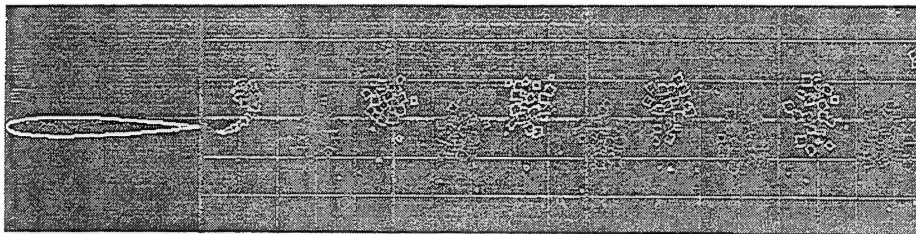
$h = +0.300c$

Figure 41. Wake geometry for $k=8.56$

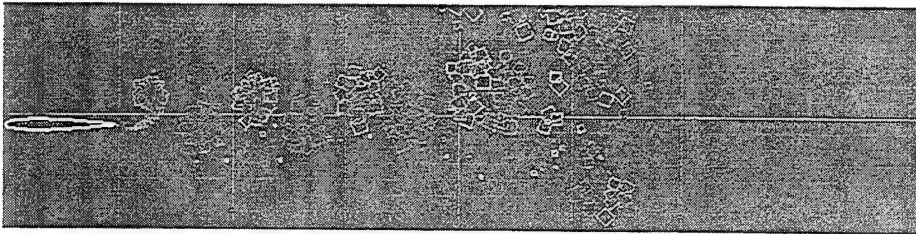
UPOTG wake geometry; $k = 10.11$, 60 time-steps/cycle, NACA 0010 airfoil defined by 100 points.



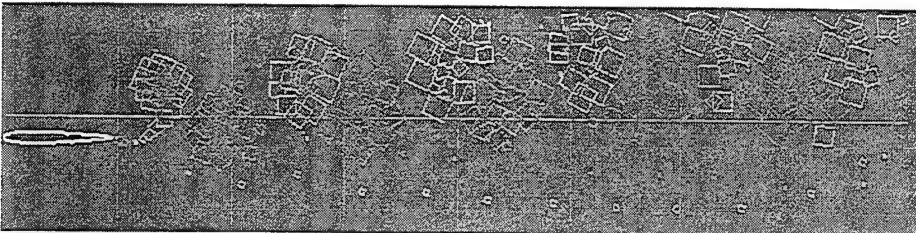
$h = \pm 0.025c$



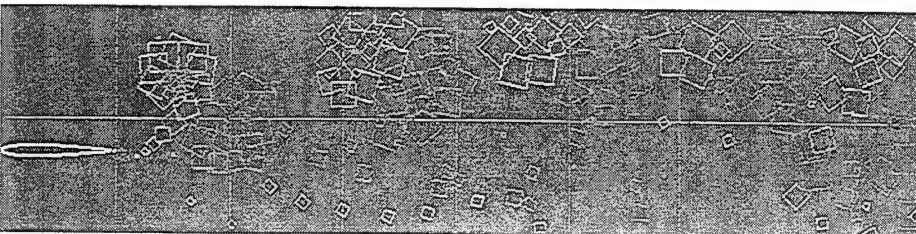
$h = \pm 0.050c$



$h = \pm 0.100c$



$h = \pm 0.200c$



$h = \pm 0.300c$

Figure 42. Wake geometry for $k=10.11$

UPOTG wake geometry; $k = 12.32$, 60 time-steps/cycle, NACA 0010 airfoil defined by 100 points.

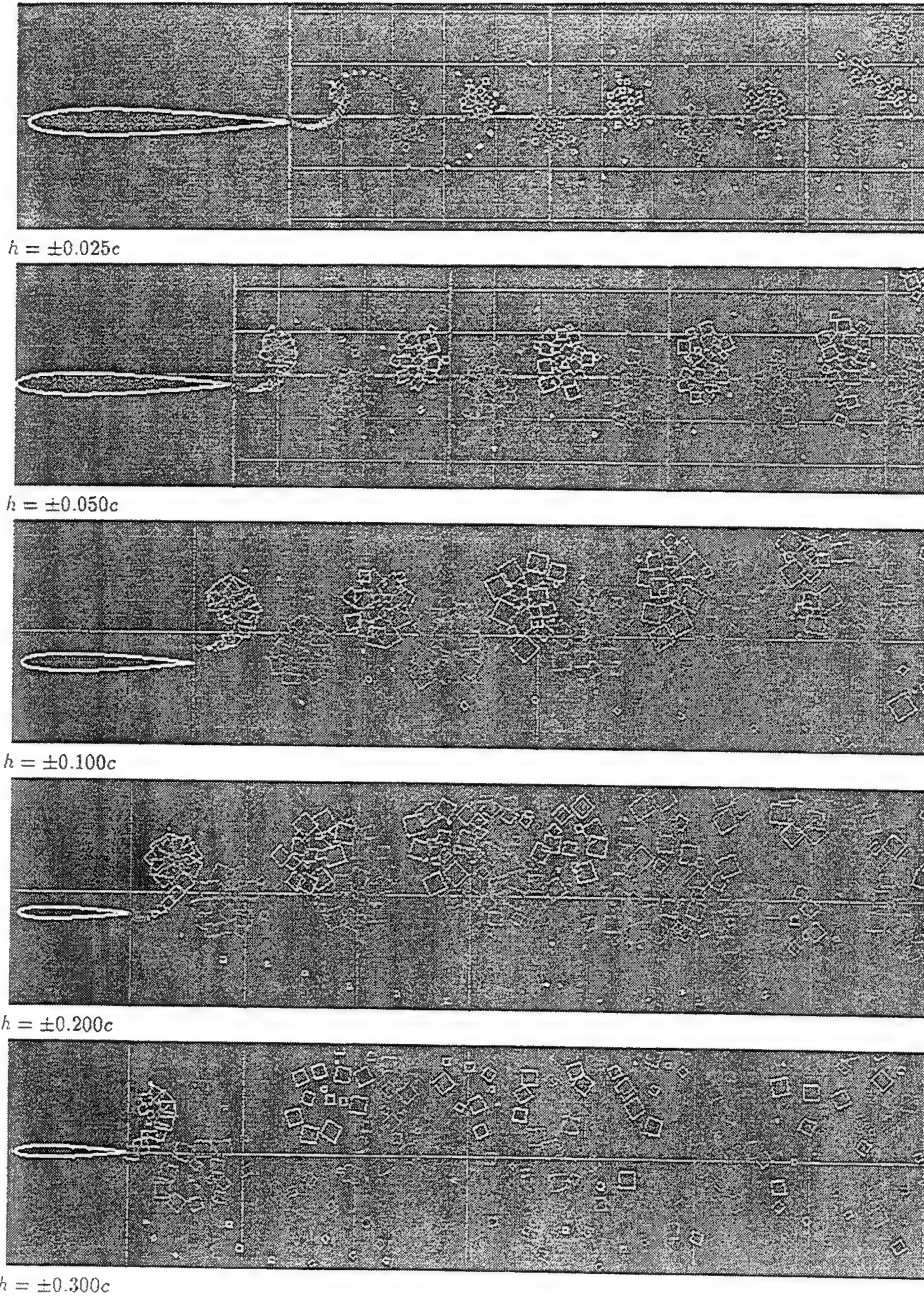


Figure 43. Wake geometry for $k=12.32$

Reduced Frequency k	Amplitude h/c				
	0.025	0.05	0.1	0.2	0.3
3.00	2.04	2.07	2.15	2.31	2.54
4.06	1.53	1.58	1.67	1.87	2.13
6.80	0.95	1.00	1.13	1.45	1.74
8.60	0.77	0.84	1.02	1.34	1.67
10.11	0.66	0.74	0.92	1.26	1.63
12.30	0.57	0.67	0.84	1.20	1.58

Table 22. Vortical Wavelength L/c as Function of Amplitude h/c and Reduced Frequency k ,
measured from Panel Code computed wake plots

LIST OF REFERENCES

1. Schmidt, W., "Der Wellpropeller, ein neuer Antrieb für Wasser-, Land- und Luftfahrzeuge", *Zeitschrift Flugwissenschaft*, Band 13, Heft 12, pp. 472-479, 1965.
2. Freymuth, P., "Propulsive Vortical Signature of Plunging and Pitching Airfoils", *AIAA Journal*, vol. 26, no. 7, pp. 881-883, July 1988.
3. Koochesfahani, M. M., "Vortical Patterns in the Wake of an Oscillating Airfoil", *AIAA Journal*, vol. 27, no. 9, pp. 1200-1205, Sept. 1989.
4. Freymuth, P., Gustafson, K. E., and Leben, P., "Visualization and Computation of Hovering Mode Vortex Dynamics", *Vortex Methods and Vortex Motion*, Society for Industrial and Applied Mathematics, pp. 143-169, Philadelphia, Pennsylvania, 1991.
5. Tuncer, I. H., Platzer, M. F., and Ekaterinaris, J. A., "Computational Analysis of Flapping Airfoil Aerodynamics", *ASME Fluids Engineering Division, Summer Meeting*, pp. 9-18, Lake Tahoe, Nevada, June 1994.
6. Teng, N. H., "The Development of a Computer Code for Numerical Solution of Unsteady, Inviscid and Incompressible flow over an Airfoil", Master's Thesis, Naval Postgraduate School, Monterey, California, June 1987.
7. Jones, K. D., and Center, K. B., "Numerical Wake Visualization for Airfoils Undergoing Forced and Aeroelastic Motions", submitted to the 34th AIAA Aerospace Science Meeting, Jan. 1996.
8. Instruction Manual, Electro-Seis Model 113 Shaker, APS Dynamics Inc., 1994.
9. Instruction Manual, Dual Mode Model 114 Amplifier, APS Dynamics Inc., 1994.
10. Instruction Manual, Model 9201 Colorburst Multicolor Beam Separator, TSI Inc., Aug. 1989.
11. Instruction Manual, Two Component Fiberoptic Probe System, TSI Inc., Oct. 1987.
12. Instruction Manual, Model IFA 550 Signal Processor, TSI Inc., Feb. 1988.

13. ' Instruction Manual, Flow Information Display (FIND) Software Version 3.5, TSI Inc., Jan. 1992.
14. Jones, K. D., Dohring C. M., and Platzer, M. F., "Wake Structures Behind Plunging Airfoils: a Comparison of Numerical and Experimental Results", submitted to the 34th AIAA Aerospace Science Meeting, Jan. 1996.

INITIAL DISTRIBUTION LIST

1. Defense Technical Information Center..... 2
8725 John J. Kingman Rd., STE 0944
Ft. Belvoir, Virginia 22060-6218

2. Dudley Knox Library..... 2
Naval Postgraduate School
411 Dyer Rd.
Monterey, California 93943-5101

3. Professor R. Panholzer, Code SS/PA..... 1
Space Systems Academic Group
Naval Postgraduate School
Monterey, California 93943-5101

4. Professor D. J. Collins, Code AA/CO..... 1
Department of Aeronautics and Astronautics
Naval Postgraduate School
Monterey, California 93943-5101

5. Professor M. F. Platzer, Code AA/PL..... 10
Department of Aeronautics and Astronautics
Naval Postgraduate School
Monterey, California 93943-5101

6. Professor M. S. Chandrasekhara, Code AA/CH..... 1
Department of Aeronautics and Astronautics
Naval Postgraduate School
Monterey, California 93943-5101

7. Dr. K. D. Jones, Code AA/JO..... 1
Department of Aeronautics and Astronautics
Naval Postgraduate School
Monterey, California 93943-5101

8. Dr. I. H. Tuncer, Code AA/TU..... 1
Department of Aeronautics and Astronautics
Naval Postgraduate School
Monterey, California 93943-5101

9. Professor L. Fottner..... 1
Institut für Strahlantriebe
Universität der Bundeswehr
Werner-Heisenberg-Weg 39
85577 Neubiberg
Germany
10. Dr. E. Rood..... 1
Office of Naval Research
800 North Quincy Street
Arlington, Virginia 22217-5660
11. Dr. S. Lekoudis..... 1
Office of Naval Research
800 North Quincy Street
Arlington, Virginia 22217-5660
12. CDR C. Dohring..... 2
Christianistr. 67
24113 Kiel
Germany